This is to certify that the
dissertation entitled
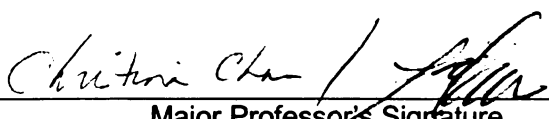

ENGINEERING *IN VITRO* CELLULAR
MICROENVIRONMENTS USING POLYELECTROLYTE
MULTILAYER FILMS TO CONTROL CELL ADHESION AND
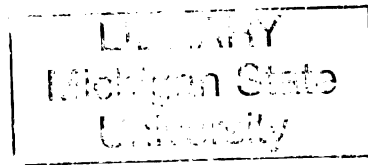FOR DRUG DELIVERY APPLICATIONS

presented by

SRIVATSAN KIDAMBI

has been accepted towards fulfillment
of the requirements for the

_____Ph.D._____ degree in _____Chemical Engineering_____

_____
Major Professor's Signature

_____03/02/07_____

Date

PLACE IN RETURN BOX to remove this checkout from your record.
TO AVOID FINES return on or before date due.
MAY BE RECALLED with earlier due date if requested.

DATE DUE	DATE DUE	DATE DUE

6/07 p:/CIRC/DateDue.indd-p.1

ENGINEERING *IN VITRO* CELLULAR MICROENVIRONMENT USING POLYELECTROLYTE MULTILAYER FILMS TO CONTROL CELL ADHESION AND FOR DRUG DELIVERY APPLICATIONS

By

SRIVATSAN KIDAMBI

A DISSERTATION

Submitted to
Michigan State University
in partial fulfillment of the requirements
for the degree of

DOCTOR OF PHILOSOPHY

Department of Chemical Engineering and Materials Science

2007

ABSTRACT

ENGINEERING *IN VITRO* CELLULAR MICROENVIRONMENT USING POLYELECTROLYTE MULTILAYER FILMS TO CONTROL CELL ADHESION AND FOR DRUG DELIVERY APPLICATIONS

By

SRIVATSAN KIDAMBI

Over the past decades, the development of new methods for fabricating thin films that provide precise control of the three-dimensional topography and cell adhesion has generated lots of interest. These films could lead to significant advances in the fields of tissue engineering, drug delivery and biosensors which have become increasingly germane areas of research in the field of chemical engineering. The ionic layer-by-layer (LbL) assembly technique called "Polyelectrolyte Multilayers (PEMs)", introduced by Decher in 1991, has emerged as a versatile and inexpensive method of constructing polymeric thin films, with nanometer-scale control of ionized species. PEMs have long been utilized in such applications as sensors, eletrochromics, and nanomechanical thin films but recently they have also been shown to be excellent candidates for biomaterial applications. In this thesis, we engineered these highly customizable PEM thin films to engineer *in vitro* cellular microenvironments to control cell adhesion and for drug delivery applications.

PEM films were engineered to control the adhesion of primary hepatocytes and primary neurons without the aid of adhesive proteins/ligands. We capitalized upon the differential cell attachment and spreading of primary hepatocytes and neurons on poly(diallyldimethylammoniumchloride) (PDAC) and sulfonated polystyrene (SPS)

surfaces to make patterned co-cultures of primary hepatocytes/fibroblasts and primary neurons /astrocytes on the PEM surfaces. In addition, we developed self-assembled monolayer (SAM) patterns of m-d-poly(ethylene glycol) (m-dPEG) acid molecules onto PEMs. The created m-dPEG acid monolayer patterns on PEMs acted as resistive templates, and thus prevented further deposits of consecutive poly(anion)/poly(cation) pairs of charged particles and resulted in the formation of three-dimensional (3-D) patterned PEM films or selective particle depositions atop the original multilayer thin films. These new patterned and structured surfaces have potential applications in microelectronic devices and electro-optical and biochemical sensors. The PEG patterns developed are tunable at certain salt conditions and be removed from the PEM surface without affecting the PEM layers underneath the patterns. These removable surfaces provide an alternative method to form patterns of multiple particles, proteins and cells. This new approach provides an environmentally friendly and biocompatible route to designing versatile salt tunable surfaces. Finally, we illustrate the use of PEM films to engineer aptamer and siRNA based drug delivery systems.

TO MY FAMILY

ACKNOWLEDGMENTS

I would like to express my deepest appreciation to my advisors Prof. Kris Chan and Prof. Ilsoon Lee, for their insight, guidance and invaluable assistance, without which this thesis would not have been possible. Co-advised projects can easily become nightmares, bogged down in conflicts and with the student struggling in the middle. Kris and Ilsoon have a wonderful working relationship, which allowed me to capitalize immensely on the synergies between the two research programs. I appreciate the freedom and space they gave me and their tolerance of my independent streak in pursuing the thesis both during times when the research was in its difficult stages and when it was sailing smoothly.

I would also like to thank the members of my Ph.D. committee, Dr. Greg Baker and Dr. Robert Ofoli, in particular for Dr.Ofoli's always insightful comments when I see him in the department hall way and Greg's critical reading of my thesis.

I am also thankful to my group members in the Chan and Lee groups whom I learned a great deal from and who made coming to lab worthwhile. From the Chan group: Shireesh, Zheng, Sachin, Lufang, Xuerei, Linxia, Yifei and Sumit; From the Lee group: Neeraj, Troy and Devesh; for making my Ph.D. a pleasant experience. In particular, I thank Shireesh for helping me get started with the assays and cell experiments, Lufang and Yifei for the numerous primary hepatocyte isolations, Deebika for the primary neurons and astrocytes isolation and also for feeding my cells when I was lazy.

Particularly due to this thesis's interdisciplinary character, I also benefited greatly from collaborative environment. Sharing lab with Pat's and Dr. Worden's group made it interesting work in the lab day in and day out without bothering about the numerous

TABLE OF CONTENTS

LIST OF TABLES

LIST OF FIGURES

LIST OF ACRONYMS

CLSM: Confocal Laser Scanning Microscopy

DMEM: Dulbecco's Modified Eagle Medium

DNA: Deoxyribonucleic acid

LbL: Layer-by-Layer

PDAC: Poly(diallyldimethylammoniumchloride)

PDMS: Poly(dimethylsiloxane)

PEG: Poly(ethylene glycol)

PEI: Poly(ethyleneimine)

PEM: Polyelectrolyte Multilayers

PLL: Poly(L-lysine)

RNA: Ribonucleic acid

SAMs: Self assembled Monolayers

SELEX: Systematic Evolution of Ligands by Exponential Amplification

siRNA: Short Interfering Ribonucleic Acids

SPS: Poly(sodium 4-styrenesulfonate)

TCPS: Tissue culture polystyrene

XPS: X-ray Photoelectron Spectroscopy

CHAPTER 1 INTRODUCTION

1.1 OVERVIEW AND SIGNIFICANCE OF PROBLEM

The ability to engineer the interactions of cells with surfaces is an important albeit demanding task in medicine and biotechnology. Proteins and cells generally attach randomly onto medical implant surfaces, which may ultimately lead to undesirable fibrous encapsulation, detrimental clinical complications, an increased risk of infection, and poor device performance. Consequently, controlled attachment may be achieved by generating so-called bioinert materials that first reduce any nonspecific physiological responses and then creating a biofunctional surface by reintroducing the attachment of only desired cells. This is achieved in a predictable fashion by using specific cell signaling molecules or adhesion ligands, often presented in precisely engineered geometries. Polymeric or oligomeric ethylene glycol (PEO, PEG, or o-EG) is often used as the bioinert background material for such approaches.[1, 2] Typically, self-assembled monolayers (SAMs), chemical grafting and polymerization methods have been employed to present these resistant materials onto a desired surface.[3, 4] However, potential problems with incomplete, nonuniform surface coverage, multiple synthetic steps and the restriction of SAMs to silicon or gold substrates greatly limit the use of these techniques to create bioinert coatings.

The ability to engineer surface properties such as hydrophobicity, charge, and adhesion at the micrometer scale are critical to the success of emerging technologies (e.g., bio-sensors, optical technologies and tissue engineering). SAMs have been extensively used to modify and control properties of gold and silicon surfaces.[5] Patterned

alkanethiol SAM surfaces have been created using microcontact printing[6] and UV photopatterning techniques,[7] however, the intricacy of surface patterns that can be created with established approaches are limited. Methods to control both the reactivity and surface properties after self-assembly are required to create more complex patterned surfaces. Existing techniques to control the reversibility and reactivity of the surfaces include sophisticated methods, such as, light and UV-induced, and electrochemical surface modifications.[8-10] These methods are not compatible when extended to biological systems involving cells and also tend to affect the morphology and properties of the surfaces underneath the SAMs. Thus, there is a need for a novel surface tuning procedure which is biocompatible and does not affect the biological systems on the surface.

In drug delivery applications, there is a need for the ability to deliver multiple biomolecules, e.g., proteins, genes, antibody, complement or drugs, to a targeted site of interest. Many delivery systems typically deliver one type of biomolecule at a time, e.g., one protein or one gene. For example, cellular processes such as opsinization, coating of a bacterium or cell with antibody and/or complement that leads to enhanced phagocytosis, require multiple complements to be present in order for phagocytosis to occur.

1.2 BACKGROUND

1.2.1 Need for New Biomaterials to Control Cell Adhesion

Advances in biotechnology often require new materials to help elucidate complex biological phenomena and to develop novel biomedical tools and devices. Since most biological processes are controlled at the molecular level, materials that can be

2

manipulated at the molecular level are ideally suited. Therefore, control of surface and interface properties are particularly important characteristics for bioactive or bioresponsive materials. The presence of micro- or nanostructures on a surface permits the manipulation of cell-substrate and cell-cell interactions to better control cellular function and behavior. Typically, proteins and cells randomly attach onto medical implant surfaces, which may ultimately lead to undesirable effects and poor device performance.[11, 12] Consequently, controlling the surface activity by first generating bioinert surfaces reduces any nonspecific physiological responses and then reintroducing the attachment of only desired cells in a predictable fashion by using specific cell signaling molecules or adhesion ligands[13] would eliminate undesired, random effects.

There is an increasing interest in developing new coatings to improve biocompatibility and to resist or enhance cellular adhesion by mimicking extracellular matrix components. The fabrication of ultrathin polymer films to improve surface characteristics is important to various scientific and biomedical applications. These surfaces are typically exposed to varying environments. The study of surfaces and materials for the purpose of growing cells is important in the field of tissue engineering. Protein adsorption and cellular adhesion are affected by different parameters, such as hydrophobicity and hydrophilicity, surface charge, roughness, and free energy. Chemical modification of biomaterial surfaces poses a major challenge in medical applications, such as implant and tissue engineering.

1.2.2 Polyelectrolyte Multilayers (PEMs)

PEMs have received much attention recently as a model system for biological applications such as biomaterials for engineering tissue constructs as well as potential

drug carriers. These multilayers can be easily constructed through layer-by-layer (LbL) assembly, in which a substrate is alternately dipped in solutions of polycations and polyanions. Such an approach offers unprecedented nanoscale control over the thin film architecture and properties, including film thickness, composition, conformation, degree of interchain ionic bonding, roughness, and wettability. The resulting films can conform to more easily coat substrate materials of any type, size, or shape (including implants with complex geometries and textures, e.g., stents and crimped blood vessel prostheses). Furthermore, a variety of materials, including synthetic polyions, biopolymers such as deoxyribonucleic acid (DNA) and enzymes, viruses, dendrimers, colloids, inorganic particles, and dyes, may be readily incorporated into the multilayers.

During the LbL assembly, functional third-party molecules can be embedded into the multilayers. The multilayer construct can be designed such that the incorporated functional molecules are either permanently embedded (e.g., for sensor or electrochromic application) or gradually released via diffusion through the films or by degradation of the film itself. Both scenarios can be used to develop novel drug delivery systems. A major advantage of LbL assemblies is that these multilayers can be deposited on surfaces of virtually any geometry, thus one can easily functionalize medical appliances, such as stents, sutures, and wound dressings. In addition, by a prudent selection of polyelectrolytes, the multilayers can degrade completely into safe biocompatible products, eliminating the need for surgical removal. Last but not least, drug delivery devices based on LbL assembly are simple and inexpensive to construct; this contrasts with microchip delivery devices, which, although capable of delivering multiple drugs with great temporal and dosage control,[14, 15] require tedious microfabrication.

1.2.3 Micropatterning and Cell Culture

Significant advances have been made in cell culture and microfabrication technologies. Integrating these two technologies has contributed to advances in cell and biological-based systems, such as diagnostics, biosensors, and prosthetics. The advantages of microfabrication and microfluidics technologies are their ability to produce miniature systems, multiple assays on one array, and multiple processes integrated on one chip.[15, 16] Advances in microfabrication and microfluidics have allowed for highly controlled cellular micropatterning, high density sample characterization using individually addressable array elements, and multiple experiments on one array. The cellular micropatterning techniques have been employed to understand fundamental cell biology such as cell-cell, cell-surface, and cell-medium interactions. [17, 18]

Recent progress in cell culture and microfabrication technologies have contributed to the development of cell-based biosensors for functional characterization and detection of drugs, pathogens, toxicants, odorants, and other chemicals. In the fields of toxicology and drug testing, *in vivo* studies have an advantage over *in vitro* studies in that it takes into account the entire biological system in determining the time-dependent response to a chemical challenge. However, it is often not easy to perform *in vivo* chemical toxicity studies with human subjects. Therefore, the development of a microscale cell culture analogue that can mimic an *in vivo* system is another promising area that capitalizes upon cell culture and microfabrication technologies.[19] In addition, cell-based systems have been used as prosthetics, especially neural protheses. Further, various macroscale techniques such as polymerase chain reaction (PCR), DNA and protein analysis, cell sorting, and cell culture have been miniaturized to the microscale

level using microfabrication techniques, and this miniaturization facilitates the integration with living cells.[20, 21] Here, we used microcontact printing to make PEM surfaces. The PEMs were used to construct patterns that ultimately would mimic tissues and organs that may be used to study *in vivo* mechanisms.

1.2.4 Aptamers and Short Interfering RNAs (siRNAs)

The development of drug delivery system with the ability to deliver multiple drug molecules could lead to important advances in treating a wide range of diseases and also to increase the efficacy of the drug molecules.[22] Typically delivery systems deliver only one type of biomolecule at a time, e.g., one protein or one gene. It is thus important to develop a method that can be used to incorporate a wide variety of molecules of different chemistry on virtually any surface including stents, sutures, and wound dressings. The delivery system should also have the ability to tune the dosage of drugs released in a time-dependent manner which would further be useful in understanding the mechanism involved in the behavior of these drug molecules. The PEM films are ideally suited for such drug delivery applications because it allows for absolute control over the order in which multiple functional molecules are incorporated into a growing film.[23] PEMs can be deposited rapidly and economically atop large area surfaces of any geometry while allowing nanometer-scale control over a range of physical properties.[24] Furthermore, the all-aqueous processing of PEM films allows for incorporation of sensitive biomolecules such as proteins and nucleic acids.[25-27]

Aptamers are ribonucleic acid (RNA) or DNA oligonucleotides that fold by intramolecular interaction into unique three-dimensional conformations capable of binding to target antigens with high affinity and specificity. Aptamers are

6

macromolecules composed of nucleic acid, such as RNA or DNA that bind tightly to a specific molecular target. Like all nucleic acids, a particular aptamer may be described by a linear sequence of nucleotides (A, U or T, C and G), typically 15-60 letters long, however, the chain of nucleotides forms intramolecular interactions that fold the molecule into a complex three-dimensional shape. The shape of the aptamer allows it to bind tightly against the surface of its target molecule. The term "aptamer" derives from the Latin aptus, "to fit", and was chosen to emphasize this lock-and-key relationship between aptamers and their binding partners. Aptamers may be obtained for a wide array of molecular targets, including most proteins and many small molecules. These novel molecules have many potential uses in medicine. Aptamers are generally produced through the SELEX Method (refer to appendix 1 for details). Considering the many favorable characteristics of aptamers (refer to appendix 1 for advantages of aptamers), including their small size, lack of immunogenicity, and ease of isolation, which together has resulted in their application in clinical trials.[28] Therefore, we propose to evaluate them as potential targeted drug delivery systems.

siRNAs has rapidly become a widely used tool for silencing gene function and validating potential therapeutic targets both in cell culture and *in vivo*. Protein production inside the cell involves a number of steps, beginning with the reading of the gene in the nucleus by a process called transcription. This process generates a messenger RNA (mRNA), which is then translated into protein in the cytoplasm. RNAi-based therapeutics specifically target and degrade mRNA using a naturally occurring cellular mechanism that regulates the expression of genes. With the recent progress in RNAi research, siRNA is poised to become a new generation of rationally designed drugs. Many diseases

7

develop from the undesired production of proteins. siRNA's technologies provide a way to halt this problem at the source. By utilizing the cellular mechanisms that already exist, drugs created with siRNA technology has the potential to halt or even cure diseases. Degrading mRNA, that is to be translated into a specific protein, results in a profound reduction in the level of that protein without directly altering the original genetic material (DNA). RNAi is a highly promising therapeutic approach for those diseases where aberrant protein production is a problem. Finally, RNAi can be applied to inhibit the expression or replication of pathogenic viruses, such as human immunodeficiency virus (HIV) and hepatitis C virus.[29, 30] However, the delivery of aptamers and siRNAs to targeted cells and tissues remains a challenge.

1.3 THESIS OUTLINE

This thesis focuses on engineering polyelectrolyte multilayer films to control cell adhesion and for drug delivery applications and is subdivided as follows: Chapter 2 describes the engineering of PEM films to control the adhesion of primary cells (primary hepatocytes and neurons) without the help of adhesive ligands/proteins and further formed patterns of these cells using microcontact printing. Chapter 3 discusses the engineering of patterned co-cultures of hepatocyte/fibroblast and neurons/astrocytes and the effect of the second cell type on the function and viability of the primary cells. Chapter 4 describes the development of novel SAM patterns of m-d-poly(ethylene glycol) (m-dPEG) acid molecules onto PEMs. The created m-dPEG acid monolayer patterns on PEMs acted as resistive templates, and thus prevented further deposits of consecutive poly(anion)/poly(cation) pairs of charged particles and resulted in the formation of three-dimensional (3-D) patterned PEM films or selective particle

depositions atop the original multilayer thin films. Chapter 5 discusses the salt tunable properties of these PEG patterns developed that can be removed from the PEM surface without affecting the PEM layers underneath the patterns. These removable surfaces provide an alternative method to form patterns of multiple particles, proteins and cells. Chapter 6 describes the use of multilayers to engineer aptamer and siRNA based drug delivery systems, and Chapter 7 concludes the thesis and suggests some future research directions.

CHAPTER 2 CONTROLLING PRIMARY CELL (HEPATOCYTES/NEURONS) ADHESION ON POLYELECTROLYTE MULTILAYER FILMS

2.1 INTRODUCTION

The ionic LbL assembly technique, introduced by Decher in 1991[23], forms films by electrostatic interactions between oppositely charged poly-ion species. The alternating layers of sequentially adsorbed poly-ions are called "Polyelectrolyte Multilayers (PEMs)". PEMs have become excellent candidates for biomaterial applications due to 1) their biocompatibility and bioinertness,[31-33] 2) the ability to incorporate biological molecules, such as proteins,[26, 34] and 3) the high degree of molecular control of the film structure and thickness providing a much simpler approach to construct complex 3D surfaces as compared with photolithography.[35] The biodegradability of PEMs have been demonstrated by Lynn and co-workers.[36] Thus far, the suitability of these films for biomedical applications have been illustrated predominantly with immortalized cell lines, such as fibroblast, osteoblast and endothelial cells.[31] Rubner and co-workers have recently developed PEM surfaces using weak polyelectrolyte system that were cytophobic and cytophilic to fibroblast attachment.[33]

Fibroblasts and astrocytes can attach to many surfaces due to its robustness and ability to secrete their own extra-cellular matrix proteins and thus provide a mechanism by which they can promote their own attachment to surfaces. On the other hand *primary hepatocytes and primary neurons*, unlike many other cell types, exhibit more selective behavior *in vitro*, preferentially attaching and spreading on tissue culture dishes or surfaces containing adhesive ligands such as collagen, poly(lysine) and fibronectin.[37]

Primary hepatocytes and primary neurons are anchorage dependent and must attach to maintain their differentiated function. A stationary suspension culture of isolated hepatocytes typically loses their differentiated function within hours. Primary hepatocytes maintain their viability in tissue culture for up to 2 weeks; nevertheless, they lose their differentiated function within a few days. To address this limitation, approaches such as overlaying the hepatocytes with a collagen gel or using cylindrical collagen gel entrapment have extended the differentiated functions *in vitro* for at least 5-6 weeks.[37, 38] Studies also show that random, dissociated primary neurons in culture develop physiological responses to neurotransmitters [39, 40] and self-organize into neuronal networks, [40-43] however, they lack the structure normally present within the nervous system, where the neurons reside in specific regions with numerous network connectivity. The advantage of patterned neurons is that it allowed for precise control of both the direction of neurite extension and degree of contact between the neurons, unlike the random neuron monoculture system, which is important for repair and regeneration of the nervous systems.[44] It has also been demonstrated by Wheeler and co-workers that patterned neurons synapse with each other, release neurotransmitters and develop electrical activity [45-47]. Furthermore, restricting neurons to patterns has been shown to enhance the cellular activity such as glutamine secretion and electrical activity as compared to the random monocultures of neurons.[48, 49]

In this chapter, we demonstrate controlling cell adhesion using PEM films by varying the surface chemistry and the surface topography. We report culturing primary hepatocytes and primary neurons on a protein free synthetic SPS surface; these cultured cells maintain a level of differentiated function similar to tissue culture polystyrene
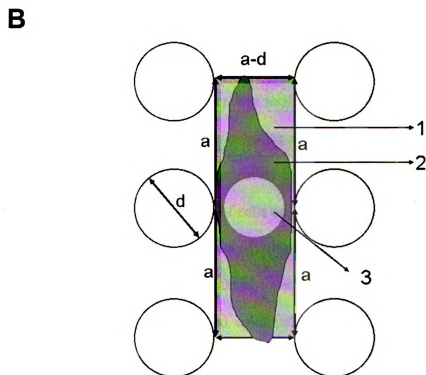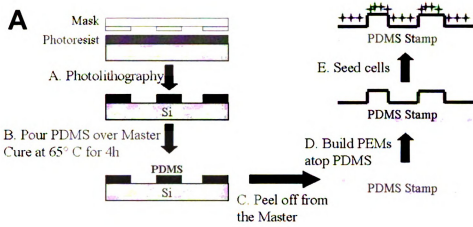
Figure 2.1. (A) Schematic diagram illustrates the method for treating the PDMS surfaces with PEMs and culturing cells on the surfaces with different topographies. PEMs (PDAC/SPS)$_{10}$ are built on top of the PDMS surface and cells are then seeded. (B) Illustration of the overlap of a cell and a flat area between the circle patterns. The diameter (d) changes while the center to center distance (a) remains constant for the features: a=18μm. Region 1 represents the area between any six adjacent patterns (features). Region 2 represents a cell attached between the patterns. Region 3 is the cell nucleus.

surface (TCPS). The advantage of PEM surfaces is its ability to construct three dimensional structures with controlled cell-cell and cell-surface interactions. On method to produce 3D structures is with the use of PDMS surfaces. Unfortunately, PDMS surfaces are known to be resistant to cell attachment. PDMS has been used extensively to study cell-substrate interactions, in medical implants and biomedical devices because of its biocompatibility,[50-53] low toxicity,[51, 54, 55] and high oxidative and thermal stability.[56, 57] Despite the many advantages of PDMS, its applications in microfluidics and medicine have been problematic because PDMS is highly hydrophobic. Even when the surface is made hydrophilic, PDMS gradually reverts to its hydrophobic state due to surface rearrangements. As a result, it is rather difficult to maintain long-term culture of cells on PDMS, due to the difficulty in irreversibly modifying PDMS surfaces to have a stable cell-adhesive layer.[58] Building a polyelectrolyte multilayer (PEM) film coating on top of the PDMS surface increases surface wettability and imparts lasting hydrophilicity thereby improving adhesion and proliferation of cells on PDMS surfaces.[23, 59, 60]Nevertheless, we noted that PEM-coated PDMS surfaces of different topographies affect the attachment, spreading and even proliferation of three types of mammalian cell, transformed 3T3 fibroblasts (3T3s), HeLa (transformed epithelial) cells and primary hepatocytes. The PEMs were built using LbL assembly of polyelectrolytes PDAC and SPS, as shown in the scheme in Figure 2.1 (A). The PDMS stamps consisted of circles with varying diameters with pitch distances of 18μm and pattern heights of 2.5μm as illustrated in Figure 2.1 B. Following cell seeding, we observed differences in the cell attachment and spreading depending on the groves and patterns on the PDMS surfaces. The cell morphology and attachment varied depending on the pattern geometries. Using imaging

techniques, we show that changes in the surface topographical features alter the attachment and spreading of cells, suggesting a physical means of controlling the interaction between the cell and its environment.

2.2 METHODS AND MATERIALS

2.2.1 Materials

Poly(diallyldimethylammoniumchloride) (PDAC) (Mw~100,000-200,000) as a 20 wt % solution, sulfonated poly(styrene), sodium salt (SPS) (Mw~70,000), linear polyethyleneimine (LPEI), branched polyethyleneimine (BPEI), poly(anetholesulfonic acid) (PAS), poly(vinylsulfonic acid) (PVS), fluorosilanes and sodium chloride were purchased from Aldrich (Milwaukee, WI). All polymers were used without further purification. Poly(dimethylsiloxane) (PDMS) from the Sylgard 184 silicone elastomer kit (Dow Corning, Midland, MI) was used to prepare stamps. The PDMS stamps were used for microcontact printing. [9]

Dulbecco's Modified Eagle Medium (DMEM) with 4.5 g/l glucose, 10X DMEM, fetal bovine serum (FBS), penicillin and streptomycin were purchased from Life Technologies (Gaithersburg, MD). Insulin and glucagon were purchased from Eli Lilly and Co. (Indianapolis, IN), epidermal growth factor from Sigma Chemical (St. Louis, MO). Type I collagen suspension (1.2 mg/ml in 1 mM HCl) was prepared from Lewis rat tail tendons as described by Dunn and co-workers.[61] Purified rat albumin was purchased from Cappel Laboratories (Aurora, OH). Urea assay was purchased from Sigma Chemical (St. Louis, MO).

2.2.2 Preparation of Polyelectrolyte Multilayers

PDAC and SPS polymer solutions were prepared with deionized (DI) water at concentrations of 0.02M and 0.01M respectively, (based on the repeating unit molecular weight) with the addition of 0.1M NaCl salt. Polyelectrolyte dipping solutions were prepared with DI water supplied by a Barnstead Nanopure-UV 4 stage purifier (Barnstead International Dubuque, Iowa), equipped with a UV source and final 0.2 μm filter. Solutions were filtered with a 0.45 μm Acrodisc syringe filter (Pall Corporation) to remove particulates. The tissue culture polystyrene (TCPS) surfaces were subjected to a Harrick plasma cleaner (Harrick Scientific Corporation, Broading Ossining, NY) for 10 min at 0.15 Torr and 50 sccm flow of O_2 in a plasma chamber. The layer-by-layer process was carried out in an automatic dipping machine (HMS programmable slide stainer from Zeiss Inc.). To form the first bilayer, the TCPS were immersed for 20 min in a polycation solution. Following two sets of 5 min rinses with agitation, the TCPS were subsequently placed in a poylanion solution and allowed to deposit for 20 min. Afterwards, the 6 well plates were rinsed twice for 5 min each. The samples were cleaned for 3 min in an ultrasonic cleaning bath after depositing a layer of polycation/polyanion pair. The sonication step removed weakly bounded polyelectrolytes on the substrate, forming uniform bilayers. This process was repeated to build multiple layers. All experiments were performed using ten (i.e., 20 layers) or ten and half bilayers (i.e., 21 layers).

2.2.3 Preparation of PDMS Stamps

An elastomeric stamp was made by curing PDMS on a microfabricated silicon master, which acts as a mold, to allow the surface topology of the stamp to form a negative replica of the master.[62] The PDMS stamps were made by pouring a 10:1 solution of

elastomer and initiator over a prepared silicon master.[63] The silicon master was pretreated

with fluorosilanes to facilitate the removal of the PDMS stamps from the silicon master.

The mixture was allowed to cure overnight at 60°C. The masters were prepared in the

BioMEMS facilities at MGH East and consisted of various features (squares and lines).

The polyelectrolytes were stamped onto the multilayer system using the polymer-on-

polymer stamping process developed by Hammond and co-workers.[35]

2.2.4 Animals and Hepatocyte Isolation

Primary rat hepatocytes were isolated from adult female Lewis rats (Charles River

Laboratories, Boston, MA) weighing 75-125 g, according to a two-step collagenase

perfusion technique described by Seglen[64] and modified by Dunn.[61] The liver isolations

yielded 150-300 x 10^6 hepatocytes. Using trypan blue exclusion the viability ranged from

90 to 98 %.

2.2.5 Hepatocyte Culture System

Hepatocytes were cultured on PEM coated 6-well tissue culture polystyrene surfaces

(TCPS). All the multilayer coated TCPS were sterilized by spraying with 70 % ethanol

and exposing them to UV light before culturing the cells onto these surfaces. The cell

culture experiments on the PEM surfaces were performed without coating the surfaces

with any adhesive proteins. Collagen coated TCPS and uncoated TCPS were used as

controls in these studies. The collagen gelling solution was prepared by mixing 9 parts of

the 1.2 mg/ml collagen suspension in 1 mM HCl with 1 part of concentrated (10X)

DMEM at 4°C. The control wells were coated with 0.5 ml of this collagen gelling

solution and the coated plates were incubated at 37°C for 1 hour. Freshly isolated

hepatocytes were seeded at a density of 4×10^5 cells per well for 7 days. The standard

hepatocyte culture medium consisted of DMEM supplemented with 10% FBS, 14 ng/ml

glucagon, 20 ng/ml epidermal growth factor, 7.5 μg/ml hydrocortisone, 200 μg/ml

streptomycin (10,000 μg/ml) – penicillin (10,000 U/ml) solution, and 0.5 U/ml insulin.

One ml of fresh medium was supplied daily to the cultures after removal of the

supernatant. Samples were kept in the incubator where the temperature and humidity

were properly controlled. A Leica inverted phase contrast microscope with Soft RT 3.5

software was used to capture images of cell density, morphology, and spreading on the

multilayer surfaces.

2.2.6 Primary Neuron Culture System

Primary cerebellar neurons were prepared from 8-day-old Sprague–Dawley rat pups

(Charles River, Sulzfeld, Germany) as described previously.[65] Cells were dissociated

from freshly dissected cerebella by mechanical disruption in the presence of trypsin and

DNase and then plated in poly l-lysine-precoated or PEM-coated six-well plates. Cells

were seeded at a density of 1×10^6 cells/cm^2 in DMEM supplemented with 10% fetal calf

serum, 2 mm glutamine, and 20 μg/mL gentamycin. Three days after incubation (37 °C,

5% CO_2), the medium was subsequently replaced with 2 ml of cerebellum medium

supplemented with 5 μM Arac to arrest the growth of non-neuronal cells. After 2 days,

the neuronal culture was switched back to cerebellum medium without Ara-C. The

experiments were performed on 6- to 7-day-old culture. Cultures generated by this

method have been shown to contain > 95% cerebellar granule neurons.[66] Astrocytes were

prepared from 7-day-old Sprague–Dawley rat pups as described previously.[67] The cells

were seeded in poly l-lysine-precoated or PEM-coated six-well plates (3×10^5/well) in

culture medium (90% DMEM, 10% FCS, 20 U/mL penicillin and 20 μg/mL streptomycin sulfate), and cultivated in an incubator (humidified, 10% CO_2). The cerebellum neurons were used in co-culture studies.

Primary cortical neurons were isolated from one-day-old Sprague–Dawley rat pups and cultured according to the published methods as described in Chandler et al.[68] The cells were plated on poly-d-lysine-coated (control) or PEM coated, six-well plates at a concentration of 2×10^6 cells per well in fresh cortical medium (DMEM supplemented with 10% horse serum, 25 mM glucose, 10 mM HEPES, 2 mM glutamine, 100 IU/ml penicillin, and 0.1 mg/ml streptomycine). Three days after incubation (37 °C, 5% CO_2), the medium was subsequently replaced with 2 ml of cortical medium supplemented with 5 μM Arac. After 2 days, the neuronal culture was switched back to cortical medium without Ara-C. The experiments were performed on 6- to 7-day-old culture. To obtain primary cultures of astroglial cells, the cortical cells from one-day-old Sprague–Dawley rat pups were cultured in DMEM/Ham's F12 medium (1:1), 10% fetal bovine serum (Biomeda, CA, USA), 100 IU/ml penicillin, and 0.1 mg/ml streptomycine. The cells were plated on poly-d-lysine or PEM coated, 6-well plates at a concentration of 2×10^6 cells per well. Cells were grown for 8–10 days (37 °C, 5% CO_2) and culture medium was changed every 2 days. Twenty-four hours prior to treatment with fatty acids, the medium was changed to neuronal cell culture medium. The cortical neurons were used in co-culture and ROS studies. Primary cortical neurons were used for the ROS studies as the oxidative stress-induced effects are higher in the affected regions (cortex and hippocampus) as compared to the unaffected areas (cerebellum).[69]

2.2.7 Biochemical Assays

The biochemical assays were performed on the collected medium supernatant. Albumin concentration was determined by an enzyme-linked immunosorbent assay described previously using a polyclonal antibody to rat albumin.[61] A standard curve was derived using chromatographically purified rat albumin dissolved in medium. Urea levels were measured with commercially available kits based upon its specific reaction with diacetyl monoxime.

2.2.8 Immunostaining of Primary Neurons

To perform confocal immunofluorescence microscopic study, neurons cultures were fixed for 20 min in 4% paraformaldehyde and permeabilized with 0.1% Triton X-100 and 5% goat serum (Invitrogen) in PBS. Cells were then labeled overnight at 4 °C with appropriate primary antibodies (1:50 neurofilament for neurons) in 5% goat serum in PBS. After three PBS washes, primary antibodies were detected with Fluorescein conjugated conjugated secondary antibodies for neurons. The cells were visualized with Leica fluorescent microscope.

2.3 RESULTS AND DISCUSSION

The aim of this study is to characterize the attachment, spreading and function of primary rat hepatocytes and primary neurons cultured on various PEM surfaces. In our study, we used synthetic polymers namely poly(diallyldimethylammoniumchloride) (PDAC) and SPS as the polycation and polyanion, respectively, to build the multilayers. We compared the attachment and spreading of primary hepatocytes and primary neurons on PEM films, with either PDAC or SPS as the top most surface, to TCPS surfaces

19

coated with adhesive proteins, as the control. The PEM surfaces used for the cell adhesion studies were not coated with collagen or other adhesive proteins.

2.3.1 Primary Hepatocyte Adhesion on PEMs

Figure 2.2 compares the morphology of primary hepatocytes on PEM surfaces with collagen coated TCPS obtained with phase contrast microscopy. Primary hepatocytes attached and spread on PEM films with SPS as the topmost surface. In contrast, the attached cells did not spread on PEM films with PDAC as the topmost surface and eventually lifted off the surface.

The difference in the projected cell area for primary hepatocytes on the different surfaces is shown in Table 2.1. The number of primary hepatocyes that attached on the SPS surfaces on Day 1 and 5 (204 and 189 cells/mm^2 respectively), was comparable to the number of hepatocytes that attached on the collagen coated TCPS control surfaces on Day 1 and Day 5 (210 and 185 cells/mm^2), see Table 2.1. In contrast, fewer cells attached and spread on PEM films with PDAC as the topmost surface on Day 1 and Day 5 (110 and 15 cells/mm^2, respectively). Primary hepatocytes attached and spread on SPS surfaces and the morphology of the cells were comparable to the control. On day 1, some cells (110 cells/mm^2) attached on the PDAC surface but did not spread. By day 5 most of the primary hepatocytes (15 cells/mm^2) lifted off the PDAC surfaces. We capitalized upon this cell adhesive/resistive property of SPS and PDAC, respectively, to make patterns of primary hepatocytes. SPS patterns were formed on PEM surfaces either by microcontact printing SPS onto PDAC surfaces or vice-versa using the polymer-on-
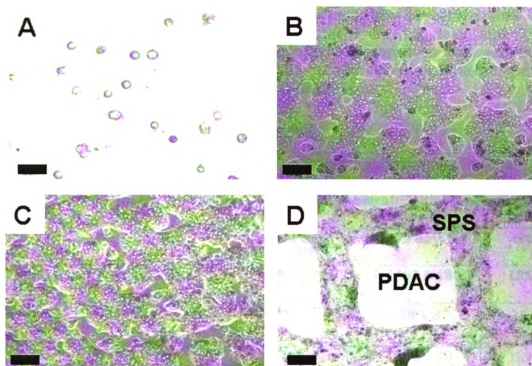
Figure 2.2. Optical micrographs of primary rat hepatocytes after 3 days for in culture on PEM surfaces. A) (PDAC/SPS)$_{10.5}$ B) (PDAC/SPS)$_{10}$ C) TCPS-Control D) PDAC patterns on SPS. The magnification is 10X. Scale bar = 50 μm

polymer stamping technique developed by Hammond and co-workers.[35] Primary hepatocytes adhered and spread only on SPS surfaces resulting in primary hepatocyte cell patterns (Figure 2.2 D) whereas fibroblasts readily attached to a variety of surfaces including both PDAC and SPS. This enabled the use of this system as a template for patterned co-culture of fibroblast and primary hepatocytes on synthetic PEM surfaces without adhesive proteins (Chapter 3). To investigate the long term effects of PEM films on cell viability and function, we assessed the morphology and maintenance of liver-specific functions over 7 days of continuous culture.

Table 2.1. Primary hepatocyte cell numbers on the projected area on the different surfaces used in the study after 1 day, 3 days and 5 days. Student's *t*-test was used for analyzing the differences between the cell adhesion on various surfaces ([a] $p<0.05$ compared with primary hepatocyte adhesion on collagen coated TCPS control)

Surfaces	Primary Hepatocytes (#cells/mm^2) (4x10^5/substrate initial concentration)		
	1 day	3 days	5 days
Collagen coated TCPS control	210 ± 21	193 ± 18	185 ± 17
PDAC	110 ± 19[a]	38 ± 8[a]	15 ± 2[a]
SPS	204 ± 16	192 ± 20	189 ± 21
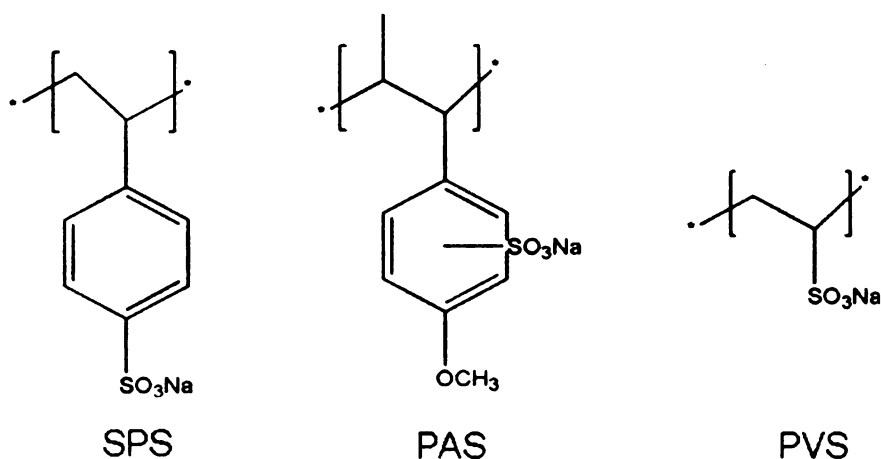
Figure 2.3. Structure formulae of the sulfonic acid polymers

One of the major challenges in studying the mechanism of cell-substrate interaction on synthetic surfaces is discerning the relative role of the chemical functional groups on this interaction. Therefore, we evaluated several synthetic sulfonic acid polymers with distinct chemical structures and molecular mass for this purpose. Figure

2.3 shows the chemical structure of three different sulfonic acid polymers, namely SPS, poly(antholesulfonic acid) (PAS), and poly(vinylsulfonic acid) (PVS), used to build PEM films for the primary hepatocytes studies. The PAS polymer has a similar structure to SPS but contains a hydrophobic ether group in the benzene ring while the PVS polymer has no benzene ring. These polymers were chosen to determine the functional group responsible for the observed cellular behavior on the PEM surfaces. Primary hepatocytes attached and spread on PEM films with all three sulfonic acid polymers as the topmost surface. The similarity in the results suggests that the sulfonate group was likely responsible for the primary hepatocyte attachment and spreading on the PEM surface. The morphology observed on SPS and other sulfonate surfaces were consistent with cells demonstrating affinity towards the surface. Similar behavior was not observed when hepatocytes were cultured on PDAC surfaces.
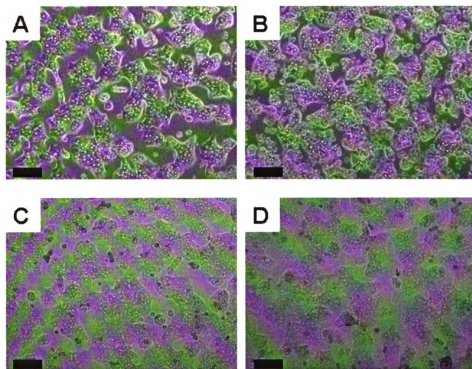
Figure 2.4. Optical micrographs of primary rat hepatocytes after 3 days in culture on PEM surfaces. A) (LPEI/SPS)$_{10.5}$ B) (SPS/LPEI)$_{10}$ C) (BPEI/SPS)$_{10.5}$ D) (SPS/BPEI)$_{10.5}$. Scale bar = 100 μm

Next, experiments were performed to determine whether the observed preferential adhesion to SPS was due to charge effect. Figure 2.4 compares the morphology of primary hepatocytes on two positively charged surfaces: $(LPEI/SPS)_{10.5}$ and $(BPEI/SPS)_{10.5}$. Primary hepatocytes were grown on positive $(LPEI/SPS)_{10.5}$ and $(BPEI/SPS)_{10.5}$ surfaces to observe the importance of charge effects on cell adhesion and spreading. Unlike the PDAC surfaces, primary hepatocytes attached and spread on positively charged LPEI and BPEI surfaces with similar morphology to that seen on the SPS surfaces, suggesting that charge effect was not likely the mechanism for cell adhesion. The functional group likely involved in enhancing cell adhesion on the LPEI and BPEI surfaces are the *primary* and *secondary* amine groups. PDAC was shown to be cell resisting for smooth muscle cells and neuronal cells by McShane and co-workers[70] and we also observe similar adhesion effect on primary hepatocytes. PEI has also been used instead of polylysine as a surface which supports attachment and growth of primary neurons.[71]

The long term metabolic response of continuous hepatocyte culture on PEM films was compared with collagen coated surfaces as shown in Figure 2.5. Figure 2.5 (A and B) illustrate the rate of albumin and urea production, respectively, for cultures up to one week. The daily production of both albumin and urea on PEM surfaces were comparable to cells cultured on collagen coated tissue culture dish. By day 7, the liver specific functions approach zero for PEM films with PDAC as the top most surface. This is likely due to the fact that the cells were unable to maintain attachment to the PDAC surfaces

24

A
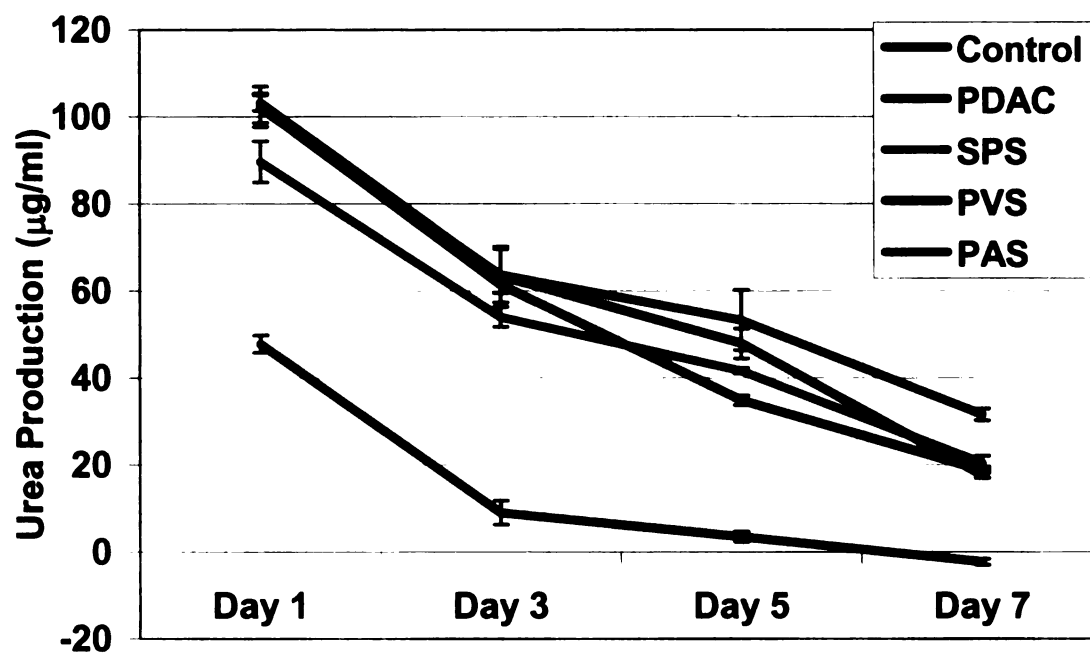
B
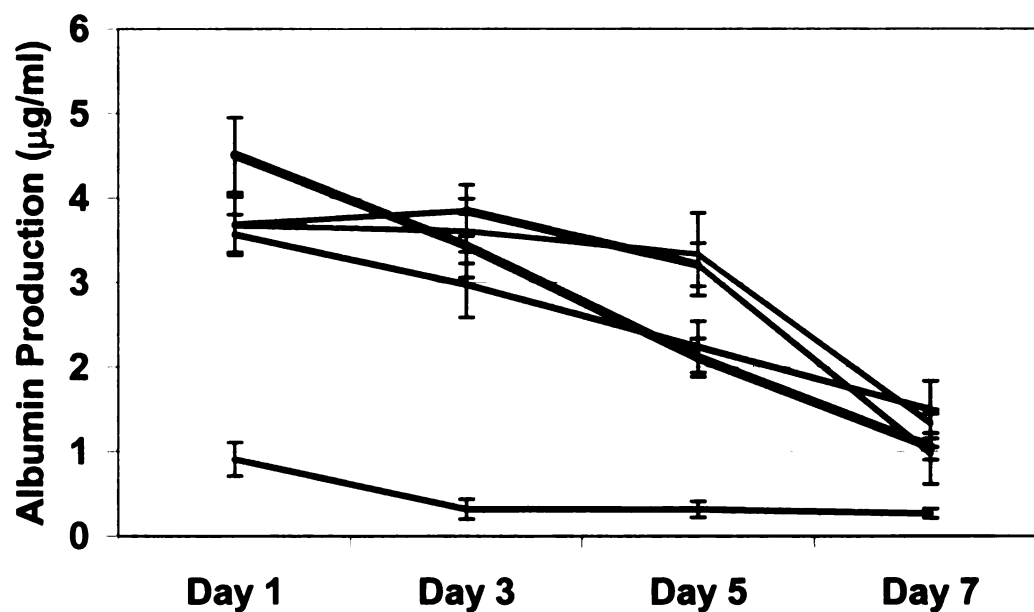
Figure 2.5. Metabolic function of primary hepatocytes on PEM surfaces. A) Total urea production per day. B) Total albumin secretion per day (n=6).

25

and had completely lifted from the surface by day 7. In contrast, PEM films with the sulfonated groups as the topmost surface had comparable urea and albumin production to the collagen coated TCPS surface. The urea and albumin secreted by the primary hepatocytes on the PDAC surfaces decreased to zero by day 7 indicating that the primary hepatocytes do not attach on the PDAC surfaces. The urea secreted by the primary hepatocytes on the SPS surfaces decreased from day 1 (112.24 ± 2.81 µg /1x10^6 cells/day) to day 7 (22.55 ± 1.30 µg /1x10^6 cells/day) suggesting that the cells were de-differentiating.

2.3.2 Primary Neuron Adhesion on PEMs

Figure 2.6 and Table 2.2 compare the adhesion of primary neurons and astrocytes on PEM surfaces to PLL coated TCPS control. The difference in the projected cell area for primary neurons and astrocytes on the different surfaces is shown in Table 2.2. The number of primary neurons that attached on the SPS surfaces on Day 7 (234 cells/mm^2) was comparable to the number of neurons that attached on the PLL coated TCPS control surfaces on Day 7 (250 cells/mm^2), see Figure 2.6 and Table 2.2. In contrast, fewer cells attached and spread on PEM films with PDAC as the topmost surface. By day 7 most of the primary neurons (10 cells/mm^2) lifted off the PDAC surfaces. Primary neurons attached and spread on SPS surfaces and the morphology of the cells were comparable to the control, see Figure 2.5 (B, C). Astrocytes attached to both PDAC and SPS surfaces as shown in Figure 2.5 (D-F). The number of astrocytes attached to both PDAC (178 cells/mm^2) and SPS surfaces (183 cells/mm^2) were comparable to the control surfaces (192 cells/mm^2), see Figure 2.5 (D-F) and Table 2.2.

Table 2.2. Primary neurons and astrocytes cell numbers on the projected area on the different surfaces used in the study after 7 days in culture. Student's *t*-test was used for analyzing the differences between the cell number on the various surfaces ([a] p<0.05 compared with cell adhesion on poly(lysine) (PLL) coated TCPS control)

Surfaces	Primary Neurons (# of cells /mm^2) (4×10^5/substrate initial conc)	Astrocytes (# of cells /mm^2) (4×10^5/substrate initial conc)
PLL coated TCPS	250 ± 19	192 ± 19
PDAC	10 ± 2 [a]	178 ± 20
SPS	234 ± 18	183 ± 17
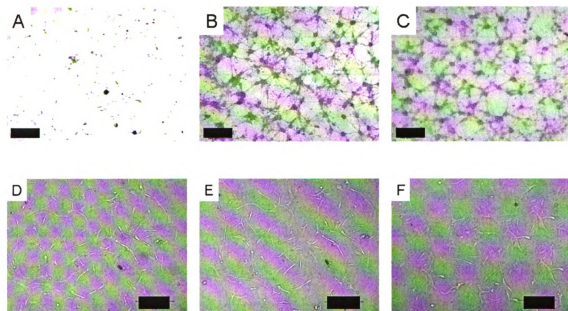
Figure 2.6. Phase contrast images of primary neurons and astrocytes after 7 days in culture on PEM surfaces. Primary neurons on (A) (PDAC/SPS)$_{10.5}$ - PDAC topmost surface (B) (PDAC/SPS)$_{10}$ - SPS topmost surface (C) poly(lysine) (PLL)-control surfaces. Astrocytes on (D) (PDAC/SPS)$_{10.5}$ - PDAC topmost surface (E) (PDAC/SPS)$_{10}$ - SPS topmost surface (F) poly(lysine)-control surfaces. (Scale bars- 250μm).

2.3.3 Fabrication of PEM Coated PDMS Substrate

Table 2.3. Dimensions of the different surface topographies used in the study

Surface	Diameter (d), μm	Pitch-Center to Center (a), μm	(a-d), μm	Area between 6 adjacent features (μm^2)
P1	1.25	18	16.75	603 ± 10
P2	2	18	16	576 ± 11
P3	3	18	15	540 ± 8
P4	4	18	14	504 ± 10
P5	5	18	13	468 ± 6
P6	6	18	12	432 ± 9
P7	7	18	11	396 ± 9
P8	8	18	10	360 ± 11
P9	9	18	9	324 ± 10

To evaluate the effect of substrate physical properties (i.e., periodic microstructures) on cell attachment and morphology, we compared the response of several cell types (fibroblasts and primary hepatocytes) cultured on various polydimethylsiloxane (PDMS) patterns. The dimensions and the topography of the patterns on the PDMS surfaces are shown in Figure 2.1B, Figure 2.7 and Table 2.3. The circle patterns have a pitch distance (center to center) of 18μm while the diameter of the circle patterns ranges from 1.25μm to 9μm. The height of the patterns was 2.5μm. The PDMS patterns were coated with PEMs (PDAC/SPS)$_{10}$ with SPS as the topmost surface, thus keeping the surface chemistry the same while changing the surface topography. In

28

the previous section, we observed the variation in cell adhesion depended on the surface chemistry. In contrast, here we studied the effect of surface topography on cell attachment while maintaining the same surface chemistry.
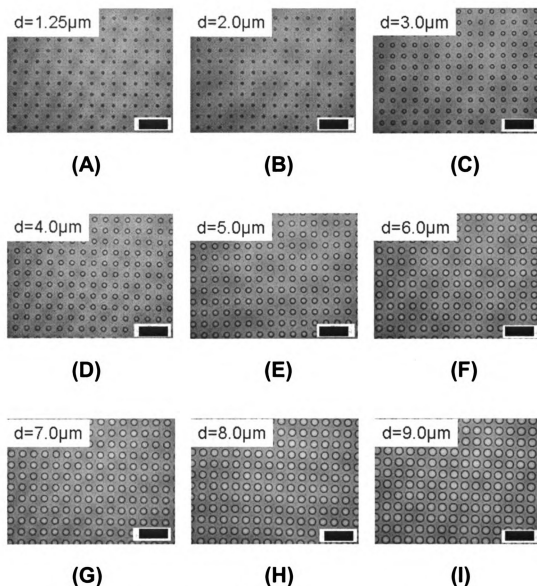
Figure 2.7. Phase contrast microscope images of circle patterns on PDMS surfaces of varying diameter (A) P1, diameter = 1.25μm, (B) P2, diameter = 2.0μm, (C) P3, diameter = 3.0μm, (D) P4, diameter = 4.0μm, (E) P5, diameter = 5.0μm, (F) P6, diameter = 6.0μm, (G) P7, diameter = 7.0μm, (H) P8, diameter = 8.0μm, (I) P9, diameter = 9.0μm. All the patterns have constant pitch distance (center to center) of 18μm and height of 2.5μm (Scale bar, 50 μm).

2.3.4 Primary Hepatocyte Adhesion on PEM Coated PDMS Surfaces
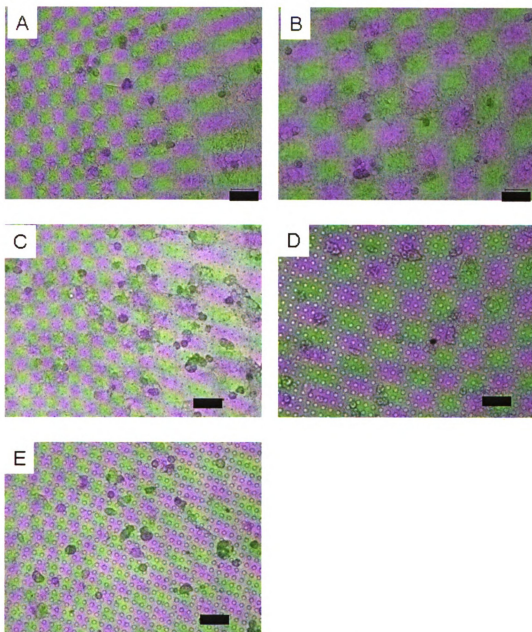
Figure 2.8. Optical micrographs of primary rat hepatocytes after 3 days in culture on various surfaces: (A) TCPS (B) PEM coated smooth PDMS surfaces (C) P1, (D) P5 (E) P9 (Scale bar, 50 μm).

Table 2.4. Cell numbers on the projected area on the different surfaces used in the study after 8h, 24h and 3 days. Student's t-test was used for analyzing the differences between the cell adhesion on various surfaces ([a-c] $p<0.05$ compared with primary hepatocyte adhesion on TCPS, [d-f] $p<0.05$ compared with fibroblast adhesion on TCPS)

Surfaces	Primary Hepatocytes (#cells/mm^2) (5×10^5, initial concentration)			Fibroblast (# of cells/mm^2) (5×10^4, initial concentration)		
	8h	24h	3 days	8h	24h	3 days
TCPS	250 ± 27	230 ± 25	210 ± 22	72 ± 2	292 ± 11	928 ± 25
PDMS	98 ± 11^a	7 ± 1^b	5 ± 1^c	16 ± 2^d	15 ± 2^e	7 ± 1^f
PEM coated PDMS	245 ± 23	210 ± 18	200 ± 19	69 ± 3	288 ± 13	893 ± 18
P1	211 ± 19	187 ± 21	176 ± 20	66 ± 1	255 ± 14	877 ± 21
P2	201 ± 18	170 ± 15	164 ± 18	62 ± 2	252 ± 12	865 ± 15
P3	191 ± 20	161 ± 14	155 ± 7	57 ± 1	242 ± 15	841 ± 19
P4	182 ± 14	75 ± 3^b	67 ± 6^c	48 ± 4^d	128 ± 11^e	357 ± 15^f
P5	189 ± 11	65 ± 2^b	56 ± 6^c	35 ± 3^d	113 ± 13^e	125 ± 14^f
P6	139 ± 17^a	59 ± 4^b	48 ± 9^c	27 ± 1^d	117 ± 18^e	79 ± 19^f
P7	142 ± 19^a	45 ± 2^b	34 ± 7^c	19 ± 2^d	69 ± 12^e	65 ± 13^f
P8	110 ± 15^a	26 ± 1^b	19 ± 4^c	15 ± 2^d	40 ± 9^e	56 ± 10^f
P9	115 ± 16^a	28 ± 2^b	17 ± 1^c	16 ± 2^d	25 ± 8^e	19 ± 9^f

31

The primary hepatocytes displayed different attachment preferences and morphologies depending on the pattern size and topography as shown in Figure 2.8. The difference in the projected cell area for primary hepatocytes on the different topographies is shown in Table 2.4. There was a general trend of decreasing cell number with increasing diameter of the circular patterns and decreasing a-d distance. The number of primary hepatocyes that attached on the P1 (211 – 176 cells/mm^2), P2 (201 – 164 cells/mm^2), and P3 (191 – 155 cells/mm^2) surfaces was comparable to the TCPS control (250 – 210 cells/mm^2) and the PEM coated PDMS surfaces (245 – 200 cells/mm^2), see Figure 2.8 and Table 2.4. Cells on the P4-P9 surfaces showed more limited cell attachment, similar to the uncoated PDMS surfaces (98 – 5 cells/mm^2), see Table 2.4. The cells on the (P4-P9) patterns did not spread and started to lift off over time resulting in a lower density of cells. From our previous studies we showed that primary hepatocytes attached and spread onto SPS surfaces without the need of adhesive proteins.[72] Hence the observed behavior in this study is independent of the surface chemistry of the substrate and is due to the effect of topography and thus provides an alternative approach to modulating the attachment of primary hepatocytes.

2.3.5 Fibroblast Adhesion on PEM Coated PDMS Surfaces

The observations were similar when these micro-patterned PDMS surface topographies were cultured with fibroblasts. The cells display varying attachment preferences and morphologies depending on the pattern size and topography as shown in Figure 2.9. Fibroblasts showed varying cell adhesion depending on the diameter of the circle patterns and the a-d distance. On smooth PEM coated PDMS surfaces the morphologies and attachment patterns of the cells were similar to those on TCPS
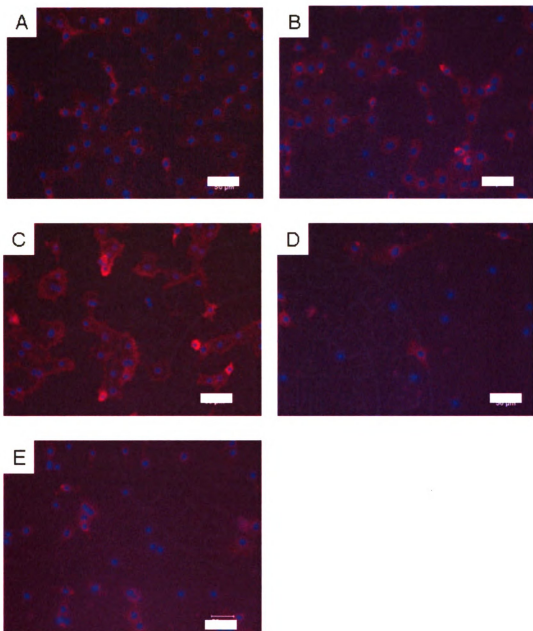
Figure 2.9. Fluorescence micrographs of focal adhesion and actin cytoskeleton in fibroblasts revealed with triple labeling using TRITC-conjugated Phalloidin (staining F-actin), anti-Vinculin (focal contacts) and DAPI (nuclei) after 3 days in culture on various surfaces: (A) TCPS (B) PEM coated smooth PDMS surfaces (C) P1, (D) P5 (E) P9 (Scale bar, 50 μm).

surfaces. On patterned PDMS surfaces, the cell attachment varied as the diameter of the circular patterns and the a-d distance changed. The cells attached preferentially on the smaller diameter patterns (P1, P2, P3), which had a correspondingly higher a-d distance, as compared to the patterns with the larger diameters and smaller a-d distance. On the P4-P9 surfaces where
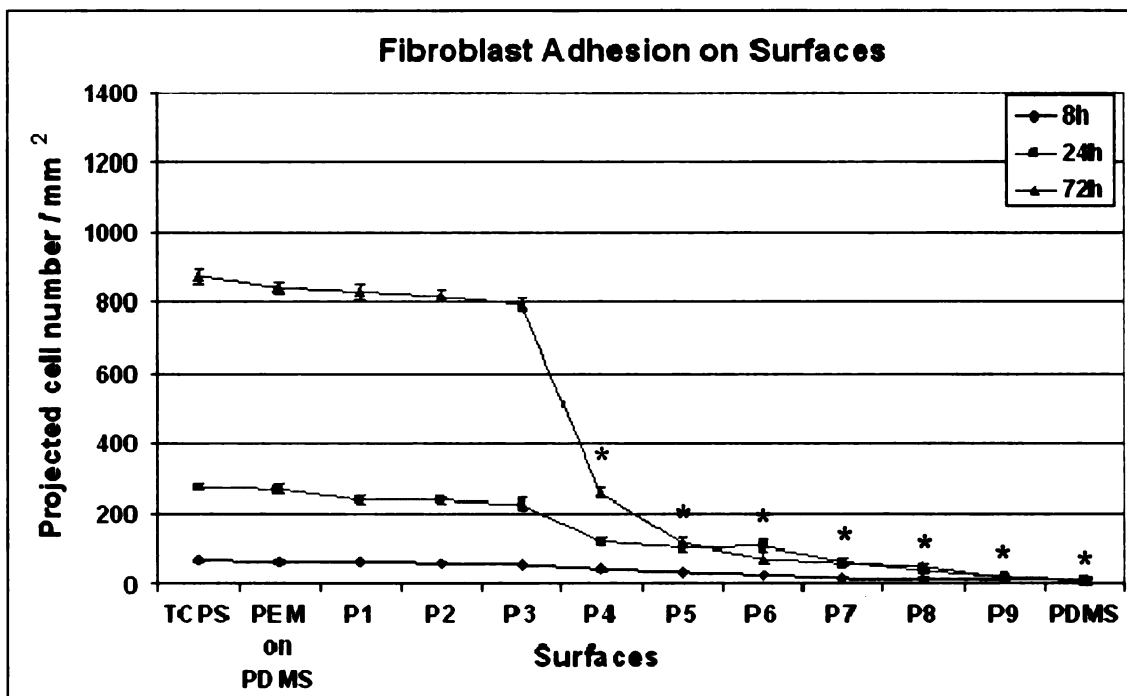
Figure 2.10. Proliferation of fibroblasts on various surfaces at 8h, 24h and 72h after cell seeding. Data represents mean ± S.E. of three independent experiments (* $p<0.05$ compared with control TCPS surfaces).

the cells detached, the cells appeared more rounded. The number of fibroblast cells that attached on the P1 (66 – 877 cells/mm^2), P2 (62 – 865 cells/mm^2), and P3 (57 – 841 cells/mm^2) surfaces was comparable to the TCPS control (72 – 928 cells/mm^2) and the PEM coated PDMS surfaces (69 – 893 cells/mm^2), see Figure 2.9 and Table 2.4. Hence, these PDMS topographies can be used to culture 3T3 fibroblasts, whereas PDMS surfaces P4-P9 were cytophobic to the fibroblast. Very few cells attached onto the uncoated PDMS surfaces (16 – 7 cells/mm^2), see Figure 2.10 and Table 2.4.

Fibroblast cells are present in almost all tissue types and organs and they play a central role in the support and repair of tissues and organs. When a tissue is injured or a device is implanted, the nearby fibroblasts proliferate and migrate into the affected area, and produce a large amount of collagenous matrix, which helps to isolate and repair the affected tissue.[73] On the other hand, overgrowth and overspreading of fibroblasts can cause diseases such as liver cirrhosis and non-functional scar tissues.[74, 75] Thus surfaces that can modulate fibroblast growth and spreading can be useful in preventing conditions, such as scar tissue formation associated with implanted medical devices or engineered tissue constructs.

2.3.6 Potential Explanation of the Observed Effect of Topography on Cell Attachment

Previous studies have shown a similar effect of topography as seen on the PDMS surface topographies, namely, the spacing and diameter of the features was critical to the attachment and spreading of the cells.[76] As seen from the data, the smaller diameter (1.25-3μm) P1-P3 surfaces appeared to have higher cell proliferation rate when compared to the larger diameter (4-9μm) P4-P9 surfaces. A possible explanation for the varying attachment and proliferation of the cells on the different topographies (P1-P9 surfaces) may be attributed to the difference in the area between the features. Figure 2.1B is a schematic illustrating the overlap of a cell and a flat area between the circle patterns (features). Using the Soft RT 3.5 software on the phase contrast images of the cells we determined the average area occupied by primary hepatocytes or mouse 3T3 cell (see Table 2.3). We observed that the area between the six adjacent circle patterns (features) decreased from 603 ± 10 μm² for the P1 surface to 324 ± 10 μm² for the P9 surface. The

35

average area occupied by a HeLa or mouse 3T3 cell was measured to be 521 ± 15 μm^2 (Region 2 in Figure 2.1B).

The fibroblast cells proliferated on the P1-P3 surfaces where the surface area between any six adjacent features (Region 1 in Figure 2.1B) ranged from 603 ± 10 μm^2 for the P1 surface to 540 ± 8 μm^2 for the P3 surface. The P4 surface, on the other hand, has a surface area of 504 ± 10 μm^2 which is on par with the size of an average cell. Even though the cells proliferated on the P4 surfaces, they proliferated significantly slower than on the control TCPS surfaces likely due to fewer cells being able to attach initially. The cells did not proliferate extensively on the P5-P9 surfaces where the surface area ranged from 468 ± 6 μm^2 for the P5 surface to 324 ± 10 μm^2 for the P9 surface, which are less than the average size of a cell. The cells proliferated on surfaces where the surface area between the features were larger than the size of an average cell (P1-P3), while the proliferation was slower on surfaces where the area between the features was on par with the size of the cells (P4) and did not proliferate extensively on surfaces where the area between the features was smaller than the average size of a cell (P5-P9). The results suggest the quantity of surface area between the features may affect the ability of the cells to attach, as well as the proliferation rate of the cells on the various topographies. Therefore, controlling the surface topography provides an alternative approach for modulating the cell attachment and proliferation for tissue engineering applications.

PDMS is a useful material for cell biology studies because it can be easily manipulated into different sizes, shapes, and dimensions with soft-lithographic techniques. We found that differences in physical environment, e.g. the surface micro-topography on the PDMS surfaces, influenced the attachment and growth of the cells.

Therefore, depending on the application requirements, the surface topography may be used as an alternative approach to chemical properties for controlling the attachment and growth of cells. These PDMS surfaces with varying topographies may be used, for example, to modulate fibroblast growth and spreading, which can be desirable in preventing conditions associated with fibroblast overproduction and overspreading. Overall, there are many advantages to fabricating devices made of PDMS, e.g., their low cost and ease of fabrication, and their biocompatability and permeability to gas. Finally, as demonstrated in this study, PDMS when appropriately modified can be a suitable substrate for culturing and controlling the adhesion of various types of mammalian cells.

2.4 CONCLUSIONS

In conclusion, the present work outlines a method for controlling cell-surface interactions by varying the surface chemistry and surface topography with the help of PEMs. PEMs were used to produce defined cell-resistant and cell-adhesive properties depending on the topmost surface and the type of cells used. We have shown using both biochemical studies and direct microscopy imaging of live cells that primary hepatocytes and neurons attach, spread and function on PEM films without the aid of adhesive proteins. These results demonstrate the feasibility of attaching primary hepatocytes and neurons directly on PEMs. We also demonstrated that patterns of primary hepatocytes and primary neurons can be formed using this layer-by-layer deposition of ionic polymers, which can be used as a template for patterned cell co-cultures. Further, PEM films permit precise control of the three dimensional topography at micro and nanometer scales. We demonstrated that the hydrophobic and cell resistant PDMS surfaces can be made to be cell adhesive surfaces by coating with PEM films. We also demonstrated that

the addition of topographical features on the PEM coated surfaces provided an alternative approach to chemistry for controlling the attachment of primary cells (hepatocyes) and the attachment and growth of transformed cells (3T3 fibroblasts and HeLa cells).Taken together, this technique may be a useful tool for fabricating controlled co-cultures with specified cell-cell and cell-surface interactions, thus providing flexibility in designing cell-specific surfaces for tissue engineering applications.

CHAPTER 3 PATTERNED CO-CULTURE OF PRIMARY HEPATOCYTES/FIBROBLASTS AND PRIMARY NEURONS/ASTROCYTES USING PEM FILMS

3.1 INTRODUCTION

Tissue formation and function *in vivo* are influenced by many factors, including cytokines, cell-matrix interactions, topology, mechanical forces, and cell-cell interactions. An important aspect in tissue formation and function is the interaction between the multiple types of cells within the tissue.[77] Cell-cell interactions are central to the function of many tissues, e.g., blood vessels form when endothelial cells are allowed to interact with smooth muscle cells[78] and nervous system function depends upon proper interactions between neuronal and glia cells.[79] Cell-cell communication between primary neurons and astrocytes is crucial for the development and repair of neuronal systems.[80] Astrocytes are glial cells that are in close proximity to the neurons and play multiple roles in the functioning of the brain. They can sense neuronal activity through neurotransmitter receptors[81] and provide direct neurotrophic factors to support the neurons.[82] Previous studies have shown that astrocytes mediate both positive and negative responses in neuronal cells. Primary neurons co-cultured randomly with astrocytes showed reduced toxicity to ammonia[83] but an increased sensitivity to the toxicity of glutamate[84] as compared to pure neuronal cultures.

Primary hepatocytes are anchorage-dependent liver cells and, therefore, require a substratum to survive and function. Primary hepatocytes, unlike many other cell types, exhibit more selective behavior *in vitro*, preferentially attaching and spreading on tissue culture dishes or surfaces containing collagen. The cells, however, eventually de-

39

differentiate and lose their hepato-specific function. To engineer liver tissues that maintain hepatic functions *in vitro* require co-cultivation of primary hepatocytes with a variety of nonparenchymal cells such as fibroblasts,[85] epithelial cells,[86] stellate cells[87] and liver epithelial cells.[88-90] The ability to mimic such interactions *in vitro* is important in cell biology studies as well as tissue engineering applications. Mimicking *in vitro* this complexity and function is difficult using traditional co-culture techniques, wherein multiple cell types are seeded randomly. Therefore, regenerating or replacing damaged tissue using *in vitro* strategies has primarily focused on manipulating the cellular environment by modulating the cell-extracellular matrix (ECM) and cell-cell interactions.[91] A challenge in engineering *in vitro* liver and brain tissue is identifying a set of minimal environmental signals required to maintain function for extended periods.[92] A limitation of traditional co-culture systems is their inability to control cell placement and manipulate cell-surface and cell-cell interactions.

Different approaches have been used to create spatially defined co-cultures of two different cell types.[91, 93] However, these techniques have certain limitations. They 1) typically require adhesive proteins for cell attachment,[91] 2) are limited to specific parallel geometries defined by laminar flow patterns,[93] and 3) have been used predominantly with cell lines rather than primary cells due to the difficulties involved in attaching primary cells onto synthetic surfaces.[61, 77, 94, 95] PEMs have been shown to be excellent candidates for biomaterial applications[26, 33] and provide flexibility in building complex three-dimensional architectures.[96] The PEM surfaces also provide an ability to control the arrangement of multiple cell types with subcellular resolution.[94, 97] We previously reported that primary hepatocytes attached and spread on PEM films.[72] This chapter

describes the engineering of patterned co-cultures of primary hepatocytes/fibroblast and primary neurons/astrocytes on polyelectrolyte multilayer (PEM) films without the aid of adhesive proteins/ligands.
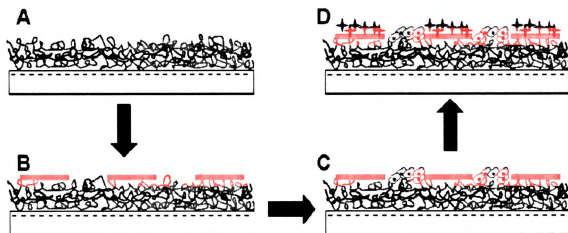
Figure 3.1. Schematic diagram illustrates the approach to patterning co-culture of primary cells on PEM surfaces. First, (PDAC/SPS)$_{10}$ PEMs were built on top of the TCPS surfaces with SPS as the topmost surface. Second, patterns of PDAC were formed on PEM surfaces by microcontact printing (μCP) PDAC onto the PEM surfaces. Third, patterns of primary hepatocytes/neurons were formed by capitalizing on the preferential attachment of primary cells to SPS surfaces. Fourth, since fibroblast/astrocytes, unlike the primary cells, attached to both surfaces, astrocytes were subsequently seeded onto the patterns of primary cells and attached onto the open PDAC regions and resulted in patterned co-cultures of primary hepatocytes/fibroblast or primary neurons/astrocytes.

We demonstrated that patterns of primary hepatocytes/neurons and patterned cell co-cultures can be formed without the aid of adhesive proteins using the layer-by-layer deposition of synthetic ionic polymers. Primary hepatocytes and primary neurons attached and spread preferentially on SPS surfaces over PDAC surfaces. We capitalized upon this differential cell attachment and spreading of primary hepatocytes and neurons on PDAC and SPS surfaces to make patterned co-cultures of primary hepatocytes/fibroblasts and primary neurons/astrocytes on the PEM surfaces. PDAC (or SPS) was patterned on the (PDAC/SPS)$_{10}$ surfaces by using a polymer-on-polymer stamping (POPS) process developed by Hammond and co-workers.[35, 98] Primary

41

hepatocytes/primary neurons were then seeded and attached preferentially attached onto the SPS surfaces. We then seeded the second cell type (fibroblasts or astrocytes) on the PDAC surface, resulting in patterned co-culture (Figure 3.1). We evaluated the cell morphology and function with an inverted microscope and biochemical assays, respectively.

3.2 METHODS AND MATERIALS

3.2.1 Materials

Poly(diallyldimethylammonium chloride) (PDAC) ($Mw\sim100,000-200,000$) as a 20 wt % solution, sulfonated poly(styrene), sodium salt (SPS) ($Mw\sim70,000$), fluorosilanes and sodium chloride were purchased from Aldrich (Milwaukee, WI). Poly(dimethylsiloxane) (PDMS) from the Sylgard 184 silicone elastomer kit (Dow Corning, Midland, MI) was used to prepare stamps. The PDMS stamps were used for microcontact printing.[9] Dulbecco's Modified Eagle Medium (DMEM) with 4.5 g/l glucose, 10X DMEM, fetal bovine serum (FBS), penicillin and streptomycin were purchased from Life Technologies (Gaithersburg, MD). Insulin and glucagon were purchased from Eli Lilly and Co. (Indianapolis, IN), epidermal growth factor from Sigma Chemical (St. Louis, MO). Purified rat albumin was purchased from Cappel Laboratories (Aurora, OH). Urea assay was purchased from Sigma Chemical (St. Louis, MO). Carboxylated polystyrene latex particles (4 μm diameter) purchased from Polysciences, were used for colloidal adsorption study on patterned polyelectrolyte multilayer films. Chloromethylbenzoylaminotetramethyl rhodamine (CMTMR) and chloromethylfluorescein diacetate (CMFDA) were purchased from Molecular Probes for

double immunofluorescent staining. Adult female Sprague-Dawley rats were obtained from Charles River Laboratories (Boston, MA).

3.2.2 Preparation of Polyelectrolyte Multilayers

The PEMs were prepared as described in Chapter 2. Briefly, PDAC and SPS polymer solutions were prepared with deionized (DI) water at concentrations of 0.02M and 0.01M, respectively, (based on the repeating unit molecular weight) with the addition of 0.1M NaCl salt. TCPS plates were subjected to a Harrick plasma cleaner (Harrick Scientific Corporation, Broading Ossining, NY) for 10 min at 0.15 torr and 50 sccm flow of O_2 in a plasma chamber. A Carl Zeiss slide stainer equipped with a custom-designed ultrasonic bath was connected to a computer to perform layer-by-layer assembly. TCPS plates were immersed for 20 min in a polycation solution, followed by two sets of 5 min rinses with agitation. TCPS plates were subsequently placed in a polyanion solution and allowed to deposit for 20 min, followed by two sets of 5 min rinses with agitation. The samples were cleaned for 3 min in an ultrasonic cleaning bath after depositing a layer of polycation/polyanion pair. The sonication step removed weakly bounded polyelectrolytes on the substrate, forming uniform bilayers. This process was repeated to build multiple layers. All experiments were performed using ten (i.e., 20 layers) or ten and half bilayers (i.e., 21 layers).

3.2.3 Primary Hepatocyte/Fibroblast Co-Culture on PEM Surfaces

Six-well plates were coated with PEM surfaces and rinsed in sterile water and sterilized under UV light overnight. Primary hepatocytes were seeded onto the PEM surfaces at a cell density of 1.0×10^6/well in a serum-free media for 36 h at 37°C, 10% CO_2, balance

air. The substrate was then rinsed three times with PBS by pipetting. On the hepatocyte-containing substrates, NIH 3T3 cells were seeded at a density of 0.5×10^6 cells/well and incubated in primary hepatocyte media at 37°C. The fibroblast/hepatocyte ratio used in this study was 0.5:1 which is the approximate physiologic ratio of stromal:parenchymal cells in the liver.[99] The reusability of these patterns was also examined. The cells were removed from the patterns with trypsin-EDTA and washed with PBS to ensure that the cells were completely removed from the patterned surfaces. A fresh batch of primary hepatocytes was subsequently seeded onto the re-used patterns. A Leica inverted phase contrast microscope with Soft RT 3.5 software was used to capture images of cell density, morphology, and spreading on the multilayer surfaces.

3.2.4 Primary Neuron/Astrocyte Co-Culture on PEM Surfaces

Primary neurons and astrocytes were cultured on PEM coated 6-well tissue culture polystyrene surfaces (TCPS). All the multilayer coated TCPS were sterilized by spraying with 70 % ethanol and exposing them to UV light before culturing the cells onto these surfaces. Poly-d-lysine-coated TCPS were used as controls in these studies. Samples were kept in the incubator where the temperature and humidity were properly controlled. A Leica inverted phase contrast microscope with Soft RT 3.5 software was used to capture images of cell density, morphology, and spreading on the multilayer surfaces.

3.2.5 Cell fluorescent staining

The patterned co-cultures of primary hepatocytes and fibroblast were observed with a double immunofluorescent staining method. The attached primary hepatocytes were rinsed three times with 1X PBS. The cells were incubated with 1mL of 10μM CMTMR

orange dye (dilution of 1:1000 in serum free media) for 45 min at 37°C. The cells were then washed three times with PBS and followed by media addition. Three hours after staining the primary hepatocytes, fibroblast cells were seeded onto the stained hepatocytes. The co-cultures were washed with PBS three times and fed hepatocyte media. Cell morphology was observed using a phase contrast and fluorescent microscope (Leica inverted microscope).

3.2.6 Immunostaining of Primary Neurons and Astrocytes

To perform confocal immunofluorescence microscopic study, neurons and astrocytes cultures were fixed for 20 min in 4% paraformaldehyde and permeabilized with 0.1% Triton X-100 and 5% goat serum (Invitrogen) in PBS. Cells were then labeled overnight at 4 °C with appropriate primary antibodies [1:50 neurofilament for neurons and 1:1000 glial fibrillary acidic protein (GFAP) for astrocytes) in 5% goat serum in PBS. After three PBS washes, primary antibodies were detected with Fluorescein conjugated and rhodamine conjugated secondary antibodies for neurons and astrocytes, respectively. The cells were visualized with Leica fluorescent microscope.

3.2.7 Biochemical Assays

Albumin synthesis is a widely accepted marker of hepatocyte synthetic function and urea production is an indicator of intact nitrogen metabolism and detoxification. The biochemical assays were performed on the collected supernatant. Albumin concentration was determined by an enzyme-linked immunosorbent assay described previously using a polyclonal antibody to rat albumin[61]. A standard curve was derived using chromatographically purified rat albumin dissolved in medium. Urea levels were

measured with commercially available kits based upon its specific reaction with diacetyl monoxime. The urea and albumin secretions were normalized to the cell number seeded on the surface (per 1 x 10^6 cells per day). Statistics was performed using the Student's t-test. A p value of 0.05 or lower was considered to be significant.

3.2.8 Determination of the number of cells on the projected area

The number of cells on the projected cell area on the different surfaces was measured using the Image J software. The projected cell area refers to the area occupied by the cells as seen under the microscope. Statistics was performed using the Student's t-test. A p value of 0.05 or lower was considered to be significant.

3.2.9 Reactive Oxygen Species (ROS) Studies

Intracellular reactive oxygen species (ROS) were detected by staining with the oxidant-sensitive dye CM-H_2DCFDA. H_2DCFDA is cleaved of the ester groups by intracellular esterases and converted into membrane impermeable, nonfluorescent derivative H_2DCF. Oxidation of H_2DCF by ROS results in highly fluorescent 2,7-dichlorofluorescein (DCF).[100] The cells were incubated for 30 min at 37 °C with 2 μM CM-H_2DCFDA in Hanks' Balanced Salt Solution without phenol red (Invitrogen, CA, USA). The cells were then washed three times with PBS and analyzed with Leica fluorescent microscopy. To quantify the fluorescence level in neurons, we used Adobe Photoshop 7.0 software (Adobe Systems). We first delineated regions of individual primary neurons from the fluorescent image, and we then chose the image → histogram menu, which graphed the number of pixels at each color intensity level, and obtained the mean of green fluorescence intensity in those regions. The fluorescence intensity was measured using all

the cells in five different areas and repeated on three different substrates and then averaged for each surface. Statistics was performed using the Student's t-test. A p value of 0.05 or lower was considered to be significant.

3.3 RESULTS

We demonstrate that patterns of primary cells (primary hepatocytes and primary neurons) and co-cultures can be formed using the LbL deposition of ionic polymers without the aid of adhesive proteins. In this study, we used synthetic polymers, PDAC and SPS as the polycation and polyanion, respectively, to build the PEMs. SPS patterns were formed on PEM surfaces either by microcontact printing SPS onto PDAC surfaces or vice-versa. When primary cells were seeded on top of the patterned PEM surfaces, they attached and spread predominantly on the SPS surfaces resulting in primary cell patterns. Once the primary cells attached, the second cell type (fibroblasts/astrocytes) were subsequently seeded and attached to the PDAC surfaces. As a result, co-culture patterns were obtained on synthetic PEM surfaces. The morphology of the cell co-cultures was characterized using phase contrast and fluorescence microscopy and their hepatic-specific function were determined by urea and albumin synthesis.

3.3.1 Patterned Culture of Primary Hepatocytes on PEMs

We capitalized upon the cell adhesive/resistive property of SPS and PDAC, respectively, to make patterns of primary hepatocytes. The technique of POPS makes the task of micropatterning polyelectrolyte multilayers a simpler process.[35] For POPS, a polyelectrolyte applied to a patterned stamp is transferred to a polyelectrolyte multilayer surface of the opposite charge. In our study, SPS patterns were formed on PEM surfaces

either by μCP SPS onto (PDAC/SPS)$_{10.5}$ surface or μCP PDAC onto (PDAC/SPS)$_{10}$ surface using the POPS technique. Figure 3.2 illustrates the attachment of primary hepatocytes on PDAC and SPS patterns after one and five days of culture. When presented with the micropatterned surface, primary hepatocytes adhered only to the SPS regions resulting in patterns of hepatocytes. On day 1, primary hepatocytes attached and preferentially on the SPS regions resulting in cell patterns irrespective of whether PDAC or SPS was stamped on top of the PEM surface (Figure 3.2 A, C). The hepatocyte
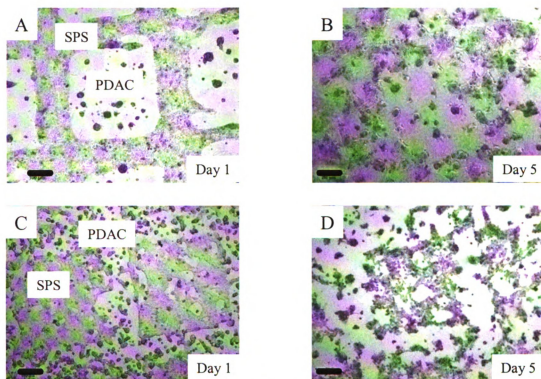
Figure 3.2. Phase contrast microscope images of primary hepatocyte cells seeded at 0.5×10^6 cells/ml on days 1 and 5 post seeding on patterned PEM surfaces. (A) and (B) primary hepatocytes on PDAC patterns on days 1 and 5, respectively. (C) and (D) primary hepatocytes on SPS patterns on days 1 and 5, respectively. PDMS stamp with 1000μm square patterns separated by 250μm width were used. (Scale bar, 100 μm).

patterns attached and maintained their differentiated morphology for the first few days but by day 5 began to detach from the PEM surfaces. Few hepatocytes remain attached to the patterns by day 6 (Figure 3.2 B, D).We also examined the reusability of these

patterns. The cells were removed from the patterns with trypsin-EDTA and washed with

PBS to ensure that the cells were completely removed from the patterned surfaces. A

fresh batch of primary hepatocytes was subsequently seeded onto the re-used patterns.

The patterns were reused 4 times and maintained their pattern design upon each re-use

(data not shown).

3.3.2 Patterned Co-Cultures of Primary Hepatocytes with Fibroblasts
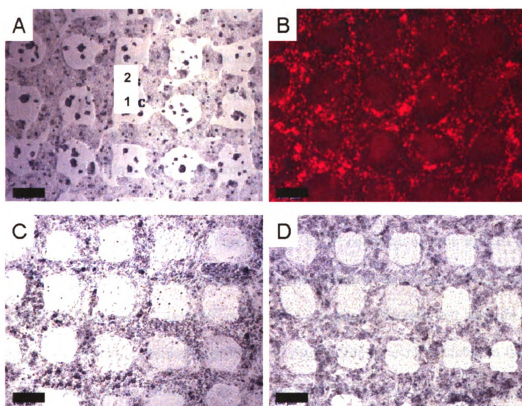
Figure 3.3. Patterned co-cultures of primary hepatocytes with fibroblasts. (A) phase contrast and (B) fluorescent images of patterned primary hepatocytes (red) on PDAC patterns on day 1, phase contrast image of co-culture of primary hepatocytes with fibroblasts on (C) day 6 (D) day 19. PDMS stamp with 250μm square patterns separated by 250μm width were used. (Scale bar, 100 μm).

Co-cultures of primary hepatocytes with nonparenchymal cells such as fibroblasts

have been shown to maintain hepatic functions *in vitro* for up to 5 weeks.[85] The

fibroblast/hepatocyte ratio used in the present study is 0.5:1 which is the approximate

physiologic ratio of stromal:parenchymal cells in the liver.[99] Figure 3.3 illustrates patterned co-cultures of primary hepatocytes with fibroblast on PEM surfaces. The preferential attachment of primary hepatocytes to SPS surfaces enabled the use of this system as a template for patterned co-cultures with fibroblasts on synthetic PEM surfaces. Primary hepatocytes remained attached (Figure 3.3 C, D) on the patterned co-culture system for up to 3 weeks.

3.3.3 Function of Primary Hepatocytes in Patterned Co-Cultures

To assess liver-specific function, we measured the levels of urea and albumin synthesis for the patterned single culture and co-cultures for up to 7 days, shown in Figure 3.4. The metabolic response of the single and co-cultures of hepatocytes on patterned PEM films were compared. Panels A and B illustrate the rate of urea and albumin production, respectively, for cultures up to one week. By day 7, liver-specific functions for the patterned co-culture (60 μg/ 1×10^6 cells/day of urea and 20 μg/1×10^6 cells/day of albumin) were much higher than the patterned single cultures (28.3 μg/ 1×10^6 cells/day of urea and 2.7 μg/1×10^6 cells/day of albumin). The urea and albumin secreted by our patterned co-culture system was also comparable to levels secreted in the culture system developed by Bhatia et al. (80 μg/1×10^6 cells/day of urea and 15 μg/1×10^6 cells/day of albumin)[99] for a similar fibroblast and hepatocyte culture ratio (0.5:1), although different pattern sizes and shapes were used in these two studies.

A)
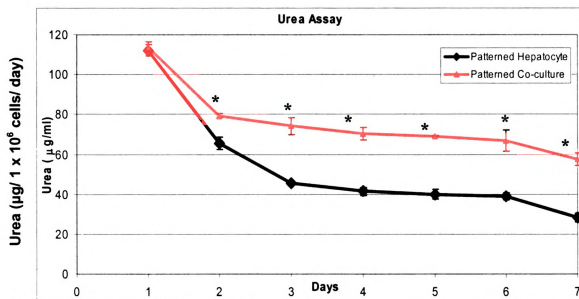
B)
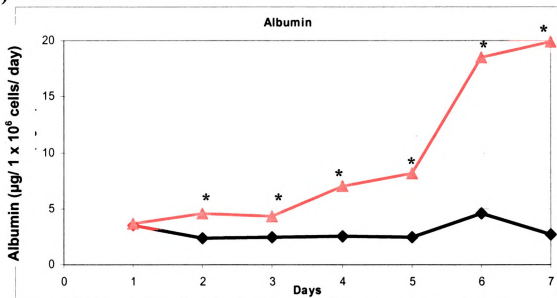
Figure 3.4. Liver-specific function of primary hepatocytes on PEM surfaces. (A) Urea synthesis of patterned hepatocytes and patterned co-cultures. (B) Albumin synthesis of patterned hepatocytes and patterned co-cultures (n=6). Data represents mean ± S.E. of six independent experiments. (* p<0.05 compared with patterned single hepatocyte culture)

Table 3.1. Comparison of maximum achievable levels of hepatic-specific function (urea and albumin secreted) in various hepatocyte culture systems. Urea and albumin secreted per 1 x 10^6 cells were approximated from experimental data and available literature

Hepatocyte Culture Systems	Urea Secreted (µg /1x10^{6}cells /h)	Albumin Secreted (µg /1x10^{6}cells /h)
Human liver *in vivo* [a]	5-8	2-3.3
Single collagen gel [b]	1.2-2.0	0.1-0.3
Sandwich gel [c]	3-4	1-2
Random co-culture of hepatocytes and fibroblast in 0.5:1 ratio [d]	2-3.5	0.25-0.4
Patterned co-culture of hepatocytes/fibroblast in 0.5:1 ratio (Bhatia et al) [d]	4-5	1-2

3.3.4 Patterned Co-Cultures of Primary Neurons with Astrocytes

Figure 3.5 illustrates the random and patterned primary neuron monoculture and co-culture of primary neurons and astrocytes. Figure 3.5 (A, B) shows the fluorescent images of mono-culture of primary neurons and random co-culture, respectively, on top of non-patterned SPS surfaces. Figure 3.5 (C, D) illustrates the fluorescent images of patterned primary neurons and patterned co-culture of neurons and astrocytes. PDAC patterns were formed on SPS surfaces (or vice-versa) and subsequently seeded with neuronal cells. Primary neurons preferentially attached on the SPS patterns when they were seeded on top of PEM surfaces (Figure 3.5 C). Astrocytes were subsequently seeded

onto the patterns of neurons and the cells attached onto the open PDAC regions and resulted in patterned co-cultures of neurons and astrocytes (Figure 3.5 D).
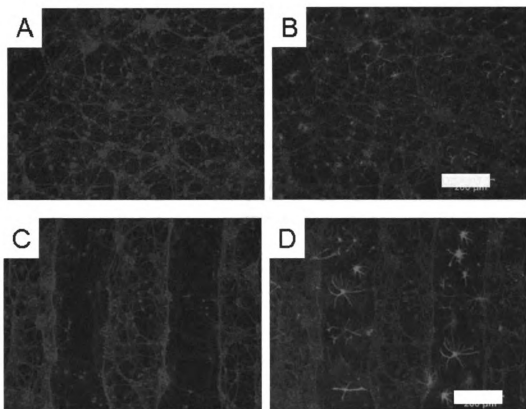
Figure 3.5. Fluorescent images of primary neurons and astrocytes co-culture on SPS surfaces (A) Random neuron monocultures (green) after 7 days in culture, (B) Random co-culture of neurons (green) and astrocytes (red) after seeding astrocytes. (C) Patterned primary neurons on SPS patterns after 7 days in culture (D) Patterned co-culture of neurons (green) and astrocytes (red) after seeding astrocytes (Scale bars-200 μm).

Studies show that random, dissociated neurons in culture develop physiological responses to neurotransmitters [39, 40] and self-organize into neuronal networks, [40-43] however, they lack the structure normally present within the nervous system, where the neurons reside in specific regions with numerous network connectivity. The advantage of patterned co-cultures of neurons and astrocytes is that it allowed for precise control of both the direction of neurite extension and degree of contact between the neurons and astrocytes, unlike the random co-culture, which is important for repair and regeneration

of the nervous systems.[44] It has also been demonstrated by Wheeler and co-workers that patterned neurons synapse with each other, release neurotransmitters and develop electrical activity [45-47]. Furthermore, restricting neurons to patterns has been shown to enhance the cellular activity such as glutamine secretion and electrical activity as compared to the random monocultures of neurons.[48, 49]

3.3.5 Reactive Oxygen Species (ROS) Studies on Co-culture Systems
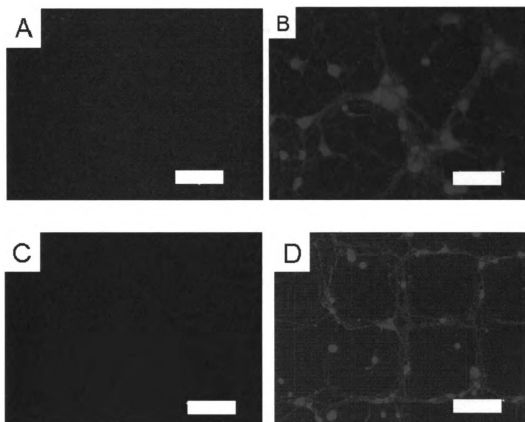
Figure 3.6. Intracellular accumulation of ROS in neurons. Astrocytes were treated for 12 h with (A) 5% BSA (control) and (B) 0.2 mM of PA, followed by transfer of the astrocytes-conditioned media to neurons for 24 h treatment. Patterned neuron-astrocytes co-culture were treated for 12h with (C) 5% BSA (control) and (D) 0.2 mM of palmitate (PA). (Scale bars- A-C: 50μm, D: 100μm)

ROS is a widely accepted marker of oxidative stress and the results indicated that elevated levels of FFAs induced astrocyte-mediated oxidative stress in the neurons.

Previously, it was shown that intracellular levels of ROS were elevated when the neurons were cultured with conditioned media from astrocytes treated with palmitic acid (PA) as compared to controls (i.e., cultured with conditioned media from astrocytes treated with 5% bovine serum albumin (BSA) media).[101] Here, we compared the astrocyte-mediated response of neurons in the present patterned co-culture system with the previous, more common, method of culture.

The earlier study used random neuronal monocultures to evaluate the effect of FFAs on primary neurons.[101, 102] As shown in Figure 3.6 (A,B), the intracellular levels of ROS were elevated in the neurons cultured in conditioned media from astrocytes treated with PA (Figure 3.6B) as compared to the controls (Figure 3.6A). The astrocytes were treated with 0.2 mM PA for 12 h prior to transfer of the conditioned media to neuronal cultures for 24h (Figure 3.6B). By contrast, random monocultures of neurons treated directly with PA did not show oxidative stress-induced effects in the neurons.[101, 102] We also exposed the co-culture system of neurons and astrocytes to elevated levels of FFAs. When the co-culture system was treated with BSA, an elevation in ROS was not observed (Figure 3.6C). In Figure 3.6D, we treated the co-culture system with 0.2 mM PA for 12 h and then performed the ROS measurements. The patterned neuron-astrocyte co-culture systems treated with fatty acids for 12h had comparable levels of ROS (Figure 3.6D) to the neurons cultured for 24h with conditioned media from astrocytes treated with fatty acids (separated monoculture system). The neuronal cells were seeded at the same density on the random monoculture (Figure 3.6A and 3.6B) and patterned co-culture systems(Figure 3.6C and 3.6D). The level of ROS was further quantified by measuring

the green fluorescence intensity of DCF from microscopic images using Photoshop software (Adobe Systems, Mountain View, CA) as shown in Figure 3.7.
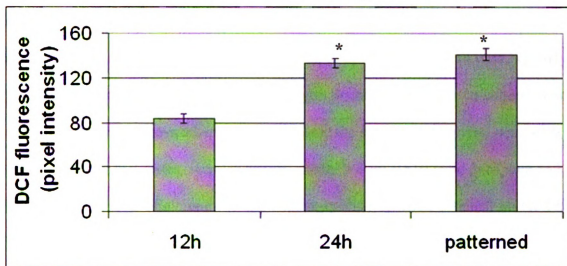
Figure 3.7. Quantification of intracellular accumulation of ROS in neurons. Data represents mean ± S.E. of three independent experiments (* $p < 0.05$ compared with 12h treatment of monocultures of neurons).

The level of ROS on the patterned neuron-astrocyte co-culture system treated with fatty acids for 12h was comparable to the random neuronal monoculture neurons systems treated in conditioned media from astrocytes treated with fatty acids for 24h. In the co-culture system, since both the astrocytes and the neuronal cells were on the same surface, the elevation in the ROS levels was observed earlier than in the separated monoculture system. This earlier response (i.e., the rapid elevation of ROS production in the co-culture) may be because 1) both types of cells were in the same culture media, which allowed the neuronal cells to response to soluble factors, such as oxidative-stress inducing cytokines or intermediate metabolites, as they were secreted by the astrocytes, or 2) the co-culture system allowed for direct contact between neurons and astrocytes.

3.4 DISCUSSIONS

In this study, we demonstrated an alternative approach to engineer patterned cell co-culture of primary hepatocytes and fibroblast without the aid of adhesive proteins using the PEM films. In Table 3.1, we compared the maximum achievable levels of hepatic-specific function in our co-culture system to *in vivo* and other *in vitro* hepatocyte co-culture systems studied, namely, the collagen double gel and the co-culture system studied by Bhatia and co-workers. By comparison, the human liver *in vivo,* consisting of 150-250 X 10^9 hepatocytes, secretes approximately 5-8 µg /1x10^6cells /h of urea and 2-3.3 µg /1x10^6cells /h of albumin.[103] The hepatic-specific function obtained on the PEM films was comparable to the collagen coated tissue-culture polystyrene (TCPS) surfaces, the collagen double gel, the co-culture system and the *in vivo* human liver. Primary hepatocytes cultured using previously well established techniques are stable, but there are certain disadvantages associated with each of these methods.

3.4.1 Advantages of our Culture System over other Hepatocyte Culture Systems

Collagen sandwich (double gel) cultures preclude direct cell-cell interaction between the sandwiched hepatocytes and other cells types that may be cultured atop the collagen sandwich. Donato et al used transwells to form co-cultures, therefore the cells were not in direct contact with each other.[104] This culture system imposed an artificial boundary that precluded cell-cell interactions. Shimaoka and co-workers developed a method whereby hepatocytes were cultured onto cover slips and the cover slips were subsequently added to the center of a confluent culture of fibroblast.[105] This method

resulted in significant cell death underneath the cover slip. Furthermore, significant topological variations in the culture existed which caused variations in the degree of cell-cell interactions. Bhatia et al. developed a patterned co-culture system using photolithography.[99] This method was very effective in controlling cell contact and adhesion, but the lithographic technique used has a number of limitations when applied to curved, nonplanar surfaces and involved multiple and cell-unfriendly processing steps to create the patterns. Furthermore, collagen must be added to the patterns in order for the primary hepatocytes to adhere onto the surface.

In the present study we used μCP which has several advantages over the method used by Bhatia et al. The advantages include its high fidelity, ease of duplication, ability to print a variety of molecules with nanometer resolution and without the need for dust-free environments and harsh chemical treatments.[18, 63, 106] In addition, we were able to achieve primary hepatocytes adhesion without the need of collagen or other adhesive proteins.

3.4.2 Advantages of our Culture System over other Neuron Culture Systems

Numerous studies use monocultures of neurons and astrocytes to study neuronal systems, however, monocultures of neurons and astrocytes do not accurately capture the diverse biological responses of living brain tissue.[107] Transwells or neurons cultured onto cover slips that were subsequently added to the center of a confluent culture of astrocytes are the most common forms of co-cultures of neurons and astrocytes.[108, 109] However, these culture systems imposed an artificial boundary that precluded cell-cell interactions. In the present study, we developed patterned neuron-astrocyte co-culture system using PEM films and μCP which has several advantages over the methods generally used for

patterning surfaces for co-cultures. The advantages include its high fidelity, ease of duplication, ability to print a variety of molecules with nanometer resolution and without the need for dust-free environments and harsh chemical treatments.[18, 63, 106] In addition, we were able to achieve primary neuron-astrocyte interactions without adhesive proteins, which was not possible with the other methods.[94, 110]

3.5 CONCLUSIONS

In conclusion, the present work outlined a method for controlling cell-surface interactions using polyions and PEMs. PEMs were used to produce defined cell-resistant and cell-adhesive properties depending on the topmost surface and the type of cells. We demonstrated using both biochemical studies and direct microscopy images of live cells that primary hepatocytes and primary neurons attached and spread onto PEM films with SPS as the top most surface. We also demonstrated that the layer-by-layer deposition and μCP of ionic polymers can be used as a template for patterned co-cultures of primary hepatocytes/fibroblasts and primary neurons/astrocytes. The patterned co-cultures of primary hepatocytes and fibroblasts maintained hepato-specific function much longer than the patterned single culture of primary hepatocytes. The patterned co-culture system where the neurons are in direct contact with the astrocytes responded quicker to elevated levels of FFAs than the separated neuronal monoculture system. Taken together, this technique provides a useful tool for engineering neuronal and hepatocyte co-culture systems, which may more accurately capture liver and neuronal function and metabolism in normal versus diseased states.

CHAPTER 4 SELECTIVE DEPOSITIONS ON POLYELECLECTROLYTE MULTILAYER FILMS: SAMS OF m-dPEG ACID AS MOLECULAR TEMPLATE

4.1 INTRODUCTION

In recent years, organic thin films have attracted a great deal of attention from researchers in many fields due to their light-weight, flexibility, ease of functionalization and application. The ionic layer-by-layer (LBL) assembly technique, introduced by Decher in 1991,[111, 112] is among the most exciting recent developments in this area. Films formed by electrostatic interactions between oppositely charged poly-ion species to create alternating layers of sequentially adsorbed poly-ions are called "Polyelectrolyte Multilayers (PEMs)". PEMs[112-114] are effective and economical approaches to depositing organic ultrathin organized films and have been further extended to functional polymers,[115, 116] organic dyes,[117, 118] colloids,[119-121] inorganic nanoparticles,[122, 123] biomaterials,[124, 125] and selective electroless metal depositions.[126]

The use of organic thin films in integrated optics, microelectronic devices, sensors and optical memory devices requires a means of patterning and controlling the device architecture. Photolithography is the conventional patterning technique of choice but lithographic techniques have limitations when applied to curved, nonplanar surfaces and involves multiple processing steps to create three dimensional, functional, and multiple-level microstructures. Microcontact printing (μCP), introduced by Whitesides and co-workers,[18, 63] provides a versatile method of chemically and molecularly patterning surfaces at the submicrometer scale. This technique is attractive due to its high fidelity and ease of duplication. μCP uses an elastomeric stamp to print a variety of molecules

60

with submicrometer resolution and without the need for dust-free environments and harsh

chemical treatments.[18, 63, 106] The stamp is coated with the desired molecules, and the

molecules residing on the raised regions of the stamp are brought in contact with the host

substrate when the stamp is printed. The transfer efficiency of the molecules from the

stamp to the substrate depends on the relative strength of the interaction of these

molecules with the substrate versus with the stamp.

$$MW = 236.26$$
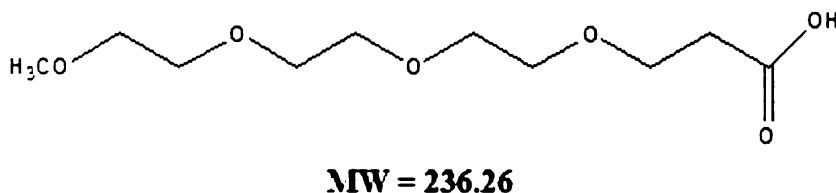
Figure 4.1. Chemical structure of PEG acid molecule (m-dPEG acid).

On the basis of the μCP and the LBL assembly techniques, Hammond and co-

workers developed a polymer-on-polymer stamping (POPS) process using charged graft

and diblock copolymers or polyelectrolytes as the ink.[35, 98] They achieved selective

deposition by introducing alternating regions of different chemical functionalities on a

surface: one promoted adsorption and another effectively resisted adsorption of poly-ions

onto the surface. We are exploring a similar approach where m-dPEG molecule with an

activated carboxylic acid group at the end can be stamped directly onto multilayer films

to form patterned monolayers of SAMs, by carefully selecting their surface chemistry and

taking advantage of electrostatic interaction between the top surface of the multilayer

film and the stamped molecule. Chemical patterning of the topmost surface of the

61

multilayer films provides a new non-lithographic approach to building and controlling device architectures.
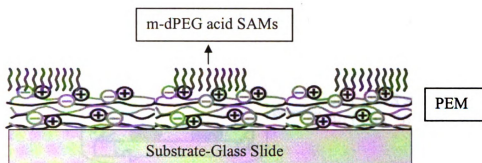
Figure 4.2. An illustration of patterned SAMs on PEM.

In this study, we describe the process of creating chemically patterned and physically structured surfaces by stamping molecules of m-dPEG acid (shown in Figure 4.1) activated with carboxylic acid at one end. Note that this is the first time patterned SAMs were created on PEMs (illustrated in Figure 4.2), as oppose to on gold or silicon substrates. The activated carboxylate functional group ionically binds to the topmost positive surface of the PEM surfaces and the other end (PEG units) resists the deposit of subsequent polymer (polyelectrolyte) layers. To create surfaces which can act as templates for selective layer-by-layer deposition, it is necessary to form surface regions that resist poly-ionic adsorption. To this end, poly(ethylene glycol) (PEG) and its oligomeric derivatives have thus far been the most effective materials to resist nonspecific adsorption of polyelectrolytes, charged particles and proteins onto surfaces from aqueous solution.[127-132] PEG is a technologically important polymer used in numerous applications.[133-145] We capitalized upon ionic interactions to deposit thin, uniform PEG self-assembled monolayer patterns atop PEM films and evaluated the

factors that influence the effective transfer of m-dPEG acid molecules onto the multilayer films as illustrated in Figure 4.3. Our motivation for exploring the m-dPEG acid molecule as the molecular template for selective deposition is that it is a small molecule compared to other polymers with the PEG backbone used in other similar studies. As a result, it will
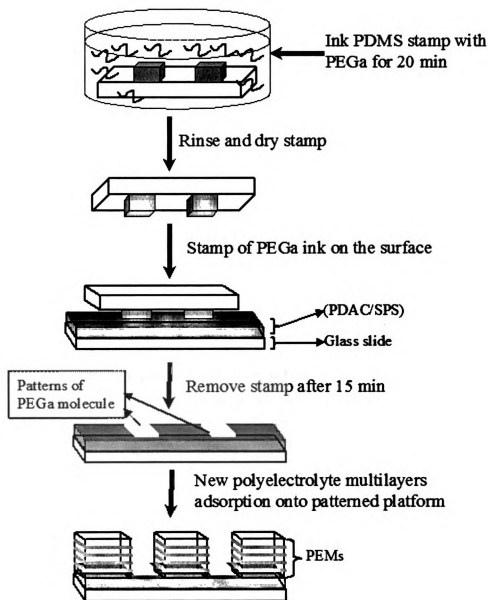
Figure 4.3. Diagram illustrating the stamping process of m-dPEG acid on a PDAC/SPS multilayer platform

63

provide us with better control in the pattern transfer onto the PEM surface. In addition, it can self-assemble to form monolayers on PEMs. The patterned SAMs on PEMs are possible like alkanethiol and alkanesilane SAMs that have been formed on gold or silicon wafers. We demonstrate that the PEG molecules create areas of selective adsorption on the multilayer films and be used in the subsequent generation of 3-D microstructure films. The patterned films were characterized by optical microscopy and atomic force microscopy (AFM).

4.2 METHODS AND MATERIALS

4.2.1 Materials

Sulfonated poly(styrene), sodium salt (SPS) (Mw ~70 000), poly(diallyldimethylammoniumchloride) (PDAC) (Mw ~ 100 000-200 000) as a 20 wt % solution and sodium chloride were purchased from Aldrich Chemical, Milwaukee, WI. The m-dPEG acid molecule (Mw=236) was obtained from Quanta biodesign. Poly(dimethylsiloxane) (PDMS) from the Sylgard 184 silicone elastomer kit (Dow Corning, Midland, MI) was used to prepare stamps. The fluorosilanes was purchased from Aldrich Chemical. These PDMS stamps were used for microcontact printing.[9] Glass slides (Corning Glass Works, Corning, NY), used for making the polyelectrolyte multilayer films, were cleaned using a Bransonic ultrasonic cleaner (Bransonic Ultrasonic Corporation, Danbury, CT). Carboxyfluorescein (6-CF), fluorescence dye, was purchased and used as received from Sigma. Carboxylated polystyrene latex particles (4 μm diameter) purchased from Polysciences, were used for colloidal adsorption study on m-dPEG self-assembled monolayer patterned polyelectrolyte templates.

4.2.2 Preparation of Polyelectrolyte Multilayer Thin Films

The strong polyelectrolytes SPS and PDAC were used to fabricate multilayer platforms using glass slides as the substrates. A Carl Zeiss slide stainer equipped with a custom-designed ultrasonic bath was connected to a computer to perform layer-by-layer assembly. Polyelectrolyte dipping solutions were prepared with DI water supplied by a Barnstead Nanopure-UV 4 stage purifier (Barnstead International Dubuque, Iowa), equipped with a UV source and final 0.2 μm filter. The concentration of SPS was 0.01 M and the concentration of PDAC solution was 0.02 M as based on the molecular repeat unit of the polymer and all polyelectrolyte solutions contained 0.1M NaCl. Solutions were filtered with a 0.45 μm Acrodisc syringe filter (Pall Corporation) to remove any particulates. The glass slides were cleaned with a dilute Lysol water mixture in a sonicator. These slides were then dried under N_2 gas and were further cleaned using Harrick plasma cleaner (Harrick Scientific Corporation, Broading Ossining, NY) for 10 min at 0.15 Torr and 50 sccm flow of O_2 in a plasma chamber. To form the first bilayer, the slides were immersed for 20 min in a PDAC solution. Following two sets of 5 min rinse with agitation, the slides were subsequently placed in a SPS solution and allowed to deposit for 20 min. They were rinsed twice for 5 min each. The samples were cleaned for 3 min in an ultrasonic cleaning bath after depositing a layer of polycation/polyanion pair.[128] The sonication step removes weakly bounded polyelectrolytes on the substrate, forming uniform bilayers. This process was repeated to build multiple layers. All experiments were performed using ten and half bilayers (i.e., 21 layers) and the topmost surface being PDAC (positive surface).

4.2.3 Preparation of PDMS Stamps

An elastomeric stamp is made by curing poly(dimethylsiloxane) (PDMS) on a microfabricated silicon master, which acts as a mold, to allow the surface topology of the stamp to form a negative replica of the master. The poly(dimethylsiloxane) (PDMS) stamps were made by pouring a 10:1 solution of elastomer and initiator over a prepared silicon master.[63] The silicon master was pretreated with fluorosilanes to facilitate the removal of the PDMS stamps from the silicon masters. The mixture was allowed to cure overnight at 60°C. The masters were prepared in the Microsystems Technology Lab at MIT and consisted of features (parallel lines and circles) from 1 μm to 10 μm.

4.2.4 Stamping of m-dPEG acid

The stamping conditions were varied to optimize the microcontact printing of the m-dPEG acid. PDMS stamps with and without plasma treatment were tested to stamp the ink. Ethanol/water mixtures were used as inks. Five solvents of this type were tried: pure ethanol, 75 % ethanol, 50 % ethanol, 25 % ethanol and pure water. The m-dPEG acid inks made with these solvents had concentrations of 10μM, 100μM and 1000μM. After solvent evaporation, the PDMS stamp was briefly dried under a N_2 stream and brought into contact with the substrate for 10-15 min at room temperature. Three different methods were used to ink the PDMS stamps: spin-inking, cotton swab-inking and dip-inking. For spin-inking the stamp was covered with ink and spun at 3,000 RPM for 20 s. For the cotton swab-inking, a cotton swab was soaked in ink and rubbed over the surface of the stamp. The stamp was then dried with nitrogen. Using the dip-inking the stamp was soaked in ink, typically for 10 minutes, and dried with nitrogen.[146] In this study, the stamping times were varied systematically from a few seconds to an hour and the pH of

the m-dPEG acid ink solution was varied from 2.0, 3.5, 4.5 to 6.5. Following the stamping process, the patterned surface was rinsed thoroughly with ethanol to remove unbound or loosely bound excess molecules to prepare self-assembled monolayer patterns. The stamped regions were designed to act as resists to adsorption as the oligoethylene glycol graft chains of PEG did.[98] In the procedure of creating complex 3-D microstructures, m-dPEG acid was stamped onto PEM surface (PDAC surface) followed by sequential adsorption layer-by-layer deposition process to build additional patterned polyelectrolyte multilayers outside the stamped region.

4.2.5 Characterization

Nikon Eclipse ME 600 optical microscope (Nikon, Melville, NY) was used to obtain dark field images of the m-dPEG acid patterns and the additional microfabricated PEMs. Nikon Eclipse E 400 microscope was used to obtain the fluorescence images. The 6-carboxyfluorescein (6-CF) dye was used to visualize the m-dPEG SAM patterns on PEM following the stamping and rinsing processes. The dye was dissolved directly in 0.1 M NaOH; samples were imaged by dipping the substrates into the dye solution. The dye, which is negatively charged, preferentially stained the positively charged PDAC surface. The dyed regions appear green when viewed with the fluorescence optical microscope, using a FITC filter.[147] Images were captured with a digital camera and processed on a Pentium computer running camera software. After the polymers were stamped atop the multilayer platform, the topography of the stamped polyelectrolyte layer was observed by atomic force microscope (AFM) images. The AFM images were obtained with a Nanoscale IV controller (Digital Instruments, Santa Barbara, CA) equipped with Tapping Mode Etched Silicon Probes and was operated in tapping mode.

4.3 RESULTS AND DISCUSSION

For the first time, we demonstrate that the creation of patterned SAMs on PEMs, using PEG acid molecules, can be achieved, as alkanethiol and alkanesilane molecules can form SAMs on gold or silicon wafers. In addition, we present approaches to fabricate complex 3-D microstructured functional films by incorporating the created m-dPEG SAMs on PEM surfaces. Using m-dPEG acid molecules with an activated carboxylic group facilitated the attachment of the m-dPEG acid molecules onto the topmost positive surface (PDAC) of the PEM surfaces (PDAC/SPS)$_{10.5}$ via ionic bonding. The SAM patterns of m-dPEG acid molecule act as a resistive template by resisting the addition of polyelectrolytes on the stamped regions. This helps to achieve complex 3-D microstructures atop the original set of PEMs by permitting selective building of subsequent PEMs outside the m-dPEG SAM patterns. The patterns were characterized using AFM, optical and fluorescence microscopy.

4.3.1 Patterning m-dPEG SAMs on Polyelectrolyte Multilayers

In this study, we stamped m-dPEG acid molecule directly onto an outermost PDAC layer of a PDAC/SPS multilayer film to form patterned m-dPEG SAMs on PEMs. To enhance the transfer of the m-dPEG SAM patterns and the subsequent building of complex microstructures, the stamping process required optimized conditions.

68

4.3.1.1 Optimization of Stamping Process
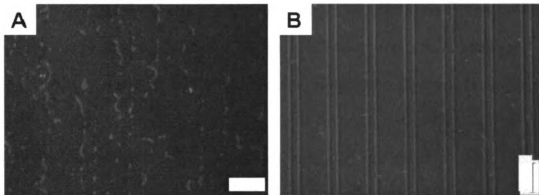
Figure 4.4. Defects occurring under non-optimized stamping conditions: (a) Rimming occurs in areas of the stamp that were insufficiently inked (bare regions were also observed). (b) Streaking due to uneven application of the m-dPEG acid ink solution on the PDMS surface. All the images are fluorescence images and the bars represent 20μm.

Figure 4.4 illustrates the various defects that occurred when m-dPEG acid molecules were stamped under non-optimized conditions. For example, rimming (Figure 4.4a) or streaking (Figure 4.4b) in the stamped areas may arise when insufficiently or uneven application of the m-dPEG acid ink solution on the PDMS surface occurs. Determining the optimal conditions is important in achieving uniform and efficient transfer of m-dPEG acid molecules to form patterned SAMs on PEMs, which in turn affects the integrity of the device architecture for further applications. Various factors were evaluated in optimizing the stamping process, such as the plasma treatment of the PDMS stamps, the type and concentration of the solvents used in making the ink solution and the contact times. The PDMS stamps were not treated with oxygen plasma since it was experimentally determined that untreated PDMS stamps resulted in more complete transfer of patterns when compared to the stamps treated with plasma. 75% (v/v) ethanol/water solvent gave the best results in terms of the effective transfer of the ink solution from the PDMS stamps onto the surface and thus was used for the rest of the

experiments. This optimal ethanol/water composition of the ink solvent was corresponded to the previous results reported by the Hammond group.[35] Three different methods were used to ink the PDMS stamps: spin-inking, cotton swab-inking and dip-inking. It was experimentally determined that the dip-inking method resulted in the most efficient transfer of the ink onto the PEM surface. The contact times were also varied from a few seconds to 30 min. The best pattern transfer resulted with a 15 min contact time. Based upon the variables discussed above, the optimal stamping condition for m-dPEG acid was determined to be a solution of 100 μM of m-dPEG acid in a 75/25 ethanol-water mixture, stamped for 15 min using the dip-inking method of inking the PDMS stamps.

4.3.1.2 Effect of pH

Among the variables, the pH of m-dPEG acid ink solution played the most important role in the transfer efficiency of the patterns onto the multilayer films. Figure 4.5 illustrates the effect of pH of the m-dPEG acid "ink" on the patterns of PEG SAM formed atop (PDAC/SPS)$_{10.5}$ using fluorescent microscopy. The fluorescence dye used stained the PDAC surface due to ionic interaction. The presence of an alternating positive/m-dPEG SAM pattern is made clear by the presence of the negatively charged green dye on the positive PDAC regions. The dark regions represent the m-dPEG acid patterns, which are not stained by the dye due to the lack of ionic interaction between the dye and m-dPEG acid surface. The carboxylic group of m-dPEG acid is responsible for the ionic interaction between m-dPEG SAM and the PDAC surface of the PEM. The extent of ionization of the acid group affects the strength of the ionic bond between the two ions and thus the extent of the pattern transfer. The ionization of m-dPEG acid, in

turn, depends on the pH of the solution. It is apparent from Figure 4.5 that the micropattern transferred cleanly at pH of 4.5 and 6.5 and in case of pH values less than the pKa the transfer was not efficient.
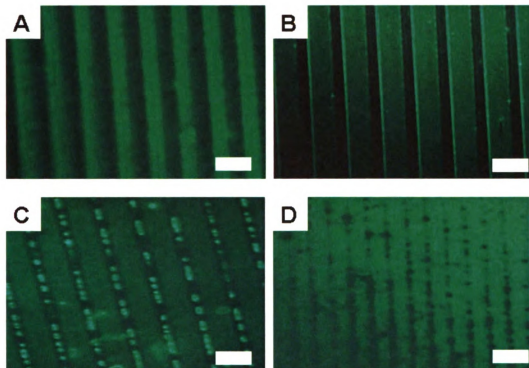
Figure 4.5. Effect of pH of m-dPEG acid "ink" on the patterns on top of (PDAC/SPS)$_{10.5}$ (a) pH=6.5; (b) pH=4.5; (c) pH=3.5; (d) pH=2.0. The green regions are the PEM films and the black regions are the m-dPEG acid surface. The m-dPEG acid ink solution was evaluated at pH of 2.0, 3.5, 4.5, and 6.5. When the pH is less than the pKa of the molecule (4.27±0.20), the acid group does not completely ionize leading to incomplete transfer of the patterns onto the multilayer films when compared to solutions with pH greater than the pKa value. At pH of 4.5 and 6.5, uniform patterns are obtained due to the complete ionization of m-dPEG acid, resulting in stronger electrostatic attraction between the PDAC layer and the m-dPEG acid molecule. All the images are fluorescence images and the bars represent 20µm.

4.3.2 3-D Microstructures Fabricated on PEMs
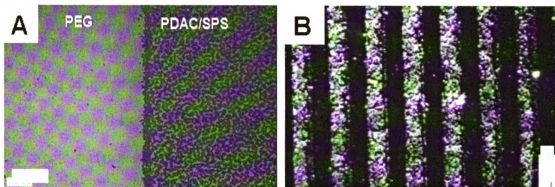
Figure 4.6. Optical microscope Image of the m-dPEG acid patterns and dark field and fluorescent images of complex microstructures built atop the m-dPEG acid patterns (a) m-dPEG acid was stamped on (PDAC/SPS)$_{10.5}$ as a resisting pattern using a blank stamp and carboxylated polystyrene beads (D=4.1 μm) were deposited on the outside regions of the m-dPEG self-assembled monolayer patterned surfaces. The left region, where there are no colloidal particles, is the m-dPEG acid region while the right region with the colloidal particles is the PEM region (b) Dark field optical images of complex microstructures formed by building PDAC/SPS atop the PEG patterns. The white regions are the PEM films and the black regions are the m-dPEG acid surface.

The fabrication of 3-D microstructures on PEMs using m-dPEG acid monolayer patterns as molecular resisting area is illustrated in Figure 4.6. PEG is known to be an effective polyelectrolyte that resists attachment of polymeric functional groups.[148] One of the goals in this work is to fabricate PEG self-assembled monolayer patterns onto PEMs by capitalizing upon ionic interactions at one end of the m-dPEG acid molecule and its resistance properties at the other end. As a further proof for the existence of m-dPEG monolayer patterns on the PEM surface, negatively charged carboxylated polystyrene PS particles (Diameter = 4 μm) were used. m-dPEG acid molecules were stamped on top of the (PDAC/SPS)$_{10.5}$ using a blank stamp (i.e., stamp with no patterns) as shown in Figure 4a and the colloidal particles deposited selectively over the positive (PDAC/SPS)$_{10.5}$ surface (right) but not on the m-dPEG self-assembled monolayer regions (left). We were able to construct complex 3-D microstructures on top of the PEG monolayer patterned

PEMs, for a variety of applications. After transferring m-dPEG monolayer patterns onto the PEM surfaces, subsequent depositing of PEMs resulted in 3-D heterostructures on the non-m-dPEG acid regions. Dark field optical microscopy and fluorescence microscopy were used to image the complex microstructures. Figure 4.6 B illustrates dark field image of the PEMs built on top of the m-dPEG acid patterns. The black regions represent the m-dPEG acid surfaces and the white regions represent the subsequent PEM films built on top of the m-dPEG SAM patterns. The white images of the patterned multilayers are due to the loopy and wavy deposits of the PEMs on the confined region (outside of the m-dPEG monolayer patterns).

To provide further confirmation of the presence of the microstructures, Figure 4.7 illustrates the corresponding AFM images of the PDAC/SPS multilayer films built atop the stamped m-dPEG acid molecules. These images show the topography and the height variations of the PEM patterns deposited on the outside regions of the m-dPEG SAM patterns (i.e. the exposed PDAC area). The AFM images were taken for different number of layers of 3-D patterned PEMs namely, 10, 20 and 40 bilayers. The height and the width of the patterns were determined using the AFM images. The height of the 3-D micropatterned PEMs (PDAC/SPS) linearly increased with the number of (PDAC/SPS) bilayers built on the outside region of the m-dPEG patterned SAM area. The heights of the 3-D microfabricated PEMs were determined by the AFM images and found to be 32-37nm for 10 bilayers, 62-67nm for 20 bilayers and 142-146nm for 40 bilayers. From these values, the average height of a pair of PDAC/SPS film was determined to be approximately 3.28-3.57 nm. This value agreed quiet well with the literature value of 3.4nm for similar deposition condition.[128]
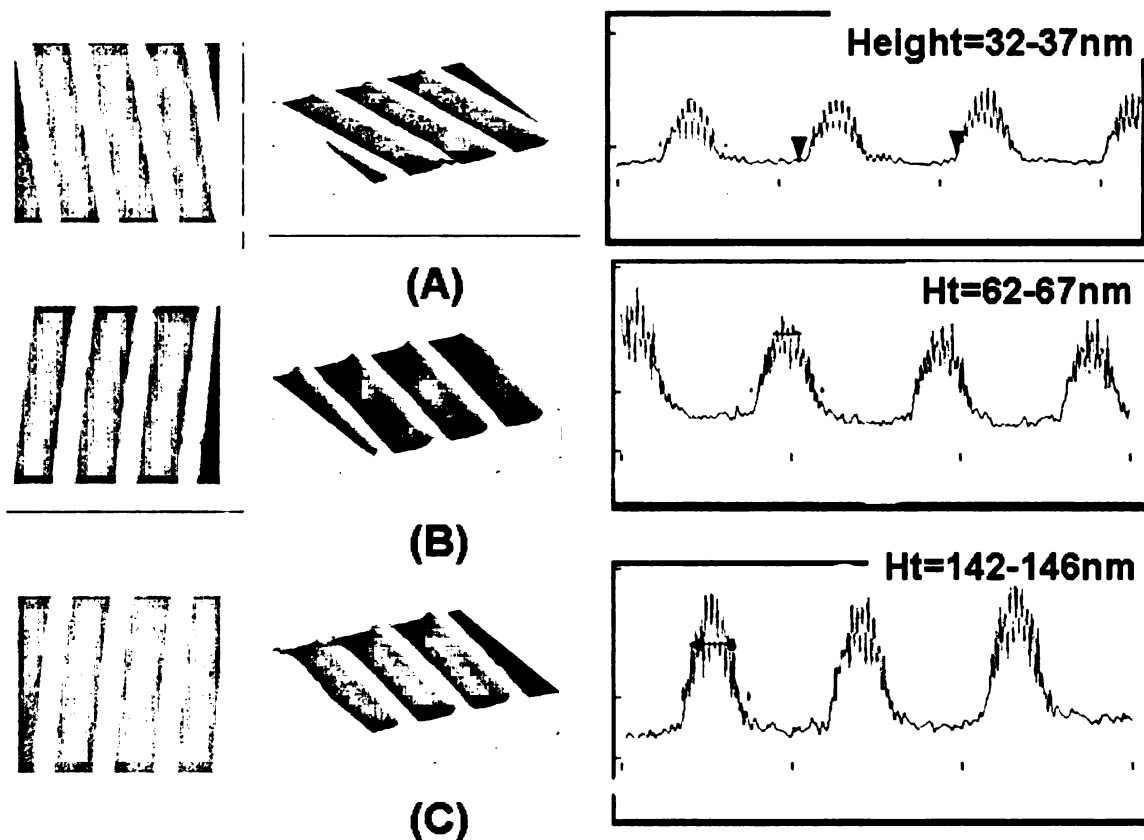
Figure 4.7. AFM images and topography of complex microstructures with different number of bilayers of PDAC/SPS built atop the m-dPEG acid patterns. (a) 10 bilayers (b) 20 bilayers and (c) 40 bilayers.

4.4 CONCLUSIONS

Micropatterning of the m-dPEG self-assembled monolayers has been demonstrated on PEM films as well as the building of subsequent 3-D micropatterned PEM structures on top of PEMs. Microfabrication of the functional and structured surfaces and interfaces were made using electrostatic interactions at the layered interfaces. In this work, the micropatterning of small PEG modified molecules, m-dPEG acid on polymer surfaces (PEM films) were achieved purely by electrostatic interactions. The stamping process was optimized by evaluating various conditions such as the inking method, the concentration, the contact times and the need for plasma treatment of the

stamps. Our results indicate that the strength of the ionic interactions between the acid and amine groups was the determining variable during the stamping process. This variable was controlled mainly by the pH of the ink solution and the contact time. Strong polyelectrolytes such as PDAC and SPS are highly ionized over all or most of the pH range. On the other hand, the m-dPEG acid molecule undergo ionic interaction with PDAC when its acid group is completely ionized, which depends on the pH of the m-dPEG acid ink solution. Clean pattern transfer occurred for pH greater than the pKa value of m-dPEG acid. By patterning an initial set of multilayer films with a resistant molecule followed by subsequent deposition of multilayer films, permitted the building of complex 3-D microstructures. These new patterned and structured surfaces have potential applications in microelectronic devices, electro-optical and biochemical sensors. Finally, possibilities also exist in a variety other areas that capitalize upon the formation of patterns and complex microstructures, including biotechnological and biomedical applications.

CHAPTER 5 SALT TUNABLE m-dPEG ACID PATTERNS ON POLYELECTROLYTE MULTILAYERS: TEMPLATES FOR DIRECTED DEPOSITION OF MACROMOLECULES

5.1 INTRODUCTION

Over the past decades, the development of new methods for fabricating thin films that provide precise control of the three-dimensional topography and cell adhesion has generated lots of interest. These films could lead to significant advances in the fields of tissue engineering, drug delivery and biosensors which have become increasingly germane applications in the field of chemical engineering. The ability to engineer surface properties such as hydrophobicity, charge, and adhesion at the micrometer scale are critical to the success of emerging technologies (e.g., bio-sensors, optical technologies and tissue engineering). Self-assembled monolayers (SAMs) have been extensively used to modify and control properties of gold and silicon surfaces.[5] Patterned alkanethiol SAM surfaces have been created using microcontact printing[6] and UV photopatterning techniques,[7] however, the intricacy of surface patterns that can be created with established approaches are limited. Methods to control both the reactivity and surface properties after self-assembly are required to create more complex patterned surfaces. Existing techniques to control the reversibility and reactivity of the surfaces include sophisticated methods, such as, light and UV-induced, and electrochemical surface modifications.[8-10] These methods tend to affect the morphology and properties of the surfaces underneath the SAMs and are not compatible when extended to biological systems involving cells and proteins.

The ionic layer-by-layer (LBL) assembly technique, introduced by Decher in 1991,[23] has emerged as a versatile and inexpensive method of constructing polymeric thin films, with nanometer-scale control of ionized species. Films formed by electrostatic interactions between oppositely charged poly-ion species to create alternating layers of sequentially adsorbed poly-ions are called "Polyelectrolyte Multilayers (PEMs)". PEMs have long been utilized in such applications as sensors, eletrochromics, and nanomechanical thin films but more recently they have also been shown to be excellent candidates for biomaterial applications due to 1) their biocompatibility and bioinertness,[31-33] 2) the ability to incorporate biological molecules, such as proteins,[26, 34] and 3) the high degree of molecular control of the film structure and thickness providing a much simpler approach to construct complex 3D surfaces as compared with photolithography.[35, 149] We, as well as others including Hammond et al, have demonstrated the ability of this layer by layer technology to readily construct complex 3D surfaces.[96, 127] This is particularly relevant in tissue engineering where ultimately the material must have the potential to rebuild a whole organ. In addition, the biodegradability of PEMs for tissue engineering and implantable device applications have been demonstrated by Lynn and co-workers[36] which is very useful in drug delivery applications.

Poly(ethylene glycol) (PEG) can serve as an excellent coating materials to augment the biocompatibility of biomaterials as it is a water soluble, nontoxic, nonantigenic and nonimmunogenic polymer, attaches to surface with very little effect on bulk properties and reduces protein adsorption and cell adhesion.[127-132] Surface modification with PEG can either be effected through physical adsorption or covalent

immobilization such as grafting and chemical coupling.[150-152] In this work, we demonstrate an alternative, dynamic approach that can switch surface properties from resistive to active by treating with high salt solutions. We have engineered this new class of salt responsive PEG patterns PEM films by first developing resistive patterns of m-d-poly(ethylene glycol) (m-dPEG) acid molecules onto PEMs and subsequently removing the SAMs from the PEM surface by treating with salt solutions creating a new active surface. Unlike other approaches, our approach is biocompatible and does not affect the properties of cells, proteins or other biological systems attached on the surface.
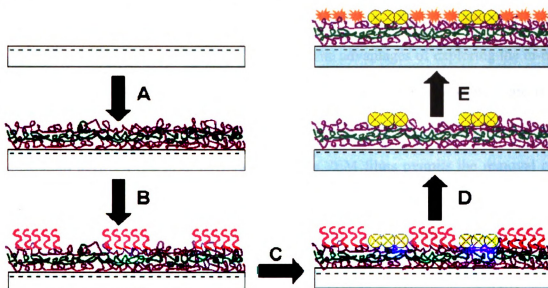
Figure 5.1. Diagram Illustrating the Formation of Salt Tunable m-dPEG Acid SAMs on a PDAC/SPS Multilayer Platform Scheme (A) PEMs (PDAC/SPS)₁₀.₅ build on top of the substrates (B) Patterned PEG SAMs on PEMs (C) Directed assembly of molecules due to the presence of resistive PEG SAMs (D) PEG SAMs are removed by treating it with salt giving rise to new active regions (E) The new active regions are filled with new set of molecules. The chemical structure of m-dPEG acid molecule.

In this chapter, we describe the process of creating chemically patterned and physically structured surfaces by stamping molecules of m-dPEG acid (scheme shown in Figure 5.1) with activated carboxylic acid group at one end. The activated carboxylate functional group ionically binds to the topmost positive surface of the PEM surfaces and

the other end (PEG units) resists the deposit of subsequent polymer (polyelectrolyte) layers. This poly-ionic adsorption enables the development of complex surface structures and templates for selective layer-by-layer deposition. In addition to the generation of complex 3-D microstructure films, [96] the PEG molecules can be used to create areas of selective adsorption on the multilayer films. PEG and its oligomeric derivatives have thus far been the most effective molecules to resist nonspecific adsorption of polyelectrolytes, charged particles, proteins and cells onto surfaces from aqueous solution.[96, 127, 130, 132] We capitalized upon the ionic interactions to deposit thin, uniform SAM patterns of PEG atop the PEM films and evaluated the factors that influence the effective transfer of m-dPEG acid molecules on and off the multilayer films. The advantages of exploring the m-dPEG acid molecule as the removable molecular template for selective deposition are i) PEG molecules can self-assemble to form resistive monolayers on PEMs, and ii) the tunable interaction between the PEG molecules and the PEM films permits the removal of the SAMs from the surface without compromising the underlying films or damaging the biological systems attached to the PEM surface. The patterned films were characterized by optical microscopy and atomic force microscopy (AFM). The effects of pH and salt on the PEG SAMs were investigated by optical microscopy, reflectance-absorption infrared spectroscopy, and spectroscopic ellipsometry. The PEG patterns were removed from the PEM surface at certain pH and salt conditions without affecting the PEM films underneath the SAMs. The removal of the PEG SAMs and the stability of the PEM films underneath it were investigated via ellipsometry and optical microscopy.

5.2 METHODS AND MATERIALS

5.2.1 Materials

Sulfonated poly(styrene), sodium salt (SPS) (M_w = 70000), poly(diallyldimethylammonium chloride) (PDAC) (M_w =100000-200000) as a 20 wt % solution, and sodium chloride were purchased from Aldrich Chemical, Milwaukee, WI. The m-dPEG acid molecule (M_w = 236) was obtained from Quanta Biodesign. Poly(dimethylsiloxane) (PDMS) from the Sylgard 184 silicone elastomer kit (Dow Corning, Midland, MI) was used to prepare stamps. The fluorosilanes was purchased from Aldrich Chemical. These PDMS stamps were used for microcontact printing.Glass slides (Corning Glass Works, Corning, NY), used for making the polyelectrolyte multilayer films, were cleaned using a Bransonic ultrasonic cleaner (Bransonic Ultrasonic Corporation, Danbury, CT). Carboxyfluorescein (6-CF), fluorescence dye, was purchased and used as received from Sigma. Carboxylated polystyrene latex particles (4 μm diameter), purchased from Polysciences, were used for colloidal adsorption study on m-dPEG self-assembled monolayer patterned polyelectrolyte templates.

5.2.2 Preparation of Polyelectrolyte Multilayers

PDAC and SPS polymer solutions were prepared with deionized (DI) water at concentrations of 0.02M and 0.01M, respectively, (based on the repeating unit molecular weight) with the addition of 0.1M NaCl salt. A Carl Zeiss slide stainer equipped with a custom-designed ultrasonic bath was connected to a computer to perform layer-by-layer assembly. To form the first bilayer, the tissue culture polystyrene (TCPS) plates were immersed for 20 min in a polycation solution. Following two sets of 5 min rinses with agitation, the TCPS plates were subsequently placed in a poylanion solution and allowed to deposit for 20 min. Afterwards, the 6 well plates were rinsed twice for 5 min each.

This process was repeated to build multiple layers. All experiments were performed using ten (i.e., 20 layers) or ten and half bilayers (i.e., 21 layers).

5.2.3 Preparation of PDMS Stamps

An elastomeric stamp is made by curing poly(dimethylsiloxane) (PDMS) on a microfabricated silicon master, which acts as a mold, to allow the surface topology of the stamp to form a negative replica of the master. The poly(dimethylsiloxane) (PDMS) stamps were made by pouring a 10:1 solution of elastomer and initiator over a prepared silicon master.[17] The silicon master was pretreated with fluorosilanes to facilitate the removal of the PDMS stamps from the silicon masters. The mixture was allowed to cure overnight at 60°C.

5.2.4 Stamping of m-dPEG Acid

The stamping conditions were varied to optimize the microcontact printing of the m-dPEG acid. PDMS stamps with and without plasma treatment were tested to stamp the ink. The optimized conditions, as determined by us in our previous work, were used for making PEG patterns.[96] The stamped regions were designed to act as resists to adsorption as the oligoethylene glycol graft chains of PEG did.[20] In the procedure of creating complex 3-D microstructures, m-dPEG acid was stamped onto the PEM surface (PDAC surface) followed by sequential adsorption layer-by-layer deposition process to build additional patterned polyelectrolyte multilayers outside the stamped region.

5.2.5 Characterization

A Nikon Eclipse ME 600 optical microscope (Nikon, Melville, NY) was used to obtain dark field images of the m-dPEG acid patterns and the additional microfabricated PEMs. A Nikon Eclipse E 400 microscope was used to obtain the fluorescence images. The 6-

carboxyfluorescein (6-CF) dye was used to visualize the m-dPEG SAM patterns on PEM following the stamping and rinsing processes. The dye was dissolved directly in 0.1 M NaOH; samples were imaged by dipping the substrates into the dye solution. The dye, which is negatively charged, preferentially stained the positively charged PDAC surface. The dyed regions appear green when viewed with the fluorescence optical microscope, using a FITC filter. Images were captured with a digital camera and processed on a Pentium computer running camera software.

5.2.6 Ellipsometry

Ellipsometric measurements were obtained with a rotating analyzer ellipsometer (model M-44; J.A. Woollam) using WVASE32 software. Substrate parameters (n and k) were measured after absorption of MPA. This ensures that any changes in substrate reflectivity due to Au-S bonds will not affect subsequent measurements. The angle of incidence was 75° for all experiments. The thickness values for PEM films were determined using 44 wavelengths between 414.0 and 736.1 nm.

5.3 RESULTS AND DISCUSSION

5.3.1. Directed Assembly of Macromolecules

The resistive nature of the PEG SAMs was demonstrated with various kinds of macromolecules such as colloid particles, proteins, nucleic acids and formation of subsequent multilayers over the PEG SAMs. We demonstrated that the PEG molecules created areas of selective adsorption on the multilayer films and be used in the subsequent generation of 3-D microstructure films. The patterned films were characterized by optical microscopy and atomic force microscopy (AFM).
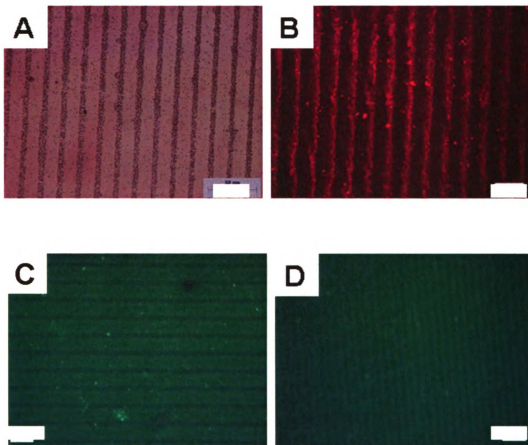
Figure 5.2. Optical microscope images of directed deposition of macromolecules on PEG patterns (A) 0.5μm colloid particles (brown lines). (B) Alexa Fluoro tagged sADH (C) Carboxyfluorescein (D) FITC tagged nucleic acid The dark lines represent the m-dPEG acid regions.

The PEG patterns resulted in the directed deposition of a wide range of macromolecules including colloidal particles, proteins, polymers such as dyes and nucleic acids as illustrated in Figure 5.2. When the negatively charged carboxylated polystyrene PS particles (Diameter = 0.5 μm) were added on top of the m-dPEG acid patterns on top of the (PDAC/SPS)$_{10.5}$, the particles attached on the PEM surface and did not attach on the PEG region resulting in the formation of patterns of particles as shown in Figure 5.2 A.
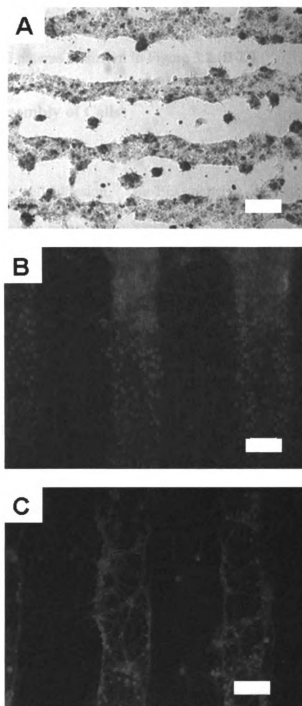
Figure 5.3. Optical microscope images of directed deposition of cells on PEG patterns (A) primary hepatocytes (B) fibroblast (C) primary neurons.

We also added alexa-fluoro tagged secondary alcohol dehydrogenase (sADH), negatively

charged carboxyfluorescein dye and FITC-tagged nucleic acids on top of the PEG

patterns and it resulted in the directed deposition of these macromolecules due to the presence of the PEG paterns as shown in Figure 5.2 (B-D).

5.3.2 Directed Assembly of Cells

PEG molecules are also known to reduce cell adhesion and commonly used in biomaterials to resist cell adhesion.[19] Our PEG patterns directed the deposition of a wide variety of cells including primary hepatocytes, primary neurons and fibroblasts as seen in Figure 5.3. can serve as an excellent coating materials to augment the biocompatibility of biomaterials as it is a water soluble, nontoxic, nonantigenic and nonimmunogenic polymer, attaches to surface with very little effect on bulk properties and reduces protein adsorption and cell adhesion.

5.3.3 Salt tunable PEG SAMs

m-dPEG acid patterns are formed on PEM films using microcontact printing and visualized with fluorescence microscopy using a dye specific to positive surfaces. As shown in Figure 5.4A, the dye (carboxyfluorescein) attaches selectively to the positive poly(diallyldimethylammoniumchloride) (PDAC) surface and results in patterns of green (PDAC) and dark (PEG) regions, thereby indicating the resistive property of the PEG patterns . When this surface is exposed to a salt solution, the PEG patterns are removed from the surface exposing the active PDAC surfaces underneath the SAMs (data not shown). As a proof-of-concept of the removable characteristic of the PEG films, a layer of SPS are added on top of the PEG patterns and due to the resistive nature of the PEG SAMs, the SPS preferentially formed a layer on the non-PEG (PDAC) surfaces resulting in alternating regions of PEG and SPS surfaces. When this surface are treated with salt,

the PEG patterns are removed from the surface resulting in alternating regions of PDAC (green) and SPS (dark) as shown in Figure 5.4 B. Further evidence of the removed PEG SAMs is obtained through ellipsometer experiments. The ellipsometric data in Figure
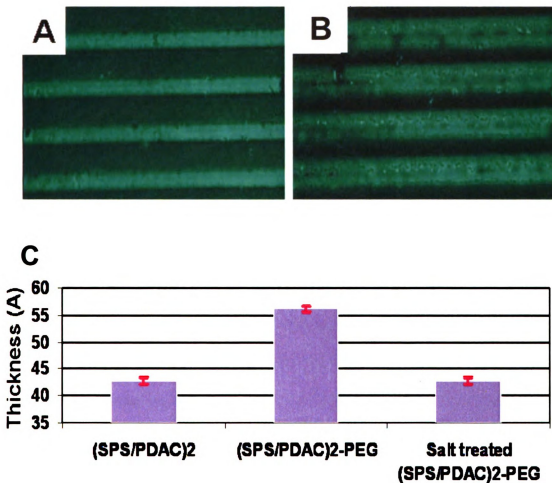
Figure 5.4. Fluorescent Images of PEG patterns (A) before and (B) after salt treatment (C) Ellipsometric data on the PEG patterns before and after salt treatment

5.4 C suggests an increase of about 13-15 Å in thickness when PEG SAMs are attached on the PEM films and upon exposure to salt the thickness of the films decreased to the original thickness.

5.3.4 Patterned Array of Multiple Particles on PEG Patterns

We evaluated the potential applications for these removable PEG patterns by attaching various molecules before and after salt treatment to demonstrate the versatility of these surfaces. The resistive nature of the PEG patterns is used to achieve directed assembly of a wide range of macromolecules such as colloid particles, proteins and formation of complex polyelectrolyte multilayer structures. As proof of the applicability of m-dPEG monolayer patterns on the PEM surface as a template for directed assembly of molecules, negatively charged carboxylated polystyrene PS particles (Diameter = 0.5 μm) were used. m-dPEG acid molecules are stamped on top of the $(PDAC/SPS)_{10.5}$ as shown in Figure 5.5 A and the colloidal particles deposited selectively over the positive $(PDAC/SPS)_{10.5}$ surface but not on the m-dPEG self-assembled monolayer regions. When the particle-deposited surfaces were treated with salt, the particles remained attached and intact while the PEG SAMs are removed exposing the underlying active PDAC surface.

Next particles of 0.2μm diameter are deposited over the exposed surfaces resulting in a two particle system as shown in Figure 5.5 B. This effective method provides a flexible and versatile approach to the fabrication of composite colloidal structures and the technique can be adapted utilizing different shaped patterned surfaces and other monodisperse colloidal particles such as silica and metal-doped particles of varying size and surface functionality, and using functionalized spheres modified with PEMs to obtain electroluminescent, conducting and other properties. This approach has potential application in electronic and optical devices, direct colloid assembly, plastic electronics and thin film power devices.
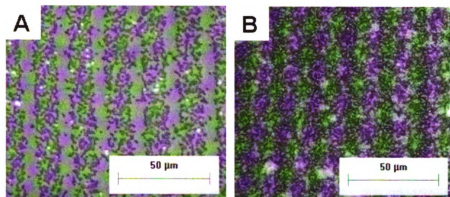
Figure 5.5. Phase constrast images of colloidal particles on PEG patterns before and after salt treatment (A) particles (D=0.5 μm) on the m-dPEG acid patterns before salt treatment (B) particles (D=0.2 μm) added onto surface A after salt treatment.

5.3.5 Patterned Array of Multiple Proteins on PEG Patterns

The applicability of removable resisting SAMs for biological applications is also evaluated using proteins and cells. Protein immobilization in micron and nano-scale patterns has importance for drug delivery, bioengineering, biosensors, and fundamental studies of cell biology, [19, 153, 154] but it is made challenging by the fragile structure of proteins and their tendency for nonspecific binding to surfaces. Several techniques such as photolithography,[155, 156] soft lithography,[19, 157] photochemical methods,[158] and dip-pen nanolithography[159] have been developed, which have primarily focused on the immobilization of one protein in defined regions surrounded by a "background" that lacks protein (and may be additionally resistant to the adsorption of other proteins from solution). However, to mimic complex cell-cell and cell-extracellular matrix interactions for studying problems in immunology, patterned surfaces comprising multiple functional protein regions on cellular and subcellular length scales would be useful. Few methods have been reported that allow patterning of multiple proteins on surfaces, and these may have limitations in spatial resolution,[160-162] in patterning fragile proteins that cannot

withstand dehydration,[163, 164] or exposure to organic solvents.[165] The removable PEG

surfaces we developed provide a template for designing multiple regions of different

proteins onto defined regions of a surface without exposing the proteins to irradiation,

organic solvents or dehydration. An advantage of this approach is that it exposes the

proteins to conditions within the narrow range of physiological pH, ionic strength and

temperature where their stability is greatest.
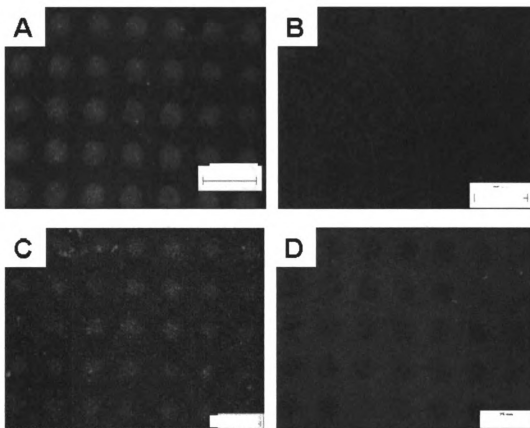
Figure 5.6. Fluorescent images of sADH protein attachment on PEG patterns before and after salt treatment (A,B) sADH tagged with Alexa-Fluoro on the m-dPEG acid patterns before salt treatment (C,D) sADH tagged with FITC added onto surface A after salt treatment. A, C are pictures taken using the red channel while B, D are taken using the green channel.

As shown in Figure 5.6, the same protein with different fluorescent tags are

attached onto the PEG patterns before and after salt treatment indicating that the salt

treatment did not affect the proteins that are attached to the PEM surface. Figure 5.6 (A,

B) shows the fluorescence images of the directed assembly of proteins on top of the PEG patterns in the red and green channel respectively before salt treatment. The red regions demonstrate the directed attachment of the sADH proteins to the PEMs and away from the resistive m-dPEG monolayer regions (black regions) while there is no proteins observed when imaged using the green channel. Alexa-Fluoro tagged sADH protein deposited selectively over the positive $(PDAC/SPS)_{10.5}$ surface but not on the m-dPEG self-assembled monolayer regions. When the protein-deposited surfaces were treated with salt, the proteins remained attached and intact while the PEG SAMs are removed exposing the underlying active PDAC surface. Next FITC-tagged sADH are deposited over the exposed surfaces resulting in a two protein array as shown in Figure 5.6 (C, D).

5.3.6 Patterned Array of Multiple Cells on PEG Patterns

Tissue formation and cellular function *in vivo* are regulated by diverse biological factors including cell–cell communication, cell–matrix interactions, and soluble factors. The ability to recreate such interactions *in vitro* may lead to advances in diverse fields, ranging from cell biology to tissue engineering. Approaches to manipulate the cell microenvironment, based on a number of fabrication strategies such as photolithography, microcontact printing, micromolding, inkjet printing and dip-pen spotting,[19, 72, 159, 166] have been conducted on micropatterned surfaces. In most approaches, the cells have been localized to adhesive regions on a substrate, thus limiting their use to one cell type. More recently, approaches have been developed to pattern two or more cell types in spatially defined co-cultures.[17] Many initial studies on patterned co-cultures have involved the selective adhesion of one cell type as compared to the adhesion of the other cell type. The removable PEG SAMs we developed provides surfaces that can be switched from cell-

repulsive to cell-adhesive using cell friendly conditions. This approach is advantageous since they can be used to form patterned co-cultures irrespective of the cell types or seeding order. In addition, this approach exposes the cells to conditions within the narrow physiological range of pH, ionic strength and temperature. As shown in Figure 5.7, the same cells with different fluorescence tags are attached onto the PEG patterns before and after salt treatment indicating that the salt treatment did not affect the cells that are attached to the PEM surface.
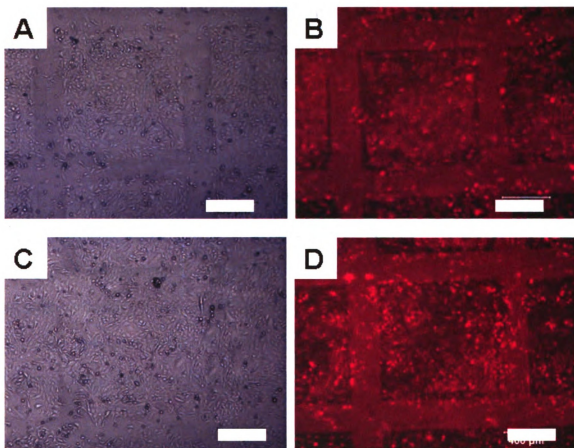
Figure 5.7. Optical microscope images of HeLa cells on PEG patterns before and after salt treatment. Phase contrast (A) and fluorescent images (B) of HeLa cells labeled red on the m-dPEG acid patterns before salt treatment. Phase contrast (C) and fluorescent images (D) of HeLa cells seeded onto the surface after salt treatment. Scale bar = 400 μm

5.4 CONCLUSIONS

In conclusion, we have shown that these PEG patterns can be removed using salt conditions that do not compromise the underlying polymers, charged particles and biological molecules, including living cells, deposited on the surface. These salt responsive PEG SAMs are ideal for optical technologies such as electroluminescent and conducting surfaces, where templates of multi-component particle arrays on PEMs are required. We have also shown that these removable surfaces can be used to form patterns of multiple proteins and cells, which may have applicability in drug delivery and tissue engineering applications. Removable surfaces provide a template for designing multiple regions of different protein, which is useful in immunology where complex cell-cell, cell-extracellular matrix interactions play important roles. Our approach avoids exposing the proteins to conditions outside the narrow range of physiological pH, ionic strength and temperature and thus maintains the stability of the proteins. This new approach provides an environmentally friendly and biocompatible route to designing versatile salt tunable surfaces. The template can be used to form arrays of nucleic acids, proteins and other biological molecules which have applications as biosensors and basic biological studies. The strategy presented here for the preparation of removable resistive SAMs provides a template to design various surfaces that can be used in a wide variety of applications.

CHAPTER 6 APTAMER AND siRNA BASED DRUG DELIVERY SYSTEM USING POLYELECTROLYTE MULTILAYERS

6.1 INTRODUCTION

For drug delivery applications, there is a need for the ability to deliver multiple biomolecules, e.g., proteins, genes, antibody, or drugs, to a targeted site of interest. Many delivery systems typically deliver one type of biomolecule at a time, e.g., one protein or one gene. The combination of targeted delivery and controlled drug release[167] is useful in treating various diseases where a cytotoxic dose of drug is required to be delivered to the unhealthy or cancerous cells over an extended period of time while leaving the surrounding healthy tissue alone. Polyelectrolyte multilayer (PEMs) are potential substrates for tissue engineering, drug delivery and implantable device applications. In this chapter, we propose using highly customizable PEM thin films to engineer surfaces for targeted drug delivery applications by integrating nucleic acid with PEM technology. The PEM technique has been applied successfully using DNA as a polyanionic building block[168, 169]. Interestingly, electrostatic interactions with positively charged polyelectrolytes have been demonstrated to protect DNA from degradation by nucleolytic activity[170]. This chapter deals with the fabrication of a novel targeted drug delivery system that attaches aptamers and small interfering RNA (siRNAs) onto PEM films.

Nucleic acid ligands, also called aptamers,[171, 172] have emerged as a novel class of ligands that rival antibodies in their potential for therapeutic and diagnostic applications.[173, 174] Aptamers are oligonucleotides that have high affinity and selectivity for various target compounds ranging from small molecules, such as drugs and dyes, to

complex biological molecules such as enzymes, peptides, and proteins.[175-177] These artificial receptors are selected from combinatorial oligonucleotide libraries for the target compound by an *in vitro* iterative process called SELEX (systematic evolution of ligands by exponential amplification).[171, 172] Use of aptamers for protein recognition instead of antibodies is of particular interest for assay developments, because the specificity and affinity of aptamers are equal or superior to those of antibodies.[178, 179] In addition, aptamers have a number of advantages as compared to antibodies, such as increased heat stability, tolerance to wide ranges of pH and salt concentrations, and ease of synthetic modification or immobilization.[178] Furthermore, unlike antibodies, aptamers are capable of being reversibly denatured, which facilitates capture and release of target compounds in reusable applications.[180] Currently, methods are being developed for aptamer immobilization onto solid surfaces for applications in protein capture, biosensors, and chromatographic separations.[181-184]

Influenza infections remain an important cause of morbidity and mortality, particularly in the elderly population, and carry the risk of pandemics; they also impose a considerable economic burden worldwide. The recently developed anti-influenza specific drug consisting of neuraminidase inhibitors, comprising of analogues of *N*-acetylneuraminic acid (*e.g.* oseltamivir and zanamivir), provide limited beneficial effect, reducing the duration of infection by 1 day, from 7 to 6 days.[185, 186] The influenza virus envelope carries two major immunogenic surface glycoproteins: hemagglutinin (HA)[187] and neuraminidase. HA plays a key role in initiating viral infection by binding to [the] sialic acid-containing receptors on host cells and mediating the subsequent viral entry and membrane fusion.[188-190] Infection by the influenza virus is initiated by the binding of the

virus to the host cell receptors via HA. Thus the approach taken in our present study is to incorporate the HA aptamer within the PEM films, which upon release from the films would bind directly to the HA protein on the virus neutralizing its ability to bind to their receptors on host cells. This would prevent the interaction of HA with the host cells, and thus infection by the virus.

siRNAs have emerged as a new and very efficient tool to downregulate gene expression in humans, animals and plants.[191] Many diseases develop from the undesired production of certain proteins. siRNA is a highly promising therapeutic approach for diseases resulting from aberrant protein production. siRNA has the potential of being a new universal drug therapy to treat a variety of human diseases such as cancer, rheumatoid arthritis, brain diseases, human immunodeficiency virus (HIV) and hepatitis C. However, the delivery of aptamers and siRNAs to targeted cells and tissues remains a challenge. There are many favorable characteristics of aptamers and siRNAs, including their small size, lack of immunogenicity, and ease of isolation, and have resulted in their application in clinical trials.[28, 192] Therefore, in this chapter we demonstrate the fabrication of aptamer and siRNA based targeted drug delivery systems using PEM films.

We have engineered aptamer and siRNA based targeted drug delivery systems using PEM films by capitalizing on electrostatic interaction between the polycations and the negatively charged nucleic acids. Nucleic acid patterns on PEMs were created by ionic interactions using microcontact printing (µCP). In this study, we chose a DNA aptamer that binds to thrombin as a model for integrating PEM and nucleic acid technologies. We selected a 15mer aptamer that forms a G-quartet for thrombin (Figure 6.1A) because it has already been screened by SELEX and has shown thrombin-

inhibiting activity.[193] This aptamer is one of the most well studied; its structure has already been determined[194-196] and the effect of its loop sequence on the G-quartet structure has also been investigated.[197] Extensive work to identify the binding site has been performed.[198-200] Additionally, the application of this thrombin-inhibiting aptamer as a drug to inhibit clot formation *in vivo*,[201-203] has been investigated along with its stability *in vitro*[204] and *in vivo*.[201]

A

5'- GGT TGG TTT GGT TGG -3'

B

5'-AATTAACCCTCACTAAAGGGCTGAG TCTCAAAACCGCAATACACTGGTTGT ATGGTCGAATAAGTTAA-3'

Figure 6.1 Structure of aptamers used in the study (A) 15mer oligonucleotide of DNA aptamer for thrombin. (B) aptamer for HA

6.2 METHODS AND MATERIALS

6.2.1 Materials

Poly(diallyldimethylammonium chloride) (PDAC) (Mw~100,000-200,000) as a 20 wt % solution, sulfonated poly(styrene), sodium salt (SPS) (Mw~70,000), poly-L-lysine (PLL), fluorosilanes and sodium chloride were purchased from Aldrich (Milwaukee, WI). Poly(dimethylsiloxane) (PDMS) from the Sylgard 184 silicone elastomer kit (Dow Corning, Midland, MI) was used to prepare stamps. The PDMS stamps were used for microcontact printing.[9] Dulbecco's Modified Eagle Medium (DMEM) with 4.5 g/l glucose, 10X DMEM, fetal bovine serum (FBS), penicillin and streptomycin were

purchased from Life Technologies (Gaithersburg, MD). Insulin and glucagon were purchased from Eli Lilly and Co. (Indianapolis, IN), epidermal growth factor, thrombin from Sigma Chemical (St. Louis, MO). Purified rat albumin was purchased from Cappel Laboratories (Aurora, OH). Adult female Sprague-Dawley rats were obtained from Charles River Laboratories (Boston, MA). DNA aptamer for thrombin (5'- GGT TGG TTT GGT TGG-3'), non-aptamer for thrombin (5'-GGT GGT GGT TGT GGT -3'), aptamer for Hemagglutinin (A22:5'-AAT TAA CCC TCA CTA AAG GGC TGA GTC TCA AAA CCG CAA TAC ACT GGT TGT ATG GTC GAA TAA GTT AA-3') and (A21:5'-AAT TAA CCC TCA CTA AAG GGC GCT TAT TTG TTC AGG TTG GGT CTT CCT ATT ATG GTC GAA TAA GTT AA-3') were obtained from Invitrogen (Carlsbad, California).

6.2.2 Preparation of Polyelectrolyte Multilayers

PDAC and SPS polymer solutions were prepared with deionized (DI) water at concentrations of 0.02M and 0.01M, respectively, (based on the repeating unit molecular weight) with the addition of 0.1M NaCl salt. A Carl Zeiss slide stainer equipped with a custom-designed ultrasonic bath was connected to a computer to perform layer-by-layer assembly. Polyelectrolyte dipping solutions were prepared with DI water supplied by a Barnstead Nanopure-UV 4 stage purifier (Barnstead International Dubuque, Iowa), equipped with a UV source and final 0.2 μm filter. Solutions were filtered with a 0.45 μm Acrodisc syringe filter (Pall Corporation) to remove particulates. TCPS plates were subjected to a Harrick plasma cleaner (Harrick Scientific Corporation, Broading Ossining, NY) for 10 min at 0.15 torr and 50 sccm flow of O_2 in a plasma chamber. To form the first bilayer, the TCPS plates were immersed for 20 min in a polycation

solution. Following two sets of 5 min rinses with agitation, the TCPS plates were subsequently placed in a polyanion solution and allowed to deposit for 20 min. Afterwards, the 6 well plates were rinsed twice for 5 min each. The samples were cleaned for 3 min in an ultrasonic cleaning bath after depositing a layer of polycation/polyanion pair. The sonication step removed weakly bounded polyelectrolytes on the substrate, forming uniform bilayers. This process was repeated to build multiple layers.

Alternating layers of PLL/nucleic acid multilayered films were assembled onto quartz slides, TCPS and gold slides depending on the experiments. The first layer of PLL was adsorbed onto the substrates by immersing them in 0.5mg/ml PLL solution for 10min. The PLL coated substrates were then washed with DI water and the nucleic acid was attached to the PLL layer by immersing the substrate in 200 μg/ml nucleic acid for 10 min. The process was alternately repeated until a desired number of bilayers were deposited.

6.2.3 Preparation of PDMS Stamps

An elastomeric stamp was made by curing PDMS on a microfabricated silicon master, which acts as a mold, to allow the surface topology of the stamp to form a negative replica of the master.[113] The PDMS stamps were made by pouring a 10:1 solution of elastomer and initiator over a prepared silicon master. The silicon master was pretreated with fluorosilanes to facilitate the removal of the PDMS stamps from the silicon master. The mixture was allowed to cure overnight at 60°C. The masters were prepared in the BioMEMS facilities at MGH East and consisted of various features (squares and lines).

6.2.4 Cell Culture

Hepatocyte Isolation

Primary rat hepatocytes were isolated from 2 months old adult female Sprague-Dawley rats (Charles River Laboratories, Boston, MA), according to a two-step collagenase perfusion technique described by Seglen [64] and modified by Dunn[61]. The liver isolations yielded 150-300 x 10^6 hepatocytes. Using trypan blue exclusion the viability ranged from 90 to 98 %. Primary hepatocyte culture medium consisted of DMEM supplemented with 10% FBS, 14 ng/ml glucagon, 20 ng/ml epidermal growth factor, 7.5μg/ml hydrocortisone, 200 μg/ml streptomycin (10,000 μg/ml) – penicillin (10,000 U/ml) solution, and 0.5 U/ml insulin.

Hepatocyte Culture

The cells were seeded under sterile tissue culture hoods and maintained at 37°C in a humidified air/CO_2 incubator (90/10 vol %). Primary hepatocytes were cultured on PEM coated 6-well TCPS. The multilayer coated TCPS plates were sterilized by spraying with 70 % ethanol and exposing them to UV light before seeding the cells onto these surfaces. The cell culture experiments were performed on PEM surfaces without adhesive proteins. Collagen coated TCPS and uncoated TCPS were used as controls in these studies. A collagen gel solution was prepared by mixing 9 parts of the 1.2 mg/ml collagen suspension in 1 mM HCl with 1 part of concentrated (10X) DMEM at 4°C. The control wells were coated with 0.5 ml of this collagen gel solution and the coated plates were incubated at 37°C for 1 hour. Freshly isolated hepatocytes were seeded at a density of 4×10^5 cells per well for 7 days. One ml of fresh medium was supplied daily to the cultures after removal of the supernatant. Samples were kept in a temperature and humidity controlled incubator.

NIH 3T3 Culture

NIH 3T3 fibroblast cell lines were purchased from American Tissue Type Collection. Cells grown to 70% confluence were trypsinized in 0.01% trypsin (ICN Biomedicals) solution in PBS for 10 min and re-suspended in 25mL media. Approximately 10% of the cells were seeded into a fresh tissue culture flask and the rest of the cells were used for the co-culture experiments. Fibroblast medium consisted of DMEM with high glucose, supplemented with 10% bovine calf serum and 200U/mL penicillin and 200μg/mL streptomycin.

6.2.5 Characterization

A Nikon Eclipse ME 600 optical microscope (Nikon, Melville, NY) was used to obtain dark field images of the m-dPEG acid patterns and the additional microfabricated PEMs. A Nikon Eclipse E 400 microscope was used to obtain the fluorescence images. The 6-carboxyfluorescein (6-CF) dye was used to visualize the m-dPEG SAM patterns on PEM following the stamping and rinsing processes. The dye was dissolved directly in 0.1 M NaOH; samples were imaged by dipping the substrates into the dye solution. The dye, which is negatively charged, preferentially stained the positively charged PDAC surface. The dyed regions appear green when viewed with the fluorescence optical microscope, using a FITC filter. Images were captured with a digital camera and processed on a Pentium computer running camera software. A Leica inverted phase contrast microscope with Soft RT 3.5 software was used to capture images of cell density, morphology, and spreading on the multilayer surfaces.

6.2.6 UV-Vis Spectroscopy and Ellispometry of PEM Films

The progressive build-up of the multilayered nucleic acid-coatings onto quartz substrates was monitored using a using a Perkin-Elmer UV/Vis (model Lambda 40) spectrophotometer. Measurements were taken after each successive layer. Growth of the multilayered nucleic acid-coatings was monitored by their incremental increases at 260 nm, the absorbance maximum of the nucleic base chromophores. All measurements were repeated three times. Ellipsometric thicknesses of films on gold-coated wafers (200 nm of Au sputtered on 20 nm of Cr on Si(100)) were determined using a rotating analyzer ellipsometer (model M-44, J. A. Woollam), assuming a film refractive index of 1.5.

6.3 Results and Discussion
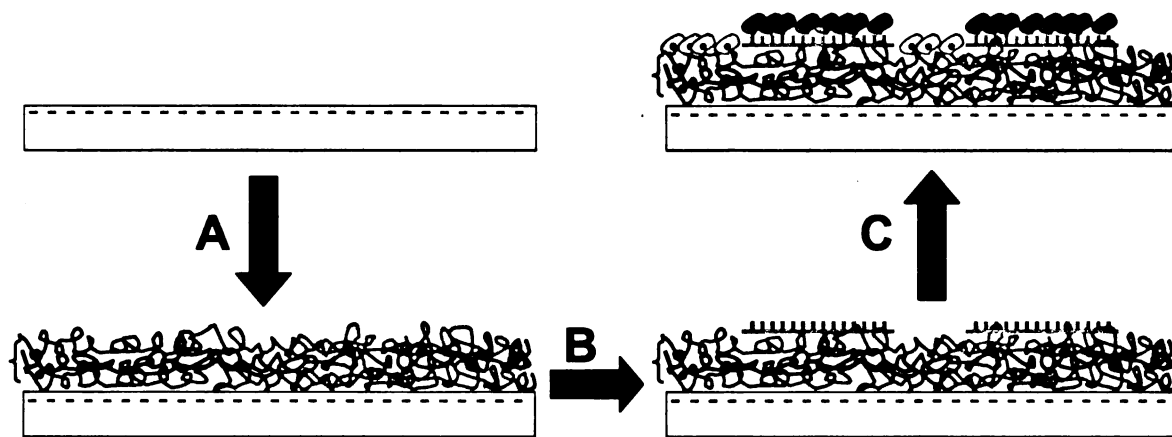
Figure 6.2. Scheme for making nucleic acid patterns on PEM surfaces (A) PEMs are built atop the substrate (B) Nucleic acids attached onto the PEM films via electrostatic interaction (C) Cells attached fluoresce due to uptake of the nucleic acid.

We capitalized upon the net negative charge of the nucleic acids of the aptamers and siRNAs to attach these nucleic acids onto positively charged PEM films. Electrostatic interactions with the positively charged polyelectrolytes have been demonstrated to protect the nucleic acids from degradation by nucleolytic activity,[170]

suggesting that this is a viable method of maintaining the activity of these molecules after surface immobilization. The overall scheme of the methodology is shown in Figure 6.2.

6.3.1 Surface Immobilization of Nuclei Acids on PEMs

The presence of nucleic acid molecules (siRNA and aptamer) on the PEM surfaces were characterized using FITC labeled oligos and with the help of µCP. We successfully immobilized and patterned nucleic acids on PEM films using electrostatic interaction of nucleic acids on top of the PEM thin films. These oligo molecules were imaged using fluorescent microscopy. We observed patterns of nucleic acids on the PEM films as shown in Figure 6.3.
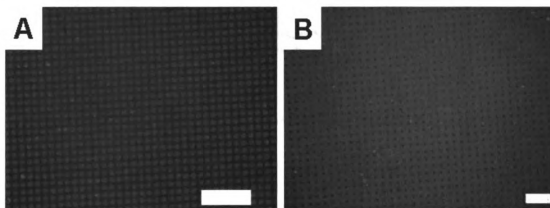
Figure 6.3. Fluorescent images of patterned FITC labeled nucleic acids on PEM surfaces (A) FITC taged HA aptamer patterns and (B) FITC tagged siRNA patterns on (PEI/SPS)$_{10.5}$.

6.3.2 Activity of Aptamer in PEM Film

To determine whether the aptamer are stable and functional upon surface immobilization, we evaluated the ability of the protein to recognize its aptamer as well as the specificity of the nucleic acids for its protein. The PEM films were µCP with patterns of thrombin and HA aptamers on the same surface (Figure 6.4A), upon which various proteins were subsequently added to the aptamer patterns to determine whether the
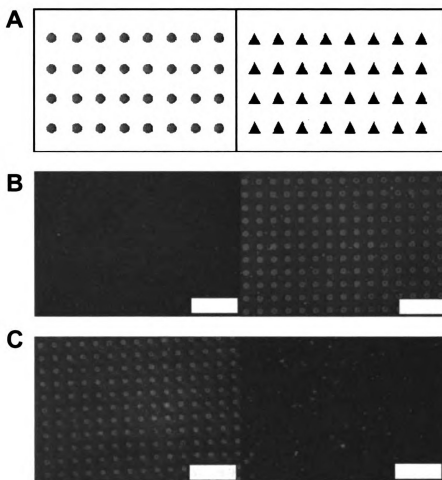
Figure 6.4. Fluorescent images of aptamer immobilized on PEM films (A) Scheme of the aptamer patterns on the PEM films. Circles represents HA aptamer and triangles represents thrombin aptamer (B) FITC tagged thrombin and (C) FITC tagged HA added on top of the aptamer patterns

immobilized aptamers maintained their specificity for their proteins, in this case the thrombin protein. Fig. 6.4 (B, C) represents typical fluorescence images of aptamer microarrays when they are incubated with a single individual analyte. Both HA and thrombin aptamers immobilized on the PEM surfaces yielded a highly specific response to their corresponding target protein and showed no cross-reactivity with the other proteins. As shown in Figure 6.4 (B,C), FITC tagged HA did not bind to the thrombin aptamer patterns and the FITC tagged thrombin did not bind to the HA aptamer patterns and the tagged proteins attached preferentially onto the corresponding aptamer regions as

demonstrated in Figure 6.4 (B,C). This study provides a proof of concept that the aptamers are still active after surface immobilization and binds specifically to its target protein.

6.3.3 Monitoring of PEM Deposition Process

(A)
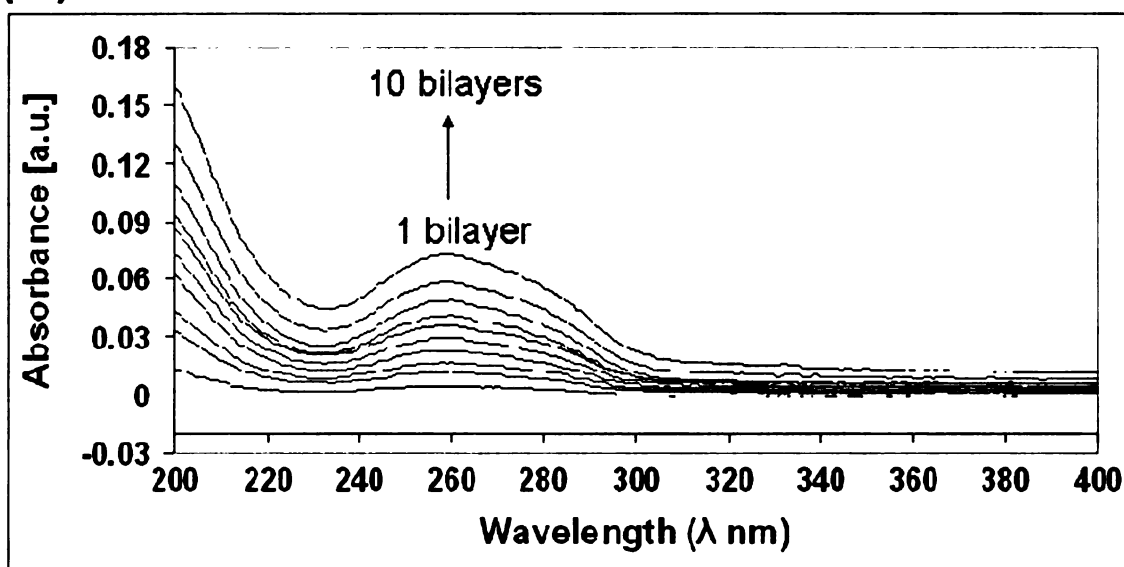
(B)
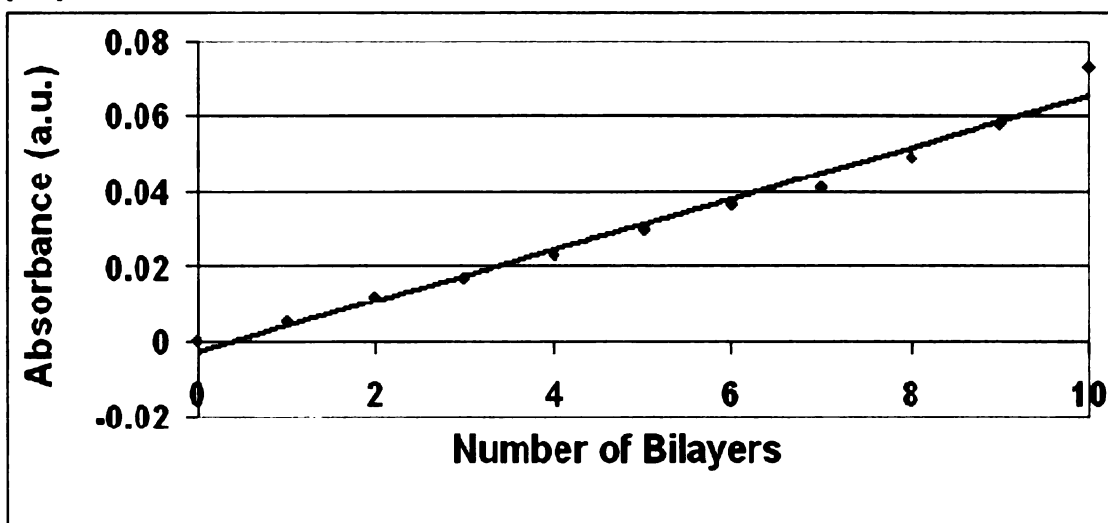
Figure 6.5 (A) UV-absorption spectra of (PLL/thrombin aptamer) multilayer coatings, and (B) plots of absorbance at 260nm. The UV-absorption spectra were monitored using quartz substrates after the deposition of 1-10 bilayers.

The build-up of multilayered nucleic acid-coatings on quartz substrates via UV-Vis spectrophotometry could be easily monitored using the DNA base chromophores (absorbance maximum at 260 nm). As illustrated in Figure 6.5, multilayered thrombin aptamer-coatings showed an increase in UV-absorbance spectrum with every successive double-layer addition. DNA contributes a characteristic absorption band at 260 nm. Two points are worth noting. First, the absorbance plot at 260 nm shows an increase with the bilayer number, suggesting that DNA molecules have been successively incorporated into the film. Second, a linear increase in the UV–vis absorbance of the films is observed with the addition of each layer (Figure 6.5 B). These observations indicate that the aptamers are being incorporated within the PEM films and the multilayers are formed due to the negative charge of the nucleic acids, i.e. acting as a polyanion. Similar experiments were performed with aptamers for the HA antigenic proteins present on the influenza virus. The build up of the films was followed by UV-Vis and ellipsometry and the change in thickness was measured after each bilayer addition. As shown in Figure 6.6, the absorbance intensity and thickness of the films increased linearly with the increase in the number of bilayers which indicates the incorporation of the HA aptamer within the PEM films.
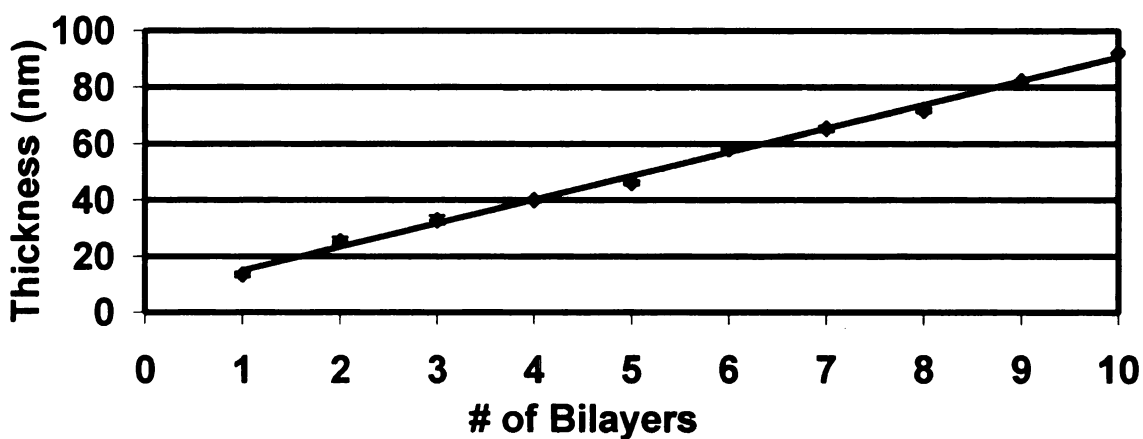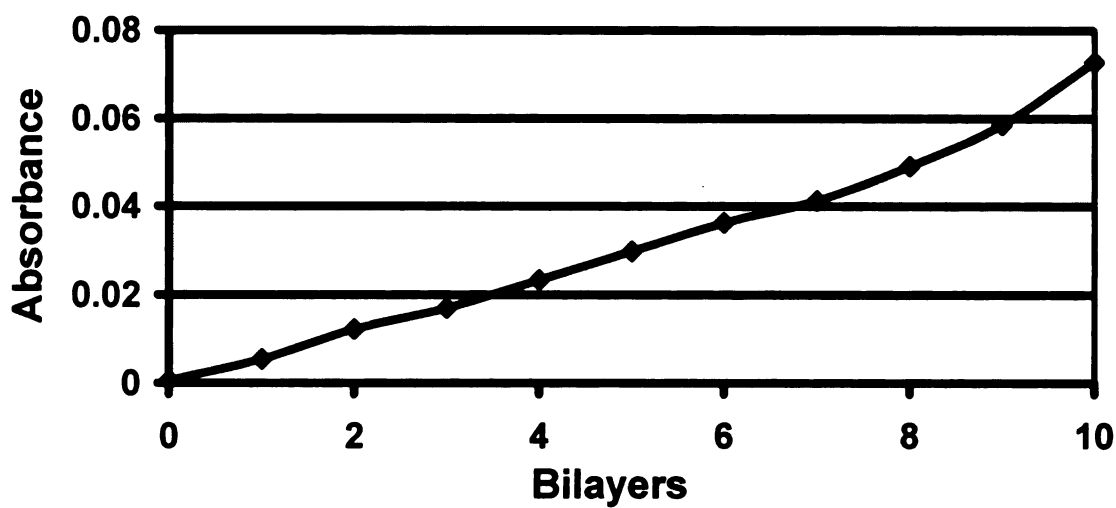
Figure 6.6 (A) Plots of UV-Vis absorbance at 260nm of (PLL/HA aptamer) multilayer coatings. The UV-absorption spectra were monitored using quartz substrates after the deposition of 1-10 bilayers The thickness of multilayered films increased as a function of number of bilayers as measured by ellipsometry. Values are given as mean ± standard deviation (n=3).

6.3.4 Deconstruction of the PEM Films
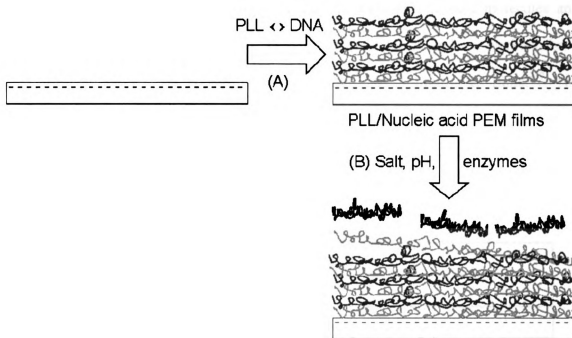
Figure 6.7 The schematic construction and deconstruction of PLL/DNA PEM films via layer-by-layer as aptamer/siRNA delivery system. (A) Construction of the films by layer-by-layer deposition of PLL and nucleic acid, and (B) deconstruction of the films

Numerous studies have shown that PEM films can be degraded under physiological conditions under enzymes, pH or changing ionic strengths.[205-207] We demonstrated that the nucleic acid encapsulated multilayer films can be deconstructed by controlling the ionic strength in the solution. The aptamers/siRNA can be released under physiological conditions, schematically illustrated in Figure 6.7. UV-Vis and ellipsometer were used to monitor the deconstruction of the PEM films and the loss of the nucleic acids embedded within the films. As seen in Figure 6.8, the film was deconstructed or dissociated after incubating the DNA aptamer/PEM films in 0.5M NaCl solution. During the construction of the films, the PLL/nucleic acid complexes or PLL/nucleic acid segment ion pairs formed, which stabilized the films.[207, 208] When the films are incubated

in concentrated salt solution, the salt ions attach to the complexes or the ion pairs. This weakens or breaks the interaction between the PLL and nucleic acid molecules and results in the loss of the nucleic acid molecules. Dubas and co-workers have demonstrated salt-induced deconstruction of (PAA/PDAC) multilayer films.[209] The kinetics of the salt induced deconstruction of PEM films varied with the NaCl concentration. Increasing the NaCl concentration increased the extent and rate of the film deconstruction.
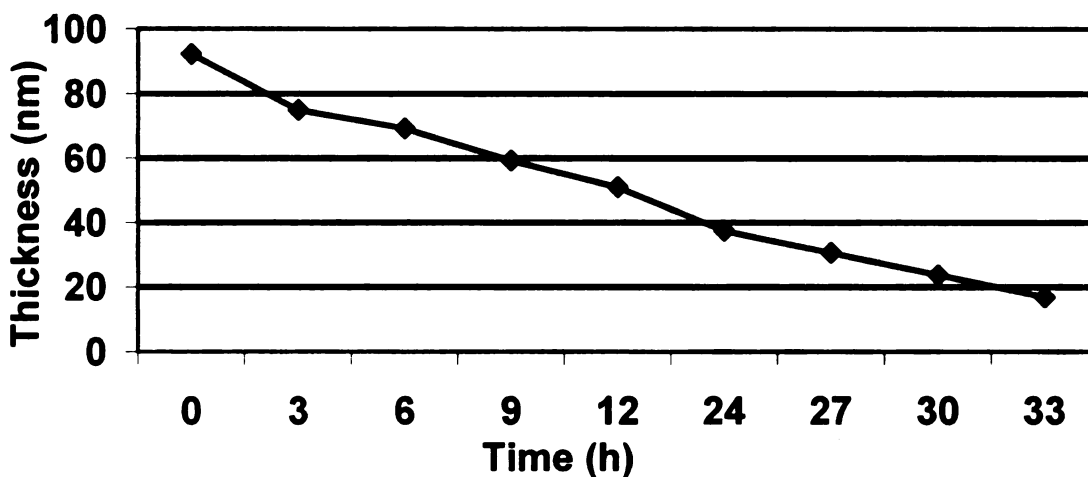
Figure 6.8 The thickness of multilayered films decreased as a function of degradation time. Values are given as mean ± standard deviation (n=3).

To further examine the stability of the released aptamers, multilayer films were constructed by incorporating FITC tagged HA aptamer within the PEM films. The PEM films were then treated with 0.25M salt solution resulting in the release of aptamers due to the deconstruction of the PEM films. The released aptamers were then added to the surface with HA and thrombin patterns. As illustrated in Figure 6.9, the released FITC tagged HA aptamers bound only to the HA peptide on the surface did not bind to the surface immobilized with thrombin surface, thereby indicating that the aptamer was

active and retained its specificity for its corresponding protein upon released from the PEM films when treated with salt.
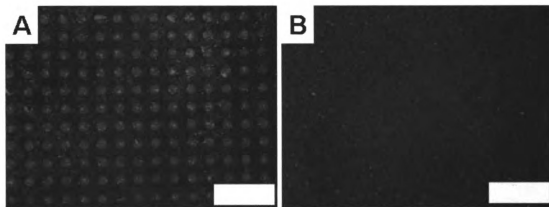
Figure 6.9. Fluorescent images of released FITC tagged HA aptamer binding onto patterns of (A) HA and (B) thrombin.

6.3.5 Cell Uptake of Released Nucleic Acids from PEM Films

In vitro experiments demonstrating the uptake by cells of nucleic acids immobilized on the PEM surfaces was performed with block-iT™ fluorescent oligo. These oligo molecules are fluorescein-labeled, double stranded RNA duplex with the same length, charge and configuration as standard siRNAs. When the cells take up this RNA, they begin to fluoresce as shown in Figure 6.9. We examined the cell uptake of the nucleic acids immobilized on the PEM surfaces using two types of mammalian cells: transformed 3T3 fibroblasts (3T3s) and primary hepatocytes. The cells started to fluoresce after 6 days which demonstrated the possibility that this effect may be extended to aptamers and siRNA molecules immobilized on PEM surfaces.
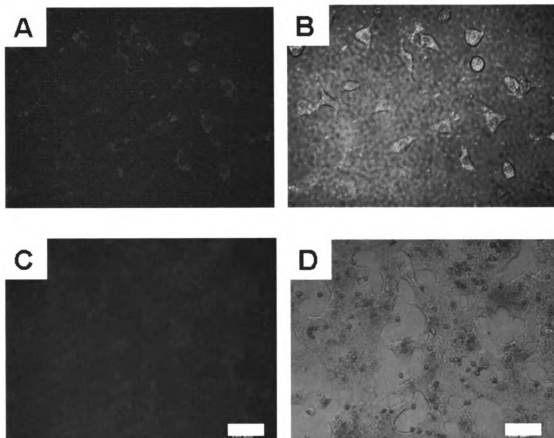
Figure 6.10. In vitro fluoroescence microscope images of cells on PEM surfaces with immobilized fluroescent oligos. Left panels show the fluorescent images and the rigth panels show the merged image of phases contrast and fluorescent images of (A,B) fibroblast and (C,D) primary hepatocytes.

6.4 Conclusions

In this chapter we demonstrated that PEM thin films can be a template for aptamer and siRNA molecules for drug delivery applications. Our preliminary studies indicated that the FITC labeled RNAs immobilized on PEM surfaces were taken up by fibroblasts and primary hepatocytes suggesting this effect may be extended to aptamers and siRNA molecules immobilized on PEM surface. Future studies will focus on targeting a specific biomolecule with aptamer or siRNA molecules attached on PEM surfaces. A comparative study with several cell types, such as cell lines and primary cells,

will be performed to determine the delivery efficiency of DNA vs RNA molecules to the

different cell types.

CHAPTER 7 CONCLUSIONS

This thesis has shown that PEMs are extremely versatile thin film assemblies for engineering surfaces to control cell adhesion and for drug delivery applications. The multilayers are chemically rich matrices in which molecules such as proteins, nucleic acids and cells can interact with the thin films. Moreover, the physical structure and chemical architecture of the multilayers are tunable and customizable by simple means such as assembly solution conditions (e.g., pH, salt) and choice of polyelectrolytes. PEMs films are excellent candidates for biomaterial applications, provide flexibility in building complex three-dimensional architectures and also provide an ability to control the arrangement of multiple cell types with subcellular resolution.

Chapter 2 demonstrated the ability of PEM films to control the adhesion of primary cells (primary hepatocytes and neurons) without the help of adhesive ligands/proteins and further formed patterns of these cells using microcontact printing. The primary cells attached preferentially on PEM films with SPS as the topmost surface. We capitalized upon this differential cell attachment and spreading of primary hepatocytes and neurons on PDAC and SPS surfaces to control the adhesion of the primary cells and form patterns of the cells. The cell patterns were achieved without the help of adhesive proteins/ligands. We demonstrated that the hydrophobic and cell resistant PDMS surfaces can be made to be cell adhesive surfaces by coating with PEM films. We also demonstrated that the addition of topographical features on the PEM coated surfaces provided an alternative approach to chemistry for controlling the attachment of primary cells (hepatocyes) and the attachment and growth of transformed cells (3T3 fibroblasts and HeLa cells). We further used these films as templates for

patterned co-cultures of primary hepatocytes/fibroblasts and primary neurons /astrocytes on the PEM surfaces as described in Chapter 3. The patterned co-cultures enhanced the function and viability of the primary cells for extended time period *in vitro*. This technique we developed provides a useful tool for engineering neuronal and hepatocyte co-culture systems, which may more accurately capture liver and neuronal cell function and metabolism in normal versus diseased states.

Chapter 4 described the development of novel self-assembled monolayer (SAM) patterns of m-d-poly(ethylene glycol) (m-dPEG) acid molecules onto PEMs. The created m-dPEG acid monolayer patterns on PEMs acted as resistive templates, and thus prevented further deposits of consecutive poly(anion)/poly(cation) pairs of charged particles and resulted in the formation of three-dimensional (3-D) patterned PEM films or selective particle depositions atop the original multilayer thin films. These new patterned and structured surfaces have potential applications in microelectronic devices and electro-optical and biochemical sensors. Chapter 5 demonstrated that the PEG patterns developed are tunable at certain salt conditions and can be removed from the PEM surface without affecting the PEM layers underneath the patterns. These removable surfaces provide an alternative method to form patterns of multiple particles, proteins and cells. This new approach provides an environmentally friendly and biocompatible route to designing versatile salt tunable surfaces.

Chapter 6 described the use of multilayers to engineer aptamer and siRNA based drug delivery systems. We capitalized on the negative charge of aptamer and siRNA molecules to attach these molecules on PEMs by electrostatic interaction. We demonstrated the successful immobilization and patterning of aptamers and siRNAs on

PEM films using electrostatic interaction of nucleic acids on top of the thin films. These films were degraded under biocompatible conditions and the nucleic acids were released to the cell culture. The cell uptake of these molecules also showed the proof of concept that these films can be designed to release a wide range of molecules after incorporating them into these films.

This thesis has laid the foundation to explore in detail the ability of PEM films to control cell adhesion for a variety of cells and also for the delivery of a wide variety of drug molecules. We found PEMs are compatible with a wide variety of cells including primary hepatocytes and primary neurons which have difficulty adhering *in vitro*. We developed PEG patterns which act as a universal resist group for a wide variety of cells and can be extended to form co-cultures without requiring a tunable adhesive/resistive surface that is cell-specific. Future work will focus on using this removable PEG surface to create patterned co-cultures of different cell combinations critical for the function of tissues *in vivo*. The tunable PEG patterns can be extended to develop targeted delivery systems that can simultaneously immobilize multiple drugs and to form arrays of proteins and nucleic acids for biosensors. The PEM films can also be used to encapsulate multiple siRNA and aptamer molecules within the films to target multiple genes for a variety of diseases. PEM films provide us with the ability to incorporate multiple drugs or biomolecules which may increase the efficiency of the delivery system and help prolong the efficacy of the drug molecules.

APPENDIX 1: Definitions

A. SELEX

In vitro selection, or **SELEX**, is a technique that allows the simultaneous screening of highly diverse pools of different RNA or DNA (dsDNA or ssDNA) molecules for a particular feature. In 1990, the laboratories of G. F. Joyce (La Jolla), J.W. Szostak (Boston), and L. Gold (Boulder) independently developed a technique which allows the simultaneous screening of more than 10^{15} individual nucleic acid molecules for different functionalities. This method is commonly known as "*in vitro* selection", "*in vitro* evolution" or "SELEX" (systematic evolution of ligands by exponential enrichment). With the *in vitro* selection-technique large random pools of nucleic acids can be screened for a particular functionality, such as the binding to small organic molecules, large proteins or the alteration or de novo generation of ribozyme-catalysis. Functional molecules ("aptamers" a linguistic chimaera composed of the latin *aptus* = to fit and the greek suffix *-mer*) are selected from the mainly non-functional pool of RNA or DNA by column chromatography or other selection techniques that are suitable for the enrichment of any desired property. The method is conceptually straightforward: in a standard DNA-oligonucleotide synthesizer a starting pool is generated. The machine synthesizes an oligonucleotide with a completely random base-sequence which is flanked by defined primer binding sites. In this way, up to 10^{15} different DNA molecules can be synthesized at once. The immense complexity of the generated pool justifies the assumption that it contains a few molecules with the correct receptor structure or with tertiary structures which lead to catalytic activity; these are selected, for example by affinity

chromatography or filter binding. Because a pool of such high complexity can be expected to contain only a very small fraction of functional molecules, several purification steps are usually required. Therefore, the very rare active molecules are amplified by the polymerase chain reaction (PCR) or in a transcription-based step. In this way, iterative cycles of selection can be carried out. Successive selection and amplification cycles result in an exponential increase in the abundance of functional sequences, until they dominate the population. The method has been applied to a number of different applications; for example, *in vitro* selection has proven to be extremely efficient for the identification of bases which cannot be changed without loss of function and are important in ribozymes, or in a protein binding site in a (ds or ss)DNA or RNA molecule. Recently, *in vitro* selection has been used for the de novo isolation of catalytic RNAs. These include ribozymes with ligation activity, isomerases and ribozymes which catalyze the ATP-dependent phosphorylation of RNA oligonucleotides. The basis for the latter two ribozymes was the isolation of RNAs for specific binding to small substrate molecules, for which several examples exist. RNA- and DNA-aptamers have been isolated, which not only bind tightly to proteins, but also are able to inhibit their biological activity.

B. Advantages of Aptamers

- are chemically stable to all but the harshest environmental conditions and can be boiled or frozen without loss of activity.

- may be produced on the benchtop using standard molecular biological techniques or they may be chemically synthesized at microgram to kilogram scales.

- As synthetic molecules, they are amenable to a nearly infinite variety of modifications designed to optimize their properties for a specific application.

- They may be circularized, linked together in pairs, or clustered onto the surface of a fat globule.

- For *in vivo* applications, aptamers can be modified to dramatically reduce their sensitivity to degradation by enzymes in the blood.

- Other chemical appendages can alter their biodistribution or plasma residence time following intravenous injection. This plasticity is a distinct advantage of aptamers over other types of molecular ligands, such as monoclonal antibodies, where chemical modification is often variable, difficult to control, and may harm the function of the molecule.

LIST OF PUBLICATIONS

The following publications were made as a direct result of the research carried out for this project.

Published and accepted journal articles:

1) "Selective Depositions on Polyelectrolyte Multilayers: Self-Assembled Monolayers of m-dPEG Acid as Molecular Templates" **Srivatsan Kidambi,** Christina Chan, Ilsoon Lee. *J. Am. Chem. Soc.* **126,** 4697-4703, **2004.**

2) "Controlling Primary Hepatocyte Adhesion and Spreading on Protein Free Polyelectrolyte Multilayer Films" **Srivatsan Kidambi,** Ilsoon Lee, Christina Chan. *J. Am. Chem. Soc.* **126** (50), 16286 -16287, **2004.**

3) "Cell Adhesion on Polyelectrolyte Multilayer coated PDMS Surfaces with Varying Topographies" **Srivatsan Kidambi,** Natasha Udpa, Stacey Schroeder, Ilsoon Lee, Christina Chan. *Tissue Engineering* (in press), **2006.**

4) "Selective Adhesion of Primary Hepatocytes on Polyelectrolyte Multilayers: Template for Patterned Cell Co-culture" **Srivatsan Kidambi,** Lufang Sheng, Mehmet Toner, Martin Yarmush, Ilsoon Lee, Christina Chan. *Macromol Biosci* (in press), **2006.**

Journal articles submitted for review or in preparation:

1) "Patterned Co-culture of Neurons and Astrocytes on Polyelectrolyte Multilayer Films for Studying Astrocyte Mediated Oxidative Stress in Neurons" **Srivatsan Kidambi,** Ilsoon Lee, Christina Chan. submitted to *Advanced Functional Materials,* **2006.**

2) "Salt Responsive m-dPEG Acid Self Assembled Monolayers on Polyelectrolyte Multilayers" **Srivatsan Kidambi,** Christina Chan, Ilsoon Lee., in preparation, *Nature Materials,* **2007.**

3) "Construction and degradation of multilayerd PLL/Aptamer films" **Srivatsan Kidambi,** Ilsoon Lee, Christina Chan., in preparation, *Nature Chemical Biology,* **2007.**

4) "Cell Targeted Delivery of siRNAs using Polyelectrolyte Multilayer Templates" **Srivatsan Kidambi,** Ilsoon Lee, Christina Chan., in preparation, *Nature Chemical Biology,* **2006.**

BIBLIOGRAPHY

1.   Amiji, M.; Park, K., Prevention of protein adsorption and platelet adhesion on surfaces by PEO/PPO/PEO triblock copolymers. *Biomaterials* **1992**, 13, (10), 682-92.

2.   Harris, J. M.; Dust, J. M.; McGill, R. A.; Harris, P. A.; Edgell, M. J.; Sedaghat-Herati, R. M.; Karr, L. J.; Donnelly, D. L., New polyethylene glycols for biomedical applications. *ACS Symposium Series* **1991**, 467, (Water-Soluble Polym.), 418-29.

3.   Singhvi, R.; Kumar, A.; Lopez, G. P.; Stephanopoulos, G. N.; Wang, D. I.; Whitesides, G. M.; Ingber, D. E., Engineering cell shape and function. *Science* **1994**, 264, (5159), 696-8.

4.   Chen, C. S.; Mrksich, M.; Huang, S.; Whitesides, G. M.; Ingber, D. E., Geometric control of cell life and death. *Science* **1997**, 276, (5317), 1425-1428.

5.   Ulman, A., An Introduction to Ultrathin Organic Films. *An Introduction to Ultrathin Organic Films* **1991**, Academic: Newyork.

6.   Kumar, A.; Whitesides, G. M., Patterned condensation figures as optical diffraction gratings. *Science* **1994**, 263, (5143), 60-2.

7.   Huang, J.; Dahlgren, D. A.; Hemminger, J. C., Photopatterning of Self-Assembled Alkanethiolate Monolayers on Gold: A Simple Monolayer Photoresist Utilizing Aqueous Chemistry. *Langmuir* **1994**, 10, (3), 626-8.

8.   Huang, J. Y.; Dahlgren, D. A.; Hemminger, J. C., Photopatterning of Self-Assembled Alkanethiolate Monolayers on Gold - a Simple Monolayer Photoresist Utilizing Aqueous Chemistry. *Langmuir* **1994**, 10, (3), 626-628.

9.   Kumar, A.; Biebuyck, H. A.; Whitesides, G. M., Patterning Self-Assembled Monolayers: Applications in Materials Science. *Langmuir* **1994**, 10, (5), 1498-511.

10.   Bain, C. D.; Whitesides, G. M., Molecular-Level Control over Surface Order in Self-Assembled Monolayer Films of Thiols on Gold. *Science* **1988**, 240, (4848), 62-63.

11.   Ratner, B. D., New ideas in biomaterials science. A path to engineered biomaterials. *Journal of Biomedical Materials Research* **1993**, 27, (7), 837-50.

12. Anderson, J. M., Biological responses to materials. *Annual Review of Materials Research* **2001**, 31, 81-110.

13. Hubbell, J. A., Bioactive biomaterials. *Current Opinion in Biotechnology* **1999**, 10, (2), 123-129.

14. Santini, J. T.; Cima, M. J.; Langer, R., A controlled-release microchip. *Nature* **1999**, 397, (6717), 335-338.

15. Tao, S. L.; Desai, T. A., Microfabricated drug delivery systems: from particles to pores. *Advanced Drug Delivery Reviews* **2003**, 55, (3), 315-328.

16. Grayson, A. C. R.; Choi, I. S.; Tyler, B. M.; Wang, P. P.; Brem, H.; Cima, M. J.; Langer, R., Multi-pulse drug delivery from a resorbable polymeric microchip device. *Nature Materials* **2003**, 2, (11), 767-772.

17. Bhatia, S. N.; Balis, U. J.; Yarmush, M. L.; Toner, M., Effect of cell-cell interactions in preservation of cellular phenotype: cocultivation of hepatocytes and nonparenchymal cells. *FASEB journal* **1999**, 13, (14), 1883-900.

18. Xia, Y.; Whitesides, G. M., Soft lithography. *Angewandte Chemie, International Edition* **1998**, 37, (5), 550-575.

19. Whitesides, G. M.; Ostuni, E.; Takayama, S.; Jiang, X.; Ingber, D. E., Soft lithography in biology and biochemistry. *Annual Review of Biomedical Engineering* **2001**, 3, 335-373.

20. Mitchell, P., Microfluidics - downsizing large-scale biology. *Nature Biotechnology* **2001**, 19, (8), 717-721.

21. Walker, G. M.; Zeringue, H. C.; Beebe, D. J., Microenvironment design considerations for cellular scale studies. *Lab on a Chip* **2004**, 4, (2), 91-97.

22. Khademhosseini, A.; Langer, R., Nanobiotechnology: drug delivery and tissue engineering. *Chemical Engineering Progress* **2006**, 102, (2), 38-42.

23. Decher, G., Fuzzy nanoassemblies: toward layered polymeric multicomposites. *Science* **1997**, 277, (5330), 1232-1237.

24. Thierry, B.; Kujawa, P.; Tkaczyk, C.; Winnik, F. M.; Bilodeau, L.; Tabrizian, M., Delivery Platform for Hydrophobic Drugs: Prodrug Approach Combined with Self-Assembled Multilayers. *Journal of the American Chemical Society* **2005**, 127, (6), 1626-1627.

25. LaVan, D. A.; Lynn, D. M.; Langer, R., Moving smaller in drug discovery and delivery. *Nature Reviews Drug Discovery* **2002**, 1, (1), 77-84.

26. Lvov, Y.; Ariga, K.; Ichinose, I.; Kunitake, T., Assembly of Multicomponent Protein Films by Means of Electrostatic Layer-by-Layer Adsorption. *Journal of the American Chemical Society* **1995**, 117, (22), 6117-23.

27. Jessel, N.; Atalar, F.; Lavalle, P.; Mutterer, J.; Decher, G.; Schaaf, P.; Voegel, J.-C.; Ogier, J., Bioactive coatings based on a polyelectrolyte multilayer architecture functionalized by embedded proteins. *Advanced Materials (Weinheim, Germany)* **2003**, 15, (9), 692-695.

28. Vinores, S. A., Technology evaluation: pegaptanib, Eyetech/Pfizer. *Current Opinion in Molecular Therapeutics* **2003**, 5, (6), 673-679.

29. Xia, H. B.; Mao, Q. W.; Paulson, H. L.; Davidson, B. L., siRNA-mediated gene silencing in vitro and in vivo. *Nature Biotechnology* **2002**, 20, (10), 1006-1010.

30. Flemming, A., Infectious disease - Topical microbicide based on siRNA. *Nature Reviews Drug Discovery* **2006**, 5, (1), 19-19.

31. Richert, L.; Lavalle, P.; Vautier, D.; Senger, B.; Stoltz, J. F.; Schaaf, P.; Voegel, J. C.; Picart, C., Cell interactions with polyelectrolyte multilayer films. *Biomacromolecules* **2002**, 3, (6), 1170-1178.

32. Elbert, D. L.; Herbert, C. B.; Hubbell, J. A., Thin Polymer Layers Formed by Polyelectrolyte Multilayer Techniques on Biological Surfaces. *Langmuir* **1999**, 15, (16), 5355-5362.

33. Mendelsohn, J. D.; Yang, S. Y.; Hiller, J.; Hochbaum, A. I.; Rubner, M. F., Rational design of cytophilic and cytophobic polyelectrolyte multilayer thin films. *Biomacromolecules* **2003**, 4, (1), 96-106.

34.   Decher, G.; Lehr, B.; Lowack, K.; Lvov, Y.; Schmitt, J., New nanocomposite films for biosensors: layer-by-layer adsorbed films of polyelectrolytes, proteins or DNA. *Biosensors & Bioelectronics* **1994**, 9, (9/10), 677-84.

35.   Jiang, X.; Zheng, H.; Gourdin, S.; Hammond, P. T., Polymer-on-Polymer Stamping: Universal Approaches to Chemically Patterned Surfaces. *Langmuir* **2002**, 18, (7), 2607-2615.

36.   Vazquez, E.; Dewitt, D. M.; Hammond, P. T.; Lynn, D. M., Construction of Hydrolytically-Degradable Thin Films via Layer-by-Layer Deposition of Degradable Polyelectrolytes. *Journal of the American Chemical Society* **2002**, 124, (47), 13992-13993.

37.   Berthiaume, F.; Moghe, P. V.; Toner, M.; Yarmush, M. L., Effect of extracellular matrix topology on cell structure, function, and physiological responsiveness: hepatocytes cultured in a sandwich configuration. *FASEB Journal* **1996**, 10, (13), 1471-1484.

38.   Grant, M. H.; Anderson, K.; McKay, G.; Wills, M.; Henderson, C.; MacDonald, C., Manipulation of the phenotype of immortalized rat hepatocytes by different culture configurations and by dimethyl sulfoxide. *Human & Experimental Toxicology* **2000**, 19, (5), 309-317.

39.   Gramowski, A.; Schiffmann, D.; Gross, G. W., Quantification of acute neurotoxic effects of trimethyltin using neuronal networks cultured on microelectrode arrays. *Neurotoxicology* **2000**, 21, (3), 331-342.

40.   Gross, R. A.; Uhler, M. D.; Macdonald, R. L., The Reduction of Neuronal Calcium Currents by Atp-Gamma-S Is Mediated by a G-Protein and Occurs Independently of Cyclic Amp-Dependent Protein-Kinase. *Brain Research* **1990**, 535, (2), 214-220.

41.   Kamioka, H.; Maeda, E.; Jimbo, Y.; Robinson, H. P. C.; Kawana, A., Spontaneous periodic synchronized bursting during formation of mature patterns of connections in cortical cultures. *Neuroscience Letters* **1996**, 206, (2-3), 109-112.

42.   Jimbo, Y.; Robinson, H. P. C.; Kawana, A., Strengthening of synchronized activity by tetanic stimulation in cortical cultures: Application of planar electrode arrays. *Ieee Transactions on Biomedical Engineering* **1998**, 45, (11), 1297-1304.

43. Shahaf, G.; Marom, S., Learning in networks of cortical neurons. *Journal of Neuroscience* **2001**, 21, (22), 8782-8788.

44. Corey, J. M.; Feldman, E. L., Substrate patterning: an emerging technology for the study of neuronal behavior. *Experimental Neurology* **2003**, 184, S89-S96.

45. Ravenscroft, M. S.; Bateman, K. E.; Shaffer, K. M.; Schessler, H. M.; Jung, D. R.; Schneider, T. W.; Montgomery, C. B.; Custer, T. L.; Schaffner, A. E.; Liu, Q. Y.; Li, Y. X.; Barker, J. L.; Hickman, J. J., Developmental neurobiology implications from fabrication and analysis of hippocampal neuronal networks on patterned silane-modified surfaces. *Journal of the American Chemical Society* **1998**, 120, (47), 12169-12177.

46. Liu, Q. Y.; Coulombe, M.; Dumm, J.; Shaffer, K. M.; Schaffner, A. E.; Barker, J. L.; Pancrazio, J. J.; Stenger, D. A.; Ma, W., Synaptic connectivity in hippocampal neuronal networks cultured on micropatterned surfaces. *Developmental Brain Research* **2000**, 120, (2), 223-231.

47. Ma, W.; Liu, Q. Y.; Jung, D.; Manos, P.; Pancrazio, J. J.; Schaffner, A. E.; Barker, J. L.; Stenger, D. A., Central neuronal synapse formation on micropatterned surfaces. *Developmental Brain Research* **1998**, 111, (2), 231-243.

48. Chang, J. C.; Brewer, G. J.; Wheeler, B. C., Modulation of neural network activity by patterning. *Biosensors & Bioelectronics* **2001**, 16, (7-8), 527-533.

49. Chang, J. C.; Brewer, G. J.; Wheeler, B. C., A modified microstamping technique enhances polylysine transfer and neuronal cell patterning. *Biomaterials* **2003**, 24, (17), 2863-2870.

50. Marois, Y.; Sigot-Luizard, M.-F.; Guidoin, R., Endothelial cell behavior on vascular prosthetic grafts: effect of polymer chemistry, surface structure, and surface treatment. *ASAIO Journal* **1999**, 45, (4), 272-280.

51. Bordenave, L.; Bareille, R.; Lefebvre, F.; Caix, J.; Baquey, C., Cytocompatibility study of NHLBI primary reference materials using human endothelial cells. *Journal of Biomaterials Science, Polymer Edition* **1992**, 3, (6), 409-16.

52. Park, J. H.; Park, K. D.; Bae, Y. H., PDMS-based polyurethanes with MPEG grafts: synthesis, characterization and platelet adhesion study. *Biomaterials* **1999**, 20, (10), 943-953.

53.   Sherman, M. A.; Kennedy, J. P.; Ely, D. L.; Smith, D., Novel polyisobutylene/polydimethyl siloxane bicomponent networks: III. Tissue compatibility. *Journal of Biomaterials Science, Polymer Edition* **1999**, 10, (3), 259-269.

54.   van Kooten, T. G.; Whitesides, J. F.; von Recum, A. F., Influence of silicone (PDMS) surface texture on human skin fibroblast proliferation as determined by cell cycle analysis. *Journal of Biomedical Materials Research* **1998**, 43, (1), 1-14.

55.   Ertel, S. I.; Ratner, B. D.; Kaul, A.; Schway, M. B.; Horbett, T. A., In vitro study of the intrinsic toxicity of synthetic surfaces to cells. *Journal of Biomedical Materials Research* **1994**, 28, (6), 667-75.

56.   Dahrouch, M.; Schmidt, A.; Leemans, L.; Linssen, H.; Goetz, H., Synthesis and properties of poly(butylene terephthalate)-poly(ethylene oxide)-poly(dimethylsiloxane) block copolymers. *Macromolecular Symposia* **2003**, 199, (Polycondensation 2002), 147-162.

57.   Interrante, L. V.; Shen, Q.; Li, J., Poly(dimethylsilylenemethylene-co-dimethylsiloxane): A Regularly Alternating Copolymer of Poly(dimethylsiloxane) and Poly(dimethylsilylenemethylene). *Macromolecules* **2001**, 34, (6), 1545-1547.

58.   Cunningham, J. J.; Nikolovski, J.; Linderman, J. J.; Mooney, D. J., Quantification of fibronectin adsorption to silicone-rubber cell culture substrates. *BioTechniques* **2002**, 32, (4), 876,878,880,882,884,886-887.

59.   Makamba, H.; Hsieh, Y. Y.; Sung, W. C.; Chen, S. H., Stable permanently hydrophilic protein-resistant thin-film coatings on poly(dimethylsiloxane) substrates by electrostatic self-assembly and chemical cross-linking. *Analytical Chemistry* **2005**, 77, (13), 3971-3978.

60.   Ai, H.; Lvov, Y. M.; Mills, D. K.; Jennings, M.; Alexander, J. S.; Jones, S. A., Coating and selective deposition of nanofilm on silicone rubber for cell adhesion and growth. *Cell Biochemistry and Biophysics* **2003**, 38, (2), 103-114.

61.   Dunn, J. C.; Tompkins, R. G.; Yarmush, M. L., Long-term in vitro function of adult hepatocytes in a collagen sandwich configuration. *Biotechnology Progress* **1991**, 7, (3), 237-45.

62.   Decher, G.; Lvov, Y.; Schmitt, J., Proof of Multilayer Structural Organization in Self-Assembled Polycation Polyanion Molecular Films. *Thin Solid Films* **1994**, 244, (1-2), 772-777.

63.   Kumar, A.; Whitesides, G. M., Features of gold having micrometer to centimeter dimensions can be formed through a combination of stamping with an elastomeric stamp and an alkanethiol \"ink\" followed by chemical etching. *Applied Physics Letters* **1993**, 63, (14), 2002-4.

64.   Seglen, P. O., Preparation of isolated rat liver cells. *Methods in Cell Biology* **1976**, 13, 29-83.

65.   Marini, A. M.; Paul, S. M., N-Methyl-D-aspartate receptor-mediated neuroprotection in cerebellar granule cells requires new RNA and protein synthesis. *Proceedings of the National Academy of Sciences of the United States of America* **1992**, 89, (14), 6555-9.

66.   Nicoletti, F.; Wroblewski, J. T.; Novelli, A.; Alho, H.; Guidotti, A.; Costa, E., The activation of inositol phospholipid metabolism as a signal-transducing system for excitatory amino acids in primary cultures of cerebellar granule cells. *Journal of Neuroscience* **1986**, 6, (7), 1905-11.

67.   Hamprecht, B.; Loeffler, F., Primary glial cultures as a model for studying hormone action. *Methods in Enzymology* **1985**, 109, (Horm. Action, Pt. 1), 341-5.

68.   Chandler, L. J.; Newsom, H.; Sumners, C.; Crews, F., Chronic ethanol exposure potentiates NMDA excitotoxicity in cerebral cortical neurons. *Journal of Neurochemistry* **1993**, 60, (4), 1578-81.

69.   Cutler, R. G.; Kelly, J.; Storie, K.; Pedersen, W. A.; Tammara, A.; Hatanpaa, K.; Troncoso, J. C.; Mattson, M. P., Involvement of oxidative stress-induced abnormalities in ceramide and cholesterol metabolism in brain aging and Alzheimer's disease. *Proceedings Of The National Academy Of Sciences Of The United States Of America* **2004**, 101, (7), 2070-2075.

70.   Mohammed, J. S.; DeCoster, M. A.; McShane, M. J., Micropatterning of nanoengineered surfaces to study neuronal cell attachment in vitro. *Biomacromolecules* **2004**, 5, (5), 1745-1755.

71.   Ruegg, U.; Hefti, F., Growth of Dissociated Neurons in Culture Dishes Coated with Synthetic Polymeric Amines. *Neuroscience Letters* **1984,** 49, (3), 319-324.

72.   Kidambi, S.; Lee, I.; Chan, C., Controlling primary hepatocyte adhesion and spreading on protein-free polyelectrolyte multilayer films. *Journal of the American Chemical Society* **2004,** 126, (50), 16286-16287.

73.   Alberts, B.; Alexander, J.; Lewis, J.; Raff, M.; Roberts, K.; Walter, P., *Molecular Biology of the Cell, 4th Edition*. 2004; p 2000 pp.

74.   McCaughan, G. W.; Gorrell, M. D.; Bishop, G. A.; Abbott, C. A.; Shackel, N. A.; McGuinness, P. H.; Levy, M. T.; Sharland, A. F.; Bowen, D. G.; Yu, D.; Slaitini, L.; Church, W. B.; Napoli, J., Molecular pathogenesis of liver disease: an approach to hepatic inflammation, cirrhosis and liver transplant tolerance. *Immunological Reviews* **2000,** 174, 172-191.

75.   Frangogiannis, N. G.; Smith, C. W.; Entman, M. L., The inflammatory response in myocardial infarction. *Cardiovascular Research* **2002,** 53, (1), 31-47.

76.   Curtis, A. S. G.; Wilkinson, C. D. W., Reactions of cells to topography. *Journal of Biomaterials Science, Polymer Edition* **1998,** 9, (12), 1313-1329.

77.   Langer, R.; Vacanti, J., Tissue Engineering. *Science* **1993,** 260, (5110), 920-926.

78.   van Breemen, C.; Skarsgard, P.; Laher, I.; McManus, B.; Wang, X., Endothelium-smooth muscle interactions in blood vessels. *Clin Exp Pharmacol Physiol* **1997,** 24, (12), 989-92.

79.   Schmidt, C.; Leach, J., Neural tissue engineering: Strategies for repair and regeneration. *Annual Review of Biomedical Engineering* **2003,** 5, 293-347.

80.   Feng, Y.; Walsh, C. A., Protein-protein interactions, cytoskeletal regulation and neuronal migration. *Nature Reviews Neuroscience* **2001,** 2, (6), 408-416.

81.   Haydon, P. G., Glia: listening and talking to the synapse. *Nature Reviews Neuroscience* **2001,** 2, (3), 185-193.

82.   Martin, E. D.; Araque, A.; Buno, W., Synaptic regulation of the slow Ca2+-activated K+ current in hippocampal CA1 pyramidal neurons: Implication in epileptogenesis. *Journal of Neurophysiology* **2001**, 86, (6), 2878-2886.

83.   Rao, K. V. R.; Panickar, K.; Jayakumar, A. R.; Norenberg, M. D., Astrocytes protect neurons from ammonia toxicity. *Neurochemical Research* **2005**, 30, (10), 1311-1318.

84.   Brown, D. R., Neurons Depend on Astrocytes in a Coculture System for Protection from Glutamate Toxicity. *Molecular and Cellular Neuroscience* **1999**, 13, (5), 379-389.

85.   Donato, M. T.; Gomez-Lechon, M. J.; Castell, J. V., Drug metabolizing enzymes in rat hepatocytes co-cultured with cell lines. *In Vitro Cellular & Developmental Biology* **1990**, 26, (11), 1057-62.

86.   Agius, L., Metabolic Interactions Of Parenchymal Hepatocytes And Dividing Epithelial-Cells In Co-Culture. *Biochemical Journal* **1988**, 252, (1), 23-28.

87.   Menzeleev, R.; Bozhkov, A.; Zvonkova, E.; Krasnopolskyii, Y.; Shvets, V., Enhancement of Liver-Cell Proliferation by Gm(3) Ganglioside. *Bullentin of Experimental Biology and Medicine* **1995**, 119, (4), 414-417.

88.   Guguen-Guillouzo, C.; Clement, B.; Baffet, G.; Beaumont, C.; Morel-Chany, E.; Glaise, D.; Guillouzo, A., Maintenance and reversibility of active albumin secretion by adult rat hepatocytes cocultured with another liver epithelial cell type. *Experimental Cell Research* **1983**, 143, (1), 47-54.

89.   Harimoto, M.; Yamato, M.; Hirose, M.; Takahashi, C.; Isoi, Y.; Kikuchi, A.; Okano, T., Novel approach for achieving double-layered cell sheets co-culture: overlaying endothelial cell sheets onto monolayer hepatocytes utilizing temperature-responsive culture dishes. *Journal of Biomedical Materials Research* **2002**, 62, (3), 464-470.

90.   Nandkumar, M. A.; Yamato, M.; Kushida, A.; Konno, C.; Hirose, M.; Kikuchi, A.; Okano, T., Two-dimensional cell sheet manipulation of heterotypically co-cultured lung cells utilizing temperature-responsive culture dishes results in long-term maintenance of differentiated epithelial cell functions. *Biomaterials* **2002**, 23, (4), 1121-1130.

91.   Bhatia, S. N.; Yarmush, M. L.; Toner, M., Controlling cell interactions by micropatterning in co-cultures: hepatocytes and 3T3 fibroblasts. *Journal of Biomedical Materials Research* **1997,** 34, (2), 189-99.

92.   Bhandari, R.; Riccalton, L.; Lewis, A.; Fry, J.; Hammond, A.; Tendler, S.; Shakesheff, K., Liver tissue engineering: A role for co-culture systems in modifying hepatocyte function and viability. *Tissue Engineering* **2001,** 7, (3), 345-357.

93.   Takayama, S.; McDonald, J. C.; Ostuni, E.; Liang, M. N.; Kenis, P. J. A.; Ismagilov, R. F.; Whitesides, G. M., Patterning cells and their environments using multiple laminar fluid flows in capillary networks. *Proceedings of the National Academy of Sciences of the United States of America* **1999,** 96, (10), 5545-5548.

94.   Yang, I. H.; Co, C. C.; Ho, C. C., Spatially controlled co-culture of neurons and glial cells. *Journal of Biomedical Materials Research Part A* **2005,** 75A, (4), 976-984.

95.   Reyes, D. R.; Perruccio, E. M.; Becerra, S. P.; Locascio, L. E.; Gaitan, M., Micropatterning neuronal cells on polyelectrolyte multilayers. *Langmuir* **2004,** 20, (20), 8805-8811.

96.   Kidambi, S.; Chan, C.; Lee, I., Selective Depositions on Polyelectrolyte Multilayers: Self-Assembled Monolayers of m-dPEG Acid as Molecular Templates. *Journal of the American Chemical Society* **2004,** 126, (14), 4697-4703.

97.   Khademhosseini, A.; Suh Kahp, Y.; Yang Jen, M.; Eng, G.; Yeh, J.; Levenberg, S.; Langer, R., Layer-by-layer deposition of hyaluronic acid and poly-L-lysine for patterned cell co-cultures. *Biomaterials* **2004,** 25, (17), 3583-92.

98.   Jiang, X.; Hammond, P. T., Selective Deposition in Layer-by-Layer Assembly: Functional Graft Copolymers as Molecular Templates. *Langmuir* **2000,** 16, (22), 8501-8509.

99.   Bhatia, S. N.; Balis, U. J.; Yarmush, M. L.; Toner, M., Probing heterotypic cell interactions: hepatocyte function in microfabricated co-cultures. *Journal of Biomaterials Science-Polymer Edition* **1998,** 9, (11), 1137-60.

100.   Sauer, H.; Klimm, B.; Hescheler, J.; Wartenberg, M., Activation of p90RSK and growth stimulation of multicellular tumor spheroids are dependent on reactive oxygen

species generated after purinergic receptor stimulation by ATP. *FASEB Journal* **2001**, 15, (13), 2539-2541, 10 1096/fj 01-0360fje.

101. Patil, S.; Chan, C., Palmitic and stearic fatty acids induce Alzheimer-like hyperphosphorylation of tau in primary rat cortical neurons. *Neuroscience Letters* **2005,** 384, (3), 288-293.

102. Blazquez, C.; Galve-Roperh, I.; Guzman, M., De novo-synthesized ceramide signals apoptosis in astrocytes via extracellular signal-regulated kinase. *FASEB Journal* **2000,** 14, (14), 2315-2322.

103. Rozga, J.; Williams, F.; Ro, M. S.; Neuzil, D. F.; Giorgio, T. D.; Backfisch, G.; Moscioni, A. D.; Hakim, R.; Demetriou, A. A., Development of a Bioartificial Liver - Properties and Function of a Hollow-Fiber Module Inoculated with Liver-Cells. *Hepatology* **1993,** 17, (2), 258-265.

104. Donato, M. T.; Castell, J. V.; Gomez-Lechon, M. J., Co-cultures of hepatocytes with epithelial-like cell lines: expression of drug-biotransformation activities by hepatocytes. *Cell Biology and Toxicology* **1991,** 7, (1), 1-14.

105. Shimaoka, S.; Nakamura, T.; Ichihara, A., Stimulation of Growth of Primary Cultured Adult-Rat Hepatocytes without Growth-Factors by Coculture with Nonparenchymal Liver-Cells. *Experimental Cell Research* **1987,** 172, (1), 228-242.

106. Quake, S. R.; Scherer, A., From micro- to nanofabrication with soft materials. *Science* **2000,** 290, (5496), 1536-1540.

107. Araque, A.; Carmignoto, G.; Haydon, P. G., Dynamic signaling between astrocytes and neurons. *Annual Review Of Physiology* **2001,** 63, 795-813.

108. Park, L. C.; Zhang, H.; Gibson, G. E., Co-culture with astrocytes or microglia protects metabolically impaired neurons. *Mechanisms of ageing and development* **2001,** 123, (1), 21-7.

109. Chen, Y.; Vartiainen, N. E.; Ying, W.; Chan, P. H.; Koistinaho, J.; Swanson, R. A., Astrocytes protect neurons from nitric oxide toxicity by a glutathione-dependent mechanism. *Journal of Neurochemistry* **2001,** 77, (6), 1601-1610.

110.   Fukuda, J.; Khademhosseini, A.; Yeh, J.; Eng, G.; Cheng, J.; Farokhzad, O. C.; Langer, R., Micropatterned cell co-cultures using layer-by-layer deposition of extracellular matrix components. *Biomaterials* **2006**, 27, (8), 1479-1486.

111.   Decher, G.; Hong, J. D., Buildup of ultrathin multilayer films by a self-assembly process. 1. Consecutive adsorption of anionic and cationic bipolar amphiphiles on charged surfaces. *Makromolekulare Chemie, Macromolecular Symposia* **1991**, 46, (Eur. Conf. Organ. Org. Thin Films, 3rd, 1990), 321-7.

112.   Decher, G.; Hong, J. D., Buildup of ultrathin multilayer films by a self-assembly process: II. Consecutive adsorption of anionic and cationic bipolar amphiphiles and polyelectrolytes on charged surfaces. *Berichte der Bunsen-Gesellschaft* **1991**, 95, (11), 1430-4.

113.   Decher, G.; Lvov, Y.; Schmitt, J., Proof of multilayer structural organization in self-assembled polycation-polyanion molecular films. *Thin Solid Films* **1994**, 244, (1-2), 772-7.

114.   Decher, G.; Schmitt, J., Fine-tuning of the film thickness of ultrathin multilayer films composed of consecutively alternating layers of anionic and cationic polyelectrolytes. *Progress in Colloid & Polymer Science* **1992**, 89, (Trends Colloid Interface Sci. VI), 160-4.

115.   Fou, A. C.; Rubner, M. F., Molecular-Level Processing of Conjugated Polymers. 2. Layer-by-Layer Manipulation of In-Situ Polymerized p-Type Doped Conducting Polymers. *Macromolecules* **1995**, 28, (21), 7115-20.

116.   Fou, A. C.; Onitsuka, O.; Ferreira, M.; Rubner, M. F.; Hsieh, B. R., Fabrication and properties of light-emitting diodes based on self-assembled multilayers of poly(phenylene vinylene). *Journal of Applied Physics*
1996, 79, (10), 7501-7509.

117.   Ariga, K.; Lvov, Y.; Kunitake, T., Assembling Alternate Dye-Polyion Molecular Films by Electrostatic Layer-by-Layer Adsorption. *Journal of the American Chemical Society* **1997**, 119, (9), 2224-2231.

118.   Zheng, H.; Zhang, R.; Wu, Y.; Shen, J., Blue-green light emission from self-assembled bipyridinium thin films. *Chemistry Letters* **1998**, (9), 909-910.

119. Kotov, N. A.; Dekany, I.; Fendler, J. H., Ultrathin graphite oxide-polyelectrolyte composites prepared by self-assembly. Transition between conductive and non-conductive states. *Advanced Materials* **1996**, **8**, (8), 637-641.

120. Lee, I.; Zheng, H. P.; Rubner, M. F.; Hammond, P. T., Controlled cluster size in patterned particle arrays via directed adsorption on confined surfaces. *Advanced Materials* **2002**, 14, (8), 572-577.

121. Zheng, H. P.; Lee, I.; Rubner, M. F.; Hammond, P. T., Two component particle arrays on patterned polyelectrolyte multilayer templates. *Advanced Materials* **2002**, 14, (8), 569-572.

122. Liu, Y.; Wang, A.; Claus, R. O., Layer-by-layer electrostatic self-assembly of nanoscale Fe3O4 particles and polyimide precursor on silicon and silica surfaces. *Applied Physics Letters* **1997**, 71, (16), 2265-2267.

123. Lvov, Y.; Ariga, K.; Onda, M.; Ichinose, I.; Kunitake, T., Alternate Assembly of Ordered Multilayers of SiO2 and Other Nanoparticles and Polyions. *Langmuir* **1997**, 13, (23), 6195-6203.

124. Lvov, Y.; Ariga, K.; Ichinose, I.; Kunitake, T., Layer-by-layer architectures of concanavalin A by means of electrostatic and biospecific interactions. *Journal of the Chemical Society, Chemical Communications* **1995**, (22), 2313-14.

125. Ichinose, I.; Fujiyoshi, K.; Mizuki, S.; Lvov, Y.; Kunitake, T., Layer-by-layer assembly of aqueous bilayer membranes on charged surfaces. *Chemistry Letters* **1996**, (4), 257-8.

126. Lee, I.; Hammond, P. T.; Rubner, M. F., Selective Electroless Nickel Plating of Particle Arrays on Polyelectrolyte Multilayers. *Chemistry of Materials* **2003 (in press)**.

127. Clark, S. L.; Montague, M.; Hammond, P. T., Selective deposition in multilayer assembly: SAMs as molecular templates. *Supramolecular Science* **1997**, 4, (1-2), 141-146.

128. Clark, S. L.; Montague, M. F.; Hammond, P. T., Ionic Effects of Sodium Chloride on the Templated Deposition of Polyelectrolytes Using Layer-by-Layer Ionic Assembly. *Macromolecules* **1997**, 30, (23), 7237-7244.

129.   Geissler, M.; Wolf, H.; Stutz, R.; Delamarche, E.; Grummt, U. W.; Michel, B.; Bietsch, A., Fabrication of metal nanowires using microcontact printing. *Langmuir* **2003**, 19, (15), 6301-6311.

130.   Ghosh, P.; Lackowski, W. M.; Crooks, R. M., Two new approaches for patterning polymer films using templates prepared by microcontact printing. *Macromolecules* **2001**, 34, (5), 1230-1236.

131.   Papra, A.; Bernard, A.; Juncker, D.; Larsen, N. B.; Michel, B.; Delamarche, E., Microfluidic networks made of poly(dimethylsiloxane), Si, and Au coated with polyethylene glycol for patterning proteins onto surfaces. *Langmuir* **2001**, 17, (13), 4090-4095.

132.   Delamarche, E.; Geissler, M.; Bernard, A.; Wolf, H.; Michel, B.; Hilborn, J.; Donzel, C., Hydrophilic poly (dimethylsloxane) stamps for microcontact printing. *Advanced Materials* **2001**, 13, (15), 1164-+.

133.   Kaneko, Y.; Sakai, K.; Okano, T., Temperature-responsive hydrogels as intelligent materials. *Biorelated Polymers and Gels* **1998**, 29-69.

134.   Henry, C. M., Chem. Eng. News. *Chem. Eng. News* **2000**, 78, 49.

135.   M.N. Mar, B. D. R., S.S. Yee, An intrinsically protein-resistant surface plasmon resonance biosensor based upon a RF-plasma-deposited thin film. *Sensors Actuators B* **1999**, 54, 125.

136.   Patel, N.; Padera, R.; Sanders, G. H. W.; Cannizzaro, S. M.; Davies, M. C.; Langer, R.; Roberts, C. J.; Tendler, S. J. B.; Williams, P. M.; Shakesheff, K. M., Spatially controlled cell engineering on biodegradable polymer surfaces. *FASEB Journal* **1998**, 12, (14), 1447-1454.

137.   Vansteenkiste, S. O.; Corneillie, S. I.; Schacht, E. H.; Chen, X.; Davies, M. C.; Moens, M.; Van Vaeck, L., Direct Measurement of Protein Adhesion at Biomaterial Surfaces by Scanning Force Microscopy. *Langmuir* **2000**, 16, (7), 3330-3336.

138.   Favia, P.; d'Agostino, R., Plasma treatments and plasma deposition of polymers for biomedical applications. *Surface and Coatings Technology* **1998**, 98, (1-3), 1102-1106.

139.   Merrill, E. W.; Salzman, E. W., Polyethylene oxide as a biomaterial. *ASAIO Journal* **1983**, 6, (2), 60-4.

140.   Sa Da Costa, V.; Brier-Russell, D.; Salzman, E. W.; Merrill, E. W., ESCA studies of polyurethanes: blood platelet activation in relation to surface composition. *Journal of Colloid and Interface Science* **1981**, 80, (2), 445-52.

141.   Sa da Costa, V.; Brier-Russell, D.; Trudel, G., III; Waugh, D. F.; Salzman, E. W.; Merrill, E. W., Polyether-polyurethane surfaces: thrombin adsorption, platelet adsorption, and ESCA scanning. *Journal of Colloid and Interface Science* **1980**, 76, (2), 594-6.

142.   Cuvelier, D.; Rossier, O.; Bassereau, P.; Nassoy, P., Micropatterned "adherent/repellent" glass surfaces for studying the spreading kinetics of individual red blood cells onto protein-decorated substrates. *European Biophysics Journal with Biophysics Letters* **2003**, 32, (4), 342-354.

143.   Csucs, G.; Michel, R.; Lussi, J. W.; Textor, M.; Danuser, G., Microcontact printing of novel co-polymers in combination with proteins for cell-biological applications. *Biomaterials* **2003**, 24, (10), 1713-1720.

144.   Ahn, D. J.; Jin, J. J.; Lee, G. S.; Kwon, G.; Pak, J. J.; Kim, J.; Lee, K. J., Hippocampal neuronal network directed geometrically by sub-patterns of microcontact printing (mu CP). *Journal of Industrial and Engineering Chemistry* **2003**, 9, (1), 25-30.

145.   Lu, L. C.; Nyalakonda, K.; Kam, L.; Bizios, R.; Gopferich, A.; Mikos, A. G., Retinal pigment epithelial cell adhesion on novel micropatterned surfaces fabricated from synthetic biodegradable polymers. *Biomaterials* **2001**, 22, (3), 291-297.

146.   Berg, M. C.; Choi, J.; Hammond, P. T.; Rubner, M. F., Tailored Micropatterns through Weak Polyelectrolyte Stamping. *Langmuir* **2003**, 19, (6), 2231-2237.

147.   Caruso, F.; Lichtenfeld, H.; Donath, E.; Moehwald, H., Investigation of Electrostatic Interactions in Polyelectrolyte Multilayer Films: Binding of Anionic Fluorescent Probes to Layers Assembled onto Colloids. *Macromolecules* **1999**, 32, (7), 2317-2328.

148.   Prime, K. L.; Whitesides, G. M., Adsorption of proteins onto surfaces containing end-attached oligo(ethylene oxide): a model system using self-assembled monolayers. *Journal of the American Chemical Society* **1993**, 115, (23), 10714-21.

149.   Jiang, X. P.; Hammond, P. T., Routes to dimensional structures: Polymer-on-polymer stamping and polyion surface sorting. *Abstracts of Papers of the American Chemical Society* **2001**, 221, U372-U372.

150.   Koh, W. G.; Revzin, A.; Pishko, M. V., Poly(ethylene glycol) hydrogel microstructures encapsulating living cells. *Langmuir* **2002**, 18, (7), 2459-62.

151.   Popat, K. C.; Johnson, R. W.; Desai, T. A., Characterization of vapor deposited poly (ethylene glycol) films on silicon surfaces for surface modification of microfluidic systems. *Journal of Vacuum Science & Technology B* **2003**, 21, (2), 645-654.

152.   Zhang, M.; Desai, T.; Ferrari, M., Proteins and cells on PEG immobilized silicon surfaces. *Biomaterials* **1998**, 19, (10), 953-960.

153.   Folch, A.; Toner, M., Microengineering of cellular interactions. *Annual Review of Biomedical Engineering* **2000**, 2, 227-256.

154.   Ito, Y., Surface micropatterning to regulate cell functions. *Biomaterials* **1999**, 20, (23/24), 2333-2342.

155.   Orth, R. N.; Clark, T. G.; Craighead, H. G., Biosensors: Avidin-biotin micropatterning methods for biosensor applications. *Biomedical Microdevices* **2003**, 5, (1), 29-34.

156.   Nicolau, D. V.; Taguchi, T.; Taniguchi, H.; Yoshikawa, S., Microsize Protein Patterning on Diazonaphthoquinone/Novolak Thin Polymeric Films. *Langmuir* **1998**, 14, (7), 1927-1936.

157.   Yang, Z.; Chilkoti, A., Microstamping of a biological ligand onto an activated polymer surface. *Advanced Materials* **2000**, 12, (6), 413-417.

158.   Willner, I.; Katz, E., Integration of layered redox proteins and conductive supports for bioelectronic applications. *Angewandte Chemie, International Edition* **2000**, 39, (7), 1181-1218.

159.   Lee, K.-B.; Park, S.-J.; Mirkin, C. A.; Smith, J. C.; Mrksich, M., Protein nanoarrays generated by dip-pen nanolithography. *Science* **2002**, 295, (5560), 1702-1705.

160. Holden, M. A.; Cremer, P. S., Light Activated Patterning of Dye-Labeled Molecules on Surfaces. *Journal of the American Chemical Society* **2003**, 125, (27), 8074-8075.

161. Blawas, A. S.; Oliver, T. F.; Pirrung, M. C.; Reichert, W. M., Step-and-Repeat Photopatterning of Protein Features Using Caged-Biotin-BSA: Characterization and Resolution. *Langmuir* **1998**, 14, (15), 4243-4250.

162. Doh, J.; Irvine, D. J., Photogenerated polyelectrolyte bilayers from an aqueous-processible photoresist for multicomponent protein patterning. *Journal of the American Chemical Society* **2004**, 126, (30), 9170-9171.

163. Lee, K.-B.; Lim, J.-H.; Mirkin, C. A., Protein nanostructures formed via direct-write dip-pen nanolithography. *Journal of the American Chemical Society* **2003**, 125, (19), 5588-5589.

164. Tien, J.; Nelson, C. M.; Chen, C. S., Fabrication of aligned microstructures with a single elastomeric stamp. *Proceedings of the National Academy of Sciences of the United States of America* **2002**, 99, (4), 1758-1762.

165. Sorribas, H.; Padeste, C.; Tiefenauer, L., Photolithographic generation of protein micropatterns for neuron culture applications. *Biomaterials* **2001**, 23, (3), 893-900.

166. Lemmo, A. V.; Rose, D. J.; Tisone, T. C., Inkjet dispensing technology: applications in drug discovery. *Current Opinion in Biotechnology* **1998**, 9, (6), 615-617.

167. Langer, R., Drug delivery and targeting. *Nature* **1998**, 392, (6679), 5-10.

168. Luo, L. Q.; Liu, J. Y.; Wang, Z. X.; Yang, X. R.; Dong, S. J.; Wang, E. K., Fabrication of layer-by-layer deposited multilayer films containing DNA and its interaction with methyl green. *Biophysical Chemistry* **2001**, 94, (1-2), 11-22.

169. Lvov, Y.; Decher, G.; Sukhorukov, G., Assembly Of Thin-Films By Means Of Successive Deposition Of Alternate Layers Of Dna And Poly(Allylamine). *Macromolecules* **1993**, 26, (20), 5396-5399.

170. Hill, I. R. C.; Garnett, M. C.; Bignotti, F.; Davis, S. S., Determination of protection from serum nuclease activity by DNA-polyelectrolyte complexes using an electrophoretic method. *Analytical Biochemistry* **2001**, 291, (1), 62-68.

171. Tuerk, C.; Gold, L., Systematic evolution of ligands by exponential enrichment: RNA ligands to bacteriophage T4 DNA polymerase. *Science (Washington, DC, United States)* **1990**, 249, (4968), 505-10.

172. Ellington, A. D.; Szostak, J. W., In vitro selection of RNA molecules that bind specific ligands. *Nature (London, United Kingdom)* **1990**, 346, (6287), 818-22.

173. Ishida, S.; Usui, T.; Yamashiro, K.; Kaji, Y.; Amano, S.; Ogura, Y.; Hida, T.; Oguchi, Y.; Ambati, J.; Miller, J. W.; Gragoudas, E. S.; Ng, Y.-S.; D'Amore, P. A.; Shima, D. T.; Adamis, A. P., VEGF164-mediated inflammation is required for pathological, but not physiological, ischemia-induced retinal neovascularization. *Journal of Experimental Medicine* **2003**, 198, (3), 483-489.

174. Brody, E. N.; Gold, L., Aptamers as therapeutic and diagnostic agents. *Reviews in Molecular Biotechnology* **2000**, 74, (1), 5-13.

175. Gold, L.; Polisky, B.; Uhlenbeck, O.; Yarus, M., Diversity of oligonucleotide functions. *Annual Review of Biochemistry* **1995**, 64, 763-97.

176. Wilson, D. S.; Szostak, J. W., In vitro selection of functional nucleic acids. *Annual Review of Biochemistry* **1999**, 68, 611-647.

177. Hesselberth, J.; Robertson, M. P.; Jhaveri, S.; Ellington, A. D., In vitro selection of nucleic acids for diagnostic applications. *Reviews in Molecular Biotechnology* **2000**, 74, (1), 15-25.

178. Jayasena, S. D., Aptamers: an emerging class of molecules that rival antibodies in diagnostics. *Clinical Chemistry (Washington, D. C.)* **1999**, 45, (9), 1628-1650.

179. Stadtherr, K.; Wolf, H.; Lindner, P., An aptamer-based protein biochip. *Analytical Chemistry* **2005**, 77, (11), 3437-3443.

180. Kirby, R.; Cho, E. J.; Gehrke, B.; Bayer, T.; Park, Y. S.; Neikirk, D. P.; McDevitt, J. T.; Ellington, A. D., Aptamer-based sensor arrays for the detection and quantitation of proteins. *Analytical Chemistry* **2004**, 76, (14), 4066-4075.

181. Potyrailo, R. A.; Conrad, R. C.; Ellington, A. D.; Hieftje, G. M., Adapting Selected Nucleic Acid Ligands (Aptamers) to Biosensors. *Analytical Chemistry* **1998**, 70, (16), 3419-3425.

137

182. Liss, M.; Petersen, B.; Wolf, H.; Prohaska, E., An aptamer-based quartz crystal protein biosensor. *Analytical Chemistry* **2002**, 74, (17), 4488-4495.

183. Xiao, Y.; Piorek, B. D.; Plaxco, K. W.; Heeger, A. J., A Reagentless Signal-On Architecture for Electronic, Aptamer-Based Sensors via Target-Induced Strand Displacement. *Journal of the American Chemical Society* **2005**, 127, (51), 17990-17991.

184. McCarley, R. L.; Vaidya, B.; Wei, S.; Smith, A. F.; Patel, A. B.; Feng, J.; Murphy, M. C.; Soper, S. A., Resist-Free Patterning of Surface Architectures in Polymer-Based Microanalytical Devices. *Journal of the American Chemical Society* **2005**, 127, (3), 842-843.

185. Couch, R. B., Prevention and treatment of influenza. *New England Journal of Medicine* **2000**, 343, (24), 1778-1787.

186. Cooper, N. J.; Sutton, A. J.; Abrams, K. R.; Wailoo, A.; Turner, D. A.; Nicholson, K. G., Effectiveness of neuraminidase inhibitors in treatment and prevention of influenza A and B: systematic review and meta-analyses of randomized controlled trials. *BMJ [British Medical Journal]* **2003**, 326, (7401), 1235-1239.

187. Demicheli, V.; Jefferson, T.; Rivetti, D.; Deeks, J., Prevention and early treatment of influenza in healthy adults. *Vaccine FIELD Full Journal Title:Vaccine* **2000**, 18, (11-12), 957-1030.

188. Skehel, J. J.; Wiley, D. C., Receptor binding and membrane fusion in virus entry: the influenza hemagglutinin. *Annual Review of Biochemistry* **2000**, 69, 531-569.

189. Skehel, J. J.; Cross, K.; Steinhauer, D.; Wiley, D. C., Influenza fusion peptides. *Biochemical Society Transactions* **2001**, 29, (4), 623-626.

190. Wilson, I. A.; Skehel, J. J.; Wiley, D. C., Structure of the hemagglutinin membrane glycoprotein of influenza virus at 3.ANG. resolution. *Nature (London, United Kingdom)* **1981**, 289, (5796), 366-73.

191. Brummelkamp, T. R.; Bernards, R., Innovation - New tools for functional mammalian cancer genetics. *Nature Reviews Cancer* **2003**, 3, (10), 781-789.

192. Ameyar-Zazoua, M.; Guasconi, V.; Ait-Si-Ali, S., siRNA as a route to new cancer therapies. *Expert Opinion on Biological Therapy* **2005**, 5, (2), 221-224.

193. Bock, L. C.; Griffin, L. C.; Latham, J. A.; Vermaas, E. H.; Toole, J. J., Selection of single-stranded DNA molecules that bind and inhibit human thrombin. *Nature (London, United Kingdom)* **1992**, 355, (6360), 564-6.

194. Macaya, R. F.; Schultze, P.; Smith, F. W.; Roe, J. A.; Feigon, J., Thrombin-Binding DNA Aptamer Forms a Unimolecular Quadruplex Structure in Solution. *Proceedings of the National Academy of Sciences of the United States of America* **1993**, 90, (8), 3745-3749.

195. Schultze, P.; Macaya, R. F.; Feigon, J., 3-Dimensional Solution Structure of the Thrombin-Binding DNA Aptamer D(Ggttggtgtggttgg). *Journal of Molecular Biology* **1994**, 235, (5), 1532-1547.

196. Kuryavyi, V.; Majumdar, A.; Shallop, A.; Chernichenko, N.; Skripkin, E.; Jones, R.; Patel, D. J., A double chain reversal loop and two diagonal loops define the architecture of a unimolecular DNA quadruplex containing a pair of stacked G(syn)center dot G(syn)center dot G(anti)center dot G(anti) tetrads flanked by a G center dot(T-T) triad and a T center dot T center dot T triple. *Journal of Molecular Biology* **2001**, 310, (1), 181-194.

197. Smirnov, I.; Shafer, R. H., Effect of loop sequence and size on DNA aptamer stability. *Biochemistry* **2000**, 39, (6), 1462-1468.

198. Paborsky, L. R.; Mccurdy, S. N.; Griffin, L. C.; Toole, J. J.; Leung, L. L. K., The Single-Stranded-DNA Aptamer-Binding Site of Human Thrombin. *Journal of Biological Chemistry* **1993**, 268, (28), 20808-20811.

199. Tsiang, M.; Gibbs, C. S.; Griffin, L. C.; Dunn, K. E.; Leung, L. L. K., Selection of a Suppressor Mutation That Restores Affinity of an Oligonucleotide Inhibitor for Thrombin Using in-Vitro Genetics. *Journal of Biological Chemistry* **1995**, 270, (33), 19370-19376.

200. Tsiang, M.; Jain, A. K.; Dunn, K. E.; Rojas, M. E.; Leung, L. L. K.; Gibbs, C. S., Functional Mapping of the Surface Residues of Human Thrombin. *Journal of Biological Chemistry* **1995**, 270, (28), 16854-16863.

201. Griffin, L. C.; Tidmarsh. George, F.; Bock, L. C.; Toole, J. J.; Leung, L. L. K., In vivo anticoagulant properties of a novel nucleotide-based thrombin inhibitor and demonstration of regional anticoagulation in extracorporeal circuits. *Blood* **1993**, 81, (12), 3271-6.

139

202. Li, W. X.; Kaplan, A. V.; Grant, G. W.; Toole, J. J.; Leung, L. L. K., A novel nucleotide-based thrombin inhibitor inhibits clot-bound thrombin and reduces arterial platelet thrombus formation. *Blood* **1994**, 83, (3), 677-82.

203. Coutre, S. E.; Griffin, L. C.; Moon, M. R.; Deanda, A.; Law, V. S.; Leung, L. L. K.; Miller, D. C., Thrombin Aptamer as an Anticoagulant for Canine Cardiopulmonary Bypass. *Thrombosis and Haemostasis* **1993**, 69, (6), 540-540.

204. Shaw, J.-P.; Fishback, J. A.; Cundy, K. C.; Lee, W. A., A novel oligodeoxynucleotide inhibitor of thrombin. I. In vitro metabolic stability in plasma and serum. *Pharmaceutical Research* **1995**, 12, (12), 1937-42.

205. Dubas, S. T.; Schlenoff, J. B., Polyelectrolyte multilayers containing a weak polyacid: Construction and deconstruction. *Macromolecules* **2001**, 34, (11), 3736-3740.

206. Wood, K. C.; Boedicker, J. Q.; Lynn, D. M.; Hammon, P. T., Tunable drug release from hydrolytically degradable layer-by-layer thin films. *Langmuir* **2005**, 21, (4), 1603-1609.

207. Ren, K. F.; Ji, J.; Shen, J. C., Construction and enzymatic degradation of multilayered poly-L-lysine/DNA films. *Biomaterials* **2006**, 27, (7), 1152-1159.

208. Putnam, D.; Gentry, C. A.; Pack, D. W.; Langer, R., Polymer-based gene delivery with low cytotoxicity by a unique balance of side-chain termini. *Proceedings of the National Academy of Sciences of the United States of America* **2001**, 98, (3), 1200-+.

209. Dubas, S. T.; Farhat, T. R.; Schlenoff, J. B., Multiple membranes from "true" polyelectrolyte multilayers. *Journal of the American Chemical Society* **2001**, 123, (22), 5368-5369.